Evaluation of Flood-Level Prediction Using Alluvial-River Models (1983)

Pages
140

Size
8.5 x 10

ISBN
0309326400

Committee on Hydrodynamic Computer Models for Flood Insurance Studies; Advisory Board on the Built Environment; Commission on Engineering and Technical Systems; National Research Council

An Evaluation of Flood-Level Prediction Using Alluvial-River Models

Committee on Hydrodynamic Computer Models
for Flood Insurance Studies
Advisory Board on the Built Environment
Commission on Engineering and Technical Systems
National Research Council

NATIONAL ACADEMY PRESS
Washington, DC 1983

NOTICE: The project that is the subject of this report was approved by the Governing Board of the National Research Council, whose members are drawn from the councils of the National Academy of Sciences, the National Academy of Engineering, and the Institute of Medicine. The members of the committee responsibile for the report were chosen for their special competences and with regard for appropriate balance.

This report has been reviewed by a group other than the authors according to procedures approved by a Report Review Committee consisting of members of the National Academy of Sciences, the National Academy of Engineering, and the Institute of Medicine.

The National Research Council was established by the National Academy of Sciences in 1916 to associate the broad community of science and technology with the Academy's purpose of furthering knowledge and of advising the federal government. The Council operates in accordance with general policies determined by the Academy under the authority of its congressional charter of 1863, which establishes the Academy as a private, nonprofit, self-governing membership corporation. The Council has become the principal operating agency of both the National Academy of Sciences and the National Academy of Engineering in the conduct of their services to the government, the public, and the scientific and engineering communities. It is administered jointly by both Academies and the Institute of Medicine. The National Academy of Engineering and the Institute of Medicine were established in 1964 and 1970, respectively, under the charter of the National Academy of Sciences.

This report was prepared under Contract Number EMW-C-0167 between the National Academy of Sciences and the Federal Emergency Management Agency.

For information contact:

Advisory Board on the Built Environment
Committee on Engineering and Technical Systems
National Research Council
2101 Constitution Avenue, N.W.
Washington, D.C. 20418

ADVISORY BOARD ON THE BUILT ENVIRONMENT

L.R. SHAFFER, Deputy Director, U.S. Army Construction Engineering Research Laboratory, Champaign, Illinois

ARTHUR C. STERN, Professor of Air Hygiene, The University of North Carolina, Chapel Hill

WARREN H. TURNER, Director, Central Office of Maintenance Engineering, American Telephone & Telegraph Company, Basking Ridge, New Jersey

SHIRLEY F. WEISS, Professor, Department of City and Regional Planning, The University of North Carolina, Chapel Hill

JOHN H. WIGGINS, Jr., President, J.H. Wiggins, Company, Redondo Beach, California

Liaision Representatives
LEE S. GARRETT, Department of the Army (Retired)
MAXINE SAVITZ, Department of Energy
RICHARD N. WRIGHT, National Bureau of Standards

Ex-Officio
JOSEPH H. ZETTEL, Chairman of the Board, Western Solar Utilization Network, Littleton, Colorado

COMMITTEE ON HYDRODYNAMIC COMPUTER MODELS FOR FLOOD INSURANCE STUDIES

Chairman
JOHN F. KENNEDY, Institute of Hydraulic Research, The University of Iowa, Iowa City, Iowa

Members
DAVID R. DAWDY, Consulting Hydrologist, San Francisco, California
CARL F. NORDIN, Jr., U.S. Geological Survey, Lakewood, Colorado
JOHN SCHAAKE, Hydrologic Services Division, National Weather Service, Silver Springs, Maryland
STANLEY A. SCHUMM, Department of Geology, Colorado State University, Fort Collins, Colorado
VITO A. VANONI, W.M. Keck Laboratory, California Institute of Technology, Pasadena, California

Liaison Representatives
FRANK TSAI, Federal Emergency Management Agency, Washington, D.C.

Consultant
TATSUAKI NAKATO, Institute of Hydraulic Research, The University of Iowa, Iowa City, Iowa

ABBE Staff
JOHN EBERHARD, Executive Director and Program Manager from 1981
JAMES R. SMITH, Program Manager until 1981
DELPHINE D. GLAZE, Administrative Secretary

CONTENTS

PREFACE

This report presents the results of one of four studies related to the National Flood Insurance Program (NFIP) conducted by the Advisory Board on the Built Environment (ABBE) during 1981-1982. The client for these studies has been the Federal Emergency Management Agency (FEMA), which administers the NFIP. This report addresses the evaluation of flood-level prediction using computer-based models of alluvial-river flows. The other three studies are: (1) an assessment of the conduct of flood insurance studies; (2) the problem of how to map areas of mudslide hazards (including recommendations on how to delineate areas prone to mudslides); and (3) an evaluation of a computer model for coastal flooding from hurricanes (and its specific application to Lee County, Florida).

The study committee was selected after consultation with experts in government, industry and academia, as well as within the National Academy of Sciences/National Academy of Engineering. The committee was chosen to include experts in river engineering, classical and numerical hydraulics, hydrology, and river morphology--the technical disciplines related to the study area under consideration. The Chairman of the Committee was Dr. John F. Kennedy, a specialist in river hydraulics and sedimentary processes. The other members of the Committee were Dr. Vito A. Vanoni and Dr. Carl F. Nordin, Jr., both specialists in sediment-transport mechanics and river hydraulics; Dr. John A. Schaake, an expert in the field of hydrology who specializes in runoff prediction and flood forecasting; Dr. David R. Dawdy, whose specialty is numerical modeling of river-flow and other hydrologic processes; and Dr. Stanley A. Schumm, a specialist in riverine geomorphology. See Appendix for biographical sketches.

The study was initiated by FEMA Regions 8, 9, and 10, primarily the western states, because they had experienced problems with modeling channel erosion and sedimentation using fixed-bed models (e.g., HEC-2) to compute flood-water elevations. The focus of these problems was flood-insurance studies in communities impacted by rivers with movable beds or alluvial channels. It was suggested to FEMA that one or more existing numerical, alluvial-river models might better serve the requirements of flood-stage prediction for the National Flood Insurance Program. This study was organized to address the question of flood-stage prediction and capabilities of computer-based flow- and sediment-routing models for alluvial streams.

The Committee decided early in their deliberations that a subcontract should be awarded to the Institute of Hydraulic Research of The University of Iowa to engage Dr. Tatsuaki Nakato to manage the technical aspects of the study. Specifically, the subcontractor was to:

1. Prepare an inventory of available computer-based flood- and sediment-routing models; a detailed description of each model's capabilities, limitations, required input and input format, and output and output format; and a general evaluation of each model's strengths, weakness and applicability for use in flood insurance studies.
2. Propose, for committee consideration, at least two U.S. river channels and corresponding flood events to be used as test cases in the evaluation and comparison of models deemed appropriate by the Committee.
3. Compile the data required by each model, in the format required, for the test cases selected and transmit these data packages to the appropriate agencies or individuals for use in performing the test-case calculations.
4. Make the arrangements required for the various agencies or individuals responsible for the selected models to perform test-case calculations using their models.
5. Perform, using the test cases selected by the Committee, a set of test-case calculations using one of the selected models in order to provide some indication of the accuracy, resolution, reproducibility, etc., that can be expected from the other models and to ensure that the test cases chosen are appropriate.
6. Prepare a report describing the test cases selected and the test-case calculations.
7. Prepare, in a form suitable for evaluation by the Committee, a compilation of the results of the test-case calculations that includes written narratives describing the technical advantages and disadvantages of the models considered.

In October of 1981 it was further determined that subcontracts should be negotiated with four computer modelers for the performance of test-case calculations, utilizing models selected from the inventory compiled by Dr. Nakato, for at least two U.S. river channels and corresponding flood events. Each modeler selected was to:

1. Supply background information consisting of:

   a. The characteristics and limitations of his model, including background documentation.

   b. A copy of the program or a functional block diagram for each computer-based flow-routing and sediment-routing model.

2. Run his computer model(s) using given input data for given test-river reaches in two phases:

   Phase I: Rigid-bed model calculation
   Phase II: Erodible-bed model calculation

   Provide rationale for selecting the various parameters utilized in his model(s) and final computational outputs tabulated in the format requested by the Committee.

3. Upon request, perform additional computation and clarify any Committee member's questions on the test results.

The four modelers selected for this purpose were:

1. Dr. Ranjan Ariathurai
   Resource Management Associates
   3738 Mt. Diablo Boulevard, Suite 200
   Lafayette, California 94549

2. Dr. Howard H. Chang
   Department of Civil Engineering
   San Diego State University
   San Diego, California 92182

3. U.S. Army Corps of Engineers
   Hydrologic Engineering Center
   609 2nd Street
   Davis, California 95616

4. Simons, Li & Associates, Inc.
   3555 Stanford Road
   Post Office Box 1816
   Fort Collins, Colorado 80552

The report is intended for the use of technical staff members of FEMA. While the report may also be of interest to other professionals in government, universities, and private consulting firms, it is not designed as a document to be used by the general public or those without previous technical background in the subject.

SUMMARY

The primary objective of this investigation was to determine whether river-bed degradation during flood passage has an effect on flood stage that should be incorporated into the calculation of flood-zone limits. The ancilliary question is whether flood-zoning studies should make use of flood-stage prediction models which incorporate river-bed mobility and degradation/aggradation, instead of utilizing fixed-bed models, which have been employed heretofore. The study involved application of six flow- and sediment-routing models for alluvial streams to study reaches of the San Lorenzo, San Dieguito, and Salt Rivers, for which relatively complete input data were available. The developers of the individual models were commissioned to perform the numerical simulations using their models.

From the results of the studies, it was concluded that the effect of river-bed degradation and aggradation on water-surface elevation during flood passage is much smaller than the effects of the uncertainties of channel roughness or flow friction factor, sediment input, and initial channel geometry. Moreover, the available input data on channel geometry, bed-material characteristics, etc., generally are inadequate to permit full utilization of the capabilities of erodible-bed models. Therefore, except in cases of severely disturbed rivers which have experienced extreme local degradation or aggradation through man's intervention, utilization of erodible-bed models instead of fixed-bed models cannot be justified in flood-insurance studies. The principal deficiencies of the erodible-bed models are:

a. Unreliable formulation of the sediment-discharge capacity of flows.

b. Inadequate formulation of the variable friction factor of erodible-bed flows, and, in particular, the dependency of friction factor on depth and velocity of flow, sediment concentration, and temperature.

c. Inadequate understanding and formulation of the mechanics of bed coarsening and armoring, and their effects on sediment-discharge capacity, friction factor, and degradation suppression of flows.

I. INTRODUCTION

The principal objective of the investigation reported herein was to provide advice and guidance to the Federal Emergency Management Agency (FEMA) concerning the capabilities, limitations, and applicability of available computer models for erodible-bed rivers to flood events, with the goal of improving flood-insurance studies conducted under the National Flood Insurance Program (NFIP). Descriptions of the Committee that was convened and the organizational aspects of the project are presented in the PREFACE. the early stages of the study, a nationwide canvass of river experts was made by the Committee to identify modelers who had developed usable, alluvial-river-flow models. Although the Committee was aware of the several alluvial-river-flow models, developed in Europe and elsewhere, such as those of the Danish Hydraulic Institute in Denmark; Delft Hydraulics Laboratory in the Netherlands, Sogreah in France; and Hydraulics Research Station of Wallingford, England, a decision was made to limit the study to models that had been developed in the USA. This decision was dictated primarily by the time and budgetary constraints of this study. From among the several modelers identified, four agreed to participate in the project: Hydrologic Engineering Center, Corps of Engineers (HEC); Resource Management Associates (RMA); San Diego State University (SDSU); and Simons, Li & Associates, Inc. (SLA). A total of six numerical models was selected by the Committee members: three from SLA, and one from each of the other organizations. The characteristics of the models are summarized in Chapter II. Chapter III presents background on the selection of the three study rivers (the San Lorenzo River (SLR); the San Dieguito River (SDR); and the Salt River (SR)), and describes the characteristics of the rivers and the input data utilized for each. The principal numerical results obtained by each modeler are summarized in Chapter IV. Chapter V describes the limitations of the alluvial-river-flow models, and the principal conclusions and recommendations arrived at by the Committee are summarized in Chapter VI.

II. DESCRIPTION OF MODELS EVALUATED

The characteristics of the six numerical models of flow and sediment transport in movable-bed channels evaluated in the present study are summarized in this chapter. The models are HEC2SR, KUWASER, UUWSR, HEC-6, FLUVIAL-11, and SEDIMENT-4H. Summaries of the models' characteristics were first prepared on the basis of the individual modelers' final reports submitted to the Committee, and the references cited therein. Each modeler then was requested to review the Committee's description of his model. The modelers' suggestions and corrections have been incorporated into the following descriptions.

A. HEC2SR (HEC-2 with Sediment Routing):

1. Developer: Simons, Li & Associates, Inc. (SLA), 1980
2. Previous Applications:
   (1) Boulder Creek, Larimer County, Colorado (SLA, 1980)
   (2) Salt River, Phoenix, Arizona (SLA, 1980)
   (3) Santa Cruz River, Tucson, Arizona (SLA, 1981)
   (4) Cañada del Oro Wash, Pima County, Arizona (SLA, 1981)
   (5) Rillito Creek, Pima County, Arizona (SLA, 1981)

3. Basic Concepts:

The model was developed for simulating watershed sediment yield and the attendant aggradation and degradation in a river system. HEC2SR uses the HEC-2 backwater-computation program developed by Eichert (1976), at the Corps of Engineers (COE), Hydrologic Engineering Center (HEC), for calculation of backwater profiles. The following assumptions are incorporated into the HEC-2 program (Eichert, 1981):

(1) Flow is steady and gradually varied.
(2) Flow is one dimensional and hydrostatic pressure prevails at any point in the channel.
(3) The total energy head is the same for all points in a cross section (one-dimensional assumption).

(4) Channel slope is small.

The following basic equations are employed:

(1) Flow-continuity equation:

$$\frac{dQ}{dx} = q \qquad \text{....(2-1)}$$

(2) Sediment-continuity equation:

$$\frac{\partial Q_s}{\partial x} + (1 - \lambda)\frac{\partial A_b}{\partial t} = q_{s\ell} \qquad \text{....(2-2)}$$

(3) Flow-energy equation:

$$y_2 + \frac{\alpha_2 V_2^2}{2g} = y_1 + \frac{\alpha_1 V_1^2}{2g} + h_e \qquad \text{....(2-3)}$$

(4) Energy head-loss equation:

$$h_e = L\bar{S}_f + C\left|\frac{\alpha_2 V_2^2}{2g} - \frac{\alpha_1 V_1^2}{2g}\right| \qquad \text{....(2-4)}$$

where Q & Q_s = water and sediment discharges in volume units

q = lateral water inflow per unit width

A_b = bed cross-section area

$q_{s\ell}$ = lateral sediment inflow in volume per unit time and length

λ = porosity of bed sediment

y_1 & y_2 = water-surface elevations at ends of reach

V_1 & V_2 = mean velocities at ends of reach

α_1 & α_2 = velocity-head correction factors for flow at ends of reach

h_e = energy head loss

L = discharge-weighted reach length

$\bar{S}_f$ = representative friction slope for reach

C = expansion or contraction loss coefficient

4. Sediment-Transport Function:

The bed-load transport rate, q_b in volume per unit width, is computed from the Meyer-Peter and Müller formula (Meyer-Peter and Müller, 1948):

$$q_b = \frac{12.85}{\sqrt{\rho}\,\gamma_s}(\tau_o - \tau_c)^{1.5} \qquad \ldots.(2\text{-}5)$$

where τ_o = bed shear stress
τ_c = critical shear stress = $0.047\,(\gamma_s - \gamma)d_s$
ρ = density of water
γ_s = specific weight of sediment
γ = specific weight of water
d_s = median sediment particle size

The suspended-load transport rate, q_s in volume per unit width, is given by the Einstein formula (Einstein, 1950):

$$q_s = \frac{q_b}{11.6}\frac{G^{w-1}}{(1-G)^w}\left((V/u_*) + 2.5\right) I_1 + 2.5\, I_2) \qquad \ldots.(2\text{-}6)$$

where G = depth of bed layer divided by sediment diameter
u_* = shear velocity
V = mean flow velocity
I_1 & I_2 = Einstein's integrals
w = Rouse Number = particle fall velocity/$(0.4u_*)$

The combined bed-material transport rates are further corrected for the fine-sediment concentration using Colby's empirical relationships (Colby, 1957). During the sediment-routing phase, armoring effect and bed-material composition changes are considered. In determining the armored layer, a functional relationship between mean flow velocity and median sediment size, which determines the size of sediment that will not move, was first derived using Shields' criterion. The channel is assumed to be armored when a layer of nonmoving sediment that is twice as thick as the smallest size of moving sediment particles is established.

5. Numerical Scheme:

HEC2SR first runs the HEC-2 program to solve (2-3) and (2-4) by the standard, iterative-step method. The computational procedure is as follows:

(1) Assume a water-surface elevation, y_2, at section 2.
(2) Based on the assumed value of y_2, determine the corresponding total conveyance and velocity head.
(3) Compute $\overline{S}_f$ and compute h_e from (2-4).
(4) Check the equality of (2-3) with the computed value using the assumed y_2.
(5) Adjust y_2 if the error in step (4) is significant, repeat steps 1 through 5 until the values agree to within 0.01 ft.

After the HEC-2 computation, the bed-material discharge, which considers both sediment availability and transport capacity, is estimated for each computational reach. The channel aggradation/degradation corresponding to the difference between the sediment inflow and outflow is also determined for each reach. This sediment-volume change is distributed uniformly along the reach. The change in elevation at each cross-section vertical is determined by a weighting factor based on flow conveyances in adjacent lateral subsections. This technique is also used in KUWASER (see Section II-B)

6. Data Requirement:

HEC2SR requires the following input data:

(1) Data on channel geometry in HEC-2 format.
(2) Information on subreaches which are divided according to hydraulic and sediment-transport characteristics, including number of cross sections, reach length, number of tributaries, surface and subsurface sediment-size distributions, and potential armor layer.
(3) Watershed data, including channel-geometry representation and sediment-size distribution; this can be neglected if the sediment inflow from the lateral tributaries is neglected and/or the upstream reach does not connect to the upland watershed area.

(4) Inflow hydrographs and downstream boundary condition (stage hydrograph if available) throughout the flood.

7. Model Limitations and Applicability:

The use of HEC2SR is limited to a reach for which the one-dimensional-flow approximation is applicable. The model accounts for neither lateral channel migration nor secondary currents. The model assumes a uniform aggradation or degradation pattern along the reach, so that localized scour or deposition cannot be predicted. The model is not suitable for studying long-term river-bed changes, because of the high cost of backwater computation using HEC-2. However, HEC2SR offers the option to input sediment inflows directly or internally to generate sediment-loading data by considering the sediment-transport capacities in the upstream main-channel and tributary reaches. The backwater results obtained using HEC-2 can be directly compared to stage predictions utilized in the conventional flood-insurance studies. The model also features modular structure, which enables users to modify each functional component.

B. KUWASER (Known discharge, Uncoupled, WAter and SEdiment Routing):

1. Developer: Simons, Li, and Brown (Colorado State University), 1979

2. Previous Applications:

(1) Yazoo River Basin (Simons, Li, and Brown, 1979)

3. Basic Concepts:

The model was developed for simulating one-dimensional, spatially-varied, steady water and sediment flows. The principal assumptions it employs are as follows:

(1) Hydraulic characteristics of flow remain constant for a specified time interval.
(2) Hydrostatic pressure distribution prevails over any channel section.
(3) Secondary flow is negligible.
(4) Friction loss at a section is the same as that for a uniform flow with the same velocity and hydraulic radius.

(5) Channel slope is small.

The following basic equations are employed:

(1) Flow-continuity equation:

$$\frac{dQ}{dx} = q \qquad \text{....(2-7)}$$

(2) Sediment-continuity equation:

$$\frac{\partial Q_s}{\partial x} + (1 - \lambda)\frac{A_b}{\partial t} = q_{s\ell} \qquad \text{....(2-8)}$$

(3) Flow-energy equation:

$$(z + D + \alpha \frac{V^2}{2g})_1 = (z + D + \alpha \frac{V^2}{2g})_2 + H_\ell + H_{\ell v} \qquad \text{....(2-9)}$$

where

Q & Q_s = water and sediment discharges

q = lateral water inflow per unit width

A_b = bed cross-section area

$q_{s\ell}$ = lateral sediment inflow

λ = porosity of bed material

z = channel bed elevation

D = flow depth

H = total head above datum

α = correction factor for velocity head

V = mean flow velocity

H_ℓ = friction loss = $S_f \Delta x$

$H_{\ell v}$ = losses due to all other factors except friction = $S_{\ell v} \Delta x$

4. Sediment-Transport Function:

The sediment discharge per unit width, q_s, is expressed by

$$q_s = a\, V^b\, y^c \qquad \text{....(2-10)}$$

where

V = mean flow velocity

y = flow depth

a, b, and c = coefficients determined by means of regression analysis

The regression coefficients are determined either from field data or by generating data using the Meyer-Peter and Müller formula and Einstein's bed-load function for bed-load and suspended-load discharges, respectively. The model does not take into account changes in bed-material composition.

5. Numerical Scheme:

KUWASER first solves (2-7) and (2-9) for a spatially-varied, steady flow by means of the first order Newton-Raphson method. Equations (2-7) and (2-9) are combined to yield the following expression for the sole unknown, flow depth at section 2, D_2:

$$a_1 \frac{Q_2^2}{2g} D_2^{a_2} + D_2 - \frac{4\Delta x\, Q_2^2}{K_1^2 + 2K_1 a_3 D_2^{a_4} + a_5 D_2^{a_6}} + a_6 \frac{\alpha_1 V_1^2}{2g} + z_2 - H_1 = 0 \qquad \ldots.(2\text{-}11)$$

where

Q_2 = water discharge at section 2

K_1 = conveyance at section 1

z_2 = bed elevation at section 2

a_1, a_2, a_3, a_4, a_5, and a_6 = regression coefficients determined from field data

Note that effective depth and width, cross-section area, conveyance, and velocity-head correction factor are all expressed in terms of power functions of the thalweg flow depth, D. Once the backwater calculation is completed, sediment-transport rates at all cross sections are computed from (2-10). The

sediment routing is then made by a two-step finite-difference algorithm. The first step is to compute the change in sediment volume between two cross sections:

$$\Delta V_i = (Q_{s_{i+1}} - Q_{s_i} + q_{s\ell_i})\Delta t \qquad \ldots.(2\text{-}12)$$

The second step is determination of the change in cross-section area at each cross section. The model assumes that one-quarter of ΔV_i is deposited or eroded in the upstream half of the segment between sections i and i+1, while three-quarters of ΔV_{i-1} is deposited or eroded in the downstream half of the reach between sections i and i-1. Therefore, when $q_{s\ell}$ is neglected, (2-8) can be expressed as

$$\Delta A_{b_i} = \frac{1}{1-\lambda} \frac{\frac{3}{2} Q_{s_{i+1}} - Q_{s_i} - \frac{1}{2} Q_{s_{i-1}}}{\Delta x_{i-1} + \Delta x_i} \Delta t \qquad \ldots.(2\text{-}13)$$

Finally, the model distributes ΔA_{bi} over the cross section to determine the new channel geometry. The method used is to relate the bed-elevation change at a point to the local conveyance. The elevation change at the j-th vertical, Δz_j, is computed as follows:

$$\Delta z_j = \frac{k_\ell + k_{\ell+1}}{K_i} \frac{\Delta A_{b_i}}{y_{j+1} - y_{j-1}} \qquad \ldots.(2\text{-}14)$$

where

k_ℓ and $k_{\ell+1}$ = conveyances of the incremental areas to the right and left of the j-th vertical

y_{j+1} and y_{j-1} = lateral coordinates of the (j+1)st and (j-1)st verticals

K_i = total conveyance of the i-th cross section

6. Data Requirements:

KUWASER requires the following input data:

(1) Number of cross sections and individual reach lengths.

(2) Number of subdivided reaches.
(3) Locations of tributaries.
(4) Cross-section geometries of all sections.
(5) Manning's n at each section.
(6) Upstream and tributary inflow hydrographs and stage data for every time step.
(7) Sediment-transport coefficients.
(8) Characteristic parameters for each dam, including its discharge coefficient, width, and height.

7. Model Limitations and Applicability:

The use of KUWASER is limited to subcritical flows. The model does not predict channel armoring or two-dimensional flow effects. KUWASER cannot effectively model a river reach with extremely irregular channel grade and geometry, but has the capability to model the main stem and tributaries in an entire river system. KUWASER can simulate divided flows associated with bars, islands, or channel breaches. The model finds its best application in long-term degradation/aggradation analysis.

C. UUWSR (Uncoupled, Unsteady Water and Sediment Routing):

1. Developer: Tucci, Chen, and Simons (Colorado State Univeristy), 1979
2. Previous Applications:
   (1) Upper Mississippi and Lower Illinois Rivers (Simons, et al., 1975)
   (2) Upper Mississippi and Lower Chippewa Rivers (Simons & Chen, 1976 & 1977; Simons et al., 1979; Simons & Chen, 1979; Chen & Simons, 1980)
   (3) Lower Mississippi River (Simons & Chen, 1978)

3. Basic Concepts:

This model was developed for simulating one-dimensional, gradually-varied, unsteady, water and sediment flows in complicated river networks. The principal assumptions included in this model are as follows:

(1) The river channel is sufficiently straight and uniform that the one-dimensional flow approximation can be employed.

(2) Hydrostatic pressure prevails at any point in the channel, and the water-surface slope is small.

(3) The density of sediment-laden water is constant over the cross section.

(4) The resistance coefficient for the unsteady flow is assumed to be the same as that for a steady flow.

The following basic equations are employed:

(1) Flow-continuity equation:

$$\frac{\partial Q}{\partial x} + T\frac{\partial y}{\partial t} - q_\ell = 0 \qquad \text{....(2-15)}$$

(2) Sediment-continuity equation:

$$\frac{\partial Q_s}{\partial x} + (1 - \lambda)\frac{\partial A_d}{\partial t} - q_s = 0 \qquad \text{....(2-16)}$$

(3) Flow-momentum equation:

$$\frac{\partial Q}{\partial t} + \frac{\partial (\beta QV)}{\partial x} + gA\frac{\partial y}{\partial x} = \rho gA(S_o - S_f + D_\ell) \qquad \text{....(2-17)}$$

where

Q & Q_s = water and sediment discharges

$T = \partial A/\partial y$

y = flow depth

A = cross-section area for water

A_d = sediment volume deposited per unit channel length

$q_\ell = q_s + q_w$

q_s = lateral sediment inflow

q_w = lateral water inflow

λ = porosity of bed material

V = mean flow velocity

β = momentum correction factor

ρ = density of water

S_o = bed slope
S_f = friction slope
D_ℓ = dynamic contribution of lateral inflow ($q_\ell V_\ell / Ag$)

To solve these three equations for the three primary unknowns, Q, y, and A_d, other variables are expressed in terms of Q, y, and A_d.

4. Sediment-Transport Function:

The sediment discharge per unit width, q_s, is expressed by

$$q_s = a\, V^b\, y^c \qquad \ldots.(2\text{-}18)$$

where

V = mean flow velocity
y = flow depth
a, b, and c = coefficients determined by means of regression analysis

The regression coefficients are determined either from field data or by generating data using the Meyer-Peter and Muller formula and Einstein's bed-load function for bed-load and suspended-load discharges, respectively. Changes in bed-material composition are not taken into account.

5. Numerical Scheme:

UUWSR first solves (2-15) and (2-17) by a four-point, implicit, finite-difference scheme (unconditionally stable) assuming a fixed bed. The resulting flow information is used to compute the sediment-transport capacity by means of (2-18). Computed sediment discharges then are applied to the sediment-continuity equation, (2-16), to estimate the change in the cross-section area. Equation (2-16) is solved using an explicit, finite-difference approximation. Therefore, UUWSR is an uncoupled, unsteady, water- and sediment-routing model.

6. Data Requirements:

UWSR requires the following input data:

(1) Number of cross sections and individual reach lengths.
(2) Number of subreaches.
(3) Locations of tributaries.
(4) Cross-section geometries of all computational sections (arranged from upstream to downstream).
(5) Manning's roughness coefficient at each cross section.
(6) Boundary conditions specified by either a discharge hydrograph, or a stage hydrograph, or a stage-discharge rating curve.
(7) Sediment-transport function.
(8) Characteristic parameters for each dam, including its discharge coefficient, width, and height.

7. Model Limitations and Applicability:

The use of UUWSR is limited to a modeling reach for which the one-dimensional flow approximation and steady-state solutions at confluences and dams are applicable. However, the model can simulate, with minimal computer cost, a complex river-network system in which islands, branches, meander loops, and tributaries are connected to the main channel. The model can also simulate effects of hydraulic structures such as dikes, locks and dams, etc. The capability of unsteady flow routing of this model enables users to simulate the flood-wave movement in a long reach.

D. HEC-6 (Hydrologic Engineering Center):

1. Developer: William A. Thomas (Hydrologic Engineering Center, Corps of Engineers), 1977

2. Previous Applications:

(1) Atchafalaya River Basin, Louisiana (Jennings & Land, 1977)
(2) Clearwater River, Idaho (Williams, 1977)
(3) Boise River, Idaho (Thomas & Prasuhn, 1977)
(4) San Lorenzo River (Jones-Tillson & Associates, 1980)
(5) Mississippi River (Nakato & Vadnal, 1981)

(6) Cottonwood Creek (Prasuhn & Sing, 1981)

3. Basic Concepts:

The model was developed to analyze scour and deposition of movable-bed channels by simulating one-dimensional, steady, gradually-varied water and sediment flows. The principal assumptions employed in the model are as follows:

(1) Flow is one dimensional and hydrostatic pressure prevails at any point in the channel.
(2) Manning's n is applicable to gradually-varied flow and is expressed as a function of either water-surface elevation or water discharge (the model incorporates indirectly the roughness effects of changes in bed forms).
(3) The entire movable-bed portion of a cross section is scoured or deposited at the same rate.
(4) Channel slope is small.

The following basic equations are employed in the model:

(1) Flow-continuity equation:

$$\frac{dQ}{dx} = q_\ell \quad \ldots.(2\text{-}18)$$

(2) Sediment-continuity equation:

$$\frac{\partial G}{\partial x} + B\frac{\partial y}{\partial t} = 0 \quad \ldots.(2\text{-}19)$$

(3) Flow-energy equation:

$$(h + \frac{\alpha Q^2}{2gA^2})_{k-1} = (h + \frac{\alpha Q^2}{2gA^2})_k + H_L \quad \ldots.(2\text{-}20)$$

where

Q = water discharge

q_ℓ = lateral water inflow per unit width
G = volumetric sediment-transport rate
B = movable-bed width
y = movable-bed elevation
h = water-surface elevation
α = velocity-head correction factor
A = cross-section area
H_L = head loss between sections k-1 and k

4. Sediment-Transport Function:

Five options are available for computing bed-material transport rates: Laursen's relationship, as modified by Madden for large rivers (Laursen, 1958); Toffaleti's formula (Toffaleti, 1968); Yang's stream-power formula (Yang, 1973); DuBoys' formula (Brown, 1950); and a special relationship between unit-width sediment-transport capacity and the product of flow depth and energy slope which is developed for a particular river reach.

Laursen's relationship is expressed by

$$q_s = 283.39\, q \sum_i p_i (d_{si}/D)^{7/6} (\tau_0'/\tau_{ci} - 1) \qquad \ldots.(2\text{-}21)$$

where

q_s = bed-material transport rate per unit width
q = water discharge per unit width
p_i = fraction by weight of the i-th fraction of the bed sediment with mean size, d_{si}
D = flow depth
τ_0' = Laursen's bed-shear stress due to grain roughness
$= \rho V^2/(58(d_{50}/D)^{1/3})$
d_{50} = median sediment size
V = mean flow velocity
τ_{ci} = critical shear stress for mean particle size, d_{si}

The second option, the Toffaleti formula, is based on Einstein's bed-load function and various empirical data and is expressed by

$$q_{si} = q_{sbi} + q_{ssLi} + q_{ssMi} + q_{ssUi} \quad \text{....(2-22)}$$

where

q_{si} = bed-material discharge for the i-th fraction of bed sediment
q_{sbi} = bed-load discharge for the i-th fraction of the bed sediment
q_{ssLi} = suspended-load discharge in lower zone
q_{ssMi} = suspended-load discharge in middle zone
q_{ssUi} = suspended-load discharge in upper zone

Detailed procedures for computation of q_{sbi}, q_{ssLi}, q_{ssMi}, and q_{ssUi} are given by Toffaleti (1966).

5. Numerical Scheme:

HEC-6 first solves the one-dimensional energy and continuity equations, (2-20) and (2-18), using an iterative, standard step-backwater method, to obtain basic hydraulic parameters such as depth, width, and slope at each section which are necessary to compute the sediment-transport capacity. Friction loss is calculated from Manning's equation with specified n values. A functional relationship between Manning's n and water discharge or flow stage can be used if available. Expansion and contraction losses are calculated using loss coefficients. The potential sediment-transport capacities at all cross sections are computed next, using one of the five optional sediment-transport functions. Note that the sediment discharge at the upstream boundary must be related to the water discharge by a rating table for different sediment-size fractions. Computations of sediment-transport capacity begin at the upstream boundary and move reach by reach to the downstream boundary. Equation (2-19) is then solved using an explicit, finite-difference scheme:

$$\frac{-(G_R - G_L)}{0.5(X_L + X_R)} + \frac{B(Y_{P'} - Y_P)}{\Delta t} = 0 \quad \text{....(2-23)}$$

or

$$Y_{P'} = Y_P + \frac{\Delta t}{0.5B}(G_R - G_L)/(X_L + X_R) \quad \text{....(2-24)}$$

where

G_R = volumetric sediment-transport rate at the (k+1)st cross section

G_L = volumetric sediment-transport rate at the (k-1)st cross section

$Y_{P'}$ = movable-bed thickness at the kth cross section at the time of $(j+1)\Delta t$

Y_P = movable-bed thickness at the kth cross section at the time of $j\Delta t$

X_L = reach length between (k-1)st and kth cross sections

X_R = reach length between kth and (k+1)st cross sections

Note that the transport capacity is calculated at the beginning of the time interval, and is not recalculated during that interval. However, the gradation of the bed material is recalculated during the time interval in order to account for armoring effects. An equilibrium water depth below which sediment with a particular grain size becomes immobile is introduced using Manning's equation, Strickler's equation, and Einstein's bed-load function:

$$D_{eq} = (q/(10.21d^{1/3}))^{6/7} \qquad \ldots.(2\text{-}25)$$

where

q = water discharge per unit width

d = sediment particle size

A zone of bed between the bed surface and the equilibrium depth is designated the active layer. When all material is removed from the layer, the bed is considered to be completely armored for that particular hydraulic condition. When a mixture of grain sizes is present, the equilibrium depth calculations utilize the given gradation curve to relate the quantity of each grain size present in the bed to the depth of scour. The armor layer formed by a previous discharge is tested for stability using Gessler's (1971) stability-analysis procedure. If Gessler's stability number is less than 0.65, the armor layer is treated as unstable and the bed-layer size distribution is computed for the next time step.

6. Data Requirements:

HEC-6 requires the following input data:

(1) Number of cross sections, individual reach lengths, and tributary locations.
(2) Geometric data on movable-bed portion of each cross section, thickness of movable bed, and bridges, and dredging information.
(3) Manning's roughness coefficient at each cross section.
(4) Data on sediment inflow, bed-material gradation, and sediment properties.
(5) Upstream and lateral inflow hydrographs, downstream boundary condition (stage-discharge curve or stage hydrograph), and water temperatures.

HEC-6 is a one-dimensional model with no provision for simulating the development of meanders or specifying a lateral distribution of the sediment-transport rate across the section. The entire movable-bed portions of the cross sections are assumed to aggrade or degrade uniformly. The model is not suitable for rapidly-changing flow conditions. The model can be applied to predict reservoir sedimentation, degradation of the stream bed downstream from a dam, and log-term trends of scour or deposition in a stream channel. The influence of dredging activity can also be simulated. The model can be run in the fixed-bed mode, similar to HEC-2, by removing all sediment-data cards.

E. FLUVIAL-11:

1. Developer: Chang and Hill (San Diego State University), 1976
2. Previous Applications:
   (1) San Dieguito River (Chang & Hill, 1976)
   (2) San Elijo Lagoon entrance channel (Chang & Hill, 1977)
   (3) San Diego River (Chang, 1982)

3. Basic Concepts:

FLUVIAL-11 was developed to simulate one-dimensional, unsteady,

gradually-varied water and sediment flows, as well as width changes, of erodible channels. The principal assumptions incorporated into this model are as follows:

(1) Flow is one dimensional, and hydrostatic pressure prevails at any point in the channel.
(2) Channel slope is small.
(3) The Manning equation and the sediment-transport formula are applicable to gradually-varied flow.
(4) Storage effect due to unsteady flow is negligible in the backwater computation.

The following basic equations are employed:

(1) Flow-continuity equation:

$$\frac{\partial Q}{\partial x} + \frac{\partial A}{\partial t} - q = 0 \qquad \text{....(2-26)}$$

(2) Sediment-continuity equation:

$$(1 - \lambda) \frac{\partial A_c}{\partial t} + \frac{\partial Q_s}{\partial x} - q_s = 0 \qquad \text{....(2-27)}$$

(3) Flow-momentum equation:

$$g \frac{\partial H}{\partial x} + \frac{1}{A} \frac{\partial Q}{\partial t} + \frac{1}{A} \frac{\partial}{\partial x} \left(\frac{Q^2}{A}\right) + gS - \frac{Q}{A^2} q = 0 \qquad \text{....(2-28)}$$

where

Q & Q_s = water and sediment discharges
A = cross-section area of flow
A_c = channel cross-section area within some reference frame
q = lateral water inflow
q_s = lateral sediment inflow
H = water-surface elevation
S = energy slope
λ = porosity of bed material

Equations (2-26) and (2-28) are solved for two unknowns, Q and H, by an iterative method. Note, however, that in this NRC study, a simpler method of computing the water-surface profile, using the energy equation, was utilized instead of solving the unsteady equations, (2-26) and (2-28). A standard step method similar to that incorporated into HEC-2 was utilized in solving the energy equation.

4. Sediment-Transport Equation:

The following formula developed by Graf (1968) was used to compute the bed-material discharge for the San Dieguito River and the Salt River:

$$\overline{C}VR/((s_s - 1)gd^{1/3})^{1/2} = 10.39((s_s-1)d/(SR))^{-2.52} \quad \ldots.(2\text{-}29)$$

where

$\overline{C}$ = mean volumetric concentration of bed-material sediment
s_s = ratio of sediment specific weight to water specific weight
d = median sediment size
S = energy slope
V = mean flow velocity
R = hydraulic radius

The Engelund-Hansen formula (1967) was used for the San Lorenzo River to compute the total-load discharge:

$$q_T = 0.05\gamma_s V^2 (d/g(\gamma_s/\gamma - 1))^{1/2} (\rho u_*^2/(\gamma_s - \gamma)d^{3/2} \quad \ldots.(2\text{-}30)$$

where

q_T = total-load discharge per unit width
γ_s = specific weight of sediment
γ = specific weight of water
u_* = shear velocity
ρ = density of water

5. Numerical Scheme:

FLUVIAL-11 first solves the water-continuity equation, (2-26), and momentum equation, (2-28), by an iterative, four-point, implicit, finite-difference scheme developed by Amein and Chu (1975). The flow information is next used to compute the sediment-transport rate from either (2-29) or (2-30). The sediment-continuity equation, (2-27), is then solved to obtain ΔA_c in the following way: from (2-27)

$$\Delta A_c = -\frac{\Delta t}{1-\lambda}\left(\frac{\partial Q_s}{\partial x} - q_s\right) \qquad \ldots.(2\text{-}31)$$

$$q_{s_i} = \frac{1}{2}\left(q_{s_i}^{j} + q_{s_i}^{j+1}\right) \qquad \ldots.(2\text{-}32)$$

$$\left(\frac{\partial Q_s}{\partial x}\right)_i = \frac{1}{\Delta x_{i-1}}\left[\frac{Q_{s_i}^{j} + Q_{s_i}^{j+1}}{2} - \frac{Q_{s_{i-1}}^{j} + Q_{s_{i-1}}^{j+1}}{2}\right] \qquad \ldots.(2\text{-}33)$$

$$(\Delta A_c)_i = \frac{\Delta t}{1-\lambda}\left[\frac{Q_{s_{i-1}}^{j} + Q_{s_{i-1}}^{j+1} - Q_{s_i}^{j} - Q_{s_i}^{j+1}}{2\Delta x_{i-1}} + \frac{q_{s_i}^{j} + q_{s_i}^{j+1}}{2}\right] \qquad \ldots.(2\text{-}34)$$

Note that a backward-difference scheme was used in x and a forward-difference scheme was used in t. The quantity ΔA_c obtained from (2-34) is then corrected for the following effects:

(1) Adjustment in channel width:
Width adjustments are made in such a way that the spatial variation in power expenditure per unit channel length (γQS) is reduced along the channel. The width is adjusted until the value which gives minimum total stream power (integration of γQS over the reach length) at each time step is found. To determine the width change at each section, the actual energy gradient at this section S_i is compared with the weighted, average energy gradient $\overline{S}_i$ of its adjacent sections given by

$$\overline{S}_i = (S_{i-1}\Delta X_i + S_{i+1}\Delta X_{i-1})/(2(\Delta X_{i-1} + \Delta X_i))$$

If S_i is greater than $\overline{S}_i$, the channel width is reduced so as to decrease S_i, and vice versa. The new channel width is determined by a trial and error technique. Width changes are subject to the physical constraints of rigid banks or the angle of repose of the bank material.

(2) Adjustment in cross-section profile:
Deposition at an aggrading section is assumed to start from the lowest point and to build up the bed in horizontal layers. At a degrading section, the change in cross-section area is distributed in proportion to the local tractive force. These types of adjustment reduce the spatial variation in power expenditure along the channel.

(3) Lateral channel migration:
The model solves the sediment-continuity equation in the transverse direction:

$$(1 - \lambda)\frac{\partial z}{\partial t} + \frac{\partial q_s'}{\partial y} = 0 \qquad \ldots.(2\text{-}35)$$

where

q_s' = $q_s \tan \beta$ = transverse sediment-transport rate per unit width

β = $\tan^{-1}(11D/r)$ = angle deviation of transverse flow from the direction tangent to the centerline of a bend given by Rozovskii(1957)

D = mean flow depth

r = radius of curvature of the bend

z = bed elevation

Using a forward-difference scheme in y, Δz_k is obtained from

$$\Delta z_k = -\frac{\Delta t}{1-\lambda}\frac{q_{s_{k+1}}' - q_{s_k}'}{\Delta y_k} \qquad \ldots.(2\text{-}36)$$

where

Δy_k = transverse distance between points k and k+1

6. Data Requirements:

FLUVIAL-11 requires the following input data:

(1) Number of cross sections and individual reach lengths.
(2) Tributary locations.
(3) Flood hydrographs for main and tributary streams.
(4) Downstream boundary conditions.
(5) Cross-section geometries of all computational sections and Manning's n at each cross section.
(6) Initial bed-material sediment compositions for the upstream and downstream ends. Sediment compositions at intermediate cross sections are computed using an exponential decay relationship.
(7) Description of channel bends, if any, by their radii of curvature.

7. Model Limitations and Applicability

The use of FLUVIAL-11 is limited to a modeling reach for which the one-dimensional flow approximation is applicable. However, the model can predict changes in erodible channel width, changes in channel-bed profile, and lateral migration of a channel in bends.

F. SEDIMENT-4H:

1. Developer: Ranjan Ariathurai (Resource Management Associates), 1977

2. Previous Applications:

(1) The Osage River, Missouri (Ariathurai, 1980)

3. Basic Concepts:

The model was developed for simulating two-dimensional, gradually-varied, unsteady, water and sediment flows. The model utilized in the present study, however, is a one-dimensional version of SEDIMENT-4H. The principal assumptions employed in this model are as follows:

(1) Flow is one dimensional and hydrostatic pressure prevails at any point in the channel.

(2) Similarity of both velocity and suspended-sediment concentration profiles in a vertical at all locations in the flow field is assumed.

(3) The resistance coefficient for the unsteady flow is the same as that for a steady flow.

(4) Channel slope is small.

The following basic equations are employed:

(1) Flow-continuity equation:

$$\frac{\partial h}{\partial t} = \frac{1}{b}\frac{\partial q}{\partial x} \pm s \qquad \text{....(2-37)}$$

(2) Sediment-continuity equation:

$$\frac{\partial C}{\partial t} + u_{\alpha s}\frac{\partial C}{\partial x} = \frac{\partial}{\partial x}\left(D_x \frac{\partial C}{\partial x}\right) + S \qquad \text{....(2-38)}$$

(3) Flow-momentum equation:

$$\frac{\partial \bar{u}}{\partial t} + u\frac{\partial \bar{u}}{\partial x} + g\frac{\partial h}{\partial x} + gS_e = 0 \qquad \text{....(2-39)}$$

where

h = water-surface elevation

b = mean channel width

q = inflow rate to a node

s = lateral inflow or outflow rate

C = mass concentration

$u_{\alpha s}$ = longitudinal component of sediment-particle velocity

D_x = turbulent mass diffusivity in the logitudinal direction

S = source/sink term produced by scour or deposition

$\bar{u}$ = mean flow velocity

S_e = friction slope

4. Sediment-Transport Function:

SEDIMENT-4H calculates total-load sediment discharge for an idealized, single, median grain size. The basic concept is similar to Einstein's bed-load function; however, in SEDIMENT-4H the sediment concentration in the bed layer is set to a maximum and is assumed to be transported at the local mass-weighted velocity. The concentration of sediment in the bed layer is assumed to be dependent on the amount of sediment in suspension, but not to exceed 100 lbs/cu ft.

The Rouse (1937) equation for the vertical distribution of suspended-sediment concentration in a fully-developed, turbulent flow is normalized by the depth-averaged sediment concentration, $\langle C \rangle$, and the concentration distribution is expressed in dimensionless terms by

$$\Phi(\lambda) = \Phi_{\Delta}(\Delta(1/\lambda - 1)/(1 - \Delta))^{\xi};\ \lambda > \Delta \qquad \ldots.(2\text{-}40)$$

and

$$\Phi(\lambda) = \Phi_{\Delta} \quad ;\ \lambda < \Delta \qquad \ldots.(2\text{-}41)$$

where

λ = y/d
d = flow depth
$\Phi(\lambda)$ = $C(y)/\langle C \rangle$
Δ = a/d (nondimensional sublayer thickness)
a = reference level where C is given
ξ = $V_s/\kappa U_*$
V_s = sediment fall velocity
κ = von Karman's constant
U_* = shear velocity

The sediment concentration in the sublayer, Φ_{Δ}, is obtained from the following relation:

$$\int_0^1 \Phi(\lambda)\, d\lambda = 1 \qquad \ldots.(2\text{-}41)$$

Therefore,

$$\Phi_{\Delta} = 1/\ (\Delta + \int_{0}^{1} (\Delta(1/\lambda - 1)/(1 - \Delta))^{\xi} d\lambda \qquad \ldots.(2\text{-}42)$$

A logarithmic-type vertical velocity distribution in normalized form is utilized:

$$\Psi = \Psi_{*}(\frac{1}{\kappa} \ell n(\lambda/\gamma) + a_r) \qquad \ldots.(2\text{-}43)$$

where

Ψ = $u/\langle U \rangle$

u = local streamwise velocity

$\langle U \rangle$ = depth-averaged streamwise velocity

Ψ_{*} = $U_{*}/\langle U \rangle$

γ = k_s/d

k_s = equivalent roughness height

Finally, depth-averaged, sediment-particle velocity, $\langle U_s \rangle$, is expressed as

$$\langle U_s \rangle = \langle U \rangle \int_{0}^{1} \beta \Phi \Psi \, d\lambda \qquad \ldots.(2\text{-}44)$$

where

$\beta(\lambda)$ = proportionality coefficient to relate sediment particle velocity, $U_s(y)$, to the mass-weighted fluid velocity, $U(y)$, such that $U_s = \beta U(y)$

Empirical formulas for the rate of scour during stream-bed erosion, E, and the rate of deposition, D, are expressed by

$$E = M(\tau/\tau_{ce} - 1)(C_{max}-C_b)/C_{max} \ ; \ \tau > \tau_{ce} \qquad \ldots.(2\text{-}45)$$

and

$$D = - V_s C_b (1 - \tau/\tau_{cd}) \ ; \ \tau < \tau_{cd} \qquad \ldots.(2\text{-}46)$$

where

M = erosion-rate constant

τ = bed shear stress

τ_{ce} = critical shear stress for erosion
τ_{cd} = critical shear stress for deposition
C_b = sediment concentration in bed layer
C_{max} = maximum concentration in bed layer

5. Numerical Scheme:

The Link-Node Hydrodynamic model first solves (2-37) and (2-39), which yield the depth-averaged mass-velocity component, u_α, and flow depth. The depth-averaged sediment-particle velocity, $\langle U_s \rangle$, then is calculated from (2-44). The convective-diffusion equation, (2-38), is next solved using the finite-element method with isoparametric, quadrilateral elements. Time marching is effected by a two-point implicit scheme. At each time step, the model provides the average sediment concentration at every computational node point and the cross-section bed profile. Note that (2-45) and (2-46) are used to determine the source/sink term, S, in (2-38).

6. Data Requirements:

SEDIMENT-4H requires the following input data:

(1) Number of cross sections.
(2) Initial cross-section geometries of all cross sections.
(3) Manning's n at each cross section.
(4) Downstream stage hydrograph.
(5) Bed-material characteristics: median size, fall velocity, critical shear stress, maximum permissible concentration in bed layer, bed-strata data, and initial suspended-sediment concentration.
(6) Diffusion coefficient in the longitudinal direction.
(7) Upstream sediment boundary condition: suspended-sediment concentration specified as a function of time.

7. Model Limitations and Applicability:

SEDIMENT-4H considers only a single sediment-particle size. Suspended-sediment particles are assumed to be convected at the local water-flow

velocities except in the vertical direction, in which the particles are allowed to settle due to the gravity effect. This assumption becomes invalid when the sediment is transported primarily in the bed-load mode, in which velocities of sediment particles and flow are significantly different. The two-dimensional version of the model is applicable to highly unsteady flow over a river bed composed of fine sediment in which the transverse velocity and concentration profiles vary significantly.

III. DESCRIPTION OF STUDY RIVERS

A. Study Rivers. The study rivers were selected on the basis of the following three criteria. First, the Federal Emergency Management Agency (FEMA) requested that rivers be selected which historically have experienced flash-flood type events with appreciable river-bed changes and channel migration during floods. Such rivers are found typically in the western United States. Second, the Committee Members wanted to include two different types of rivers: those which are characterized by stable, confined channels; and those which have unstable, disturbed channels. Third, and most importantly, it was necessary that adequate input information on the study rivers be available for testing the different numerical models. The input data generally had to satisfy the requirements of the individual numerical models, as set forth in Chapter II. In the search for appropriate study rivers which satisfy these conditions, various regional FEMA offices were contacted, including Denton, Texas; Bothell, Washington; San Francisco, California; and Denver, Colorado. After reviewing the recommended rivers, the San Lorenzo River (SLR), the San Dieguito River (SDR), and the Salt River (SR) were selected by the Committee. Note that these rivers had been previously investigated using movable-bed numerical models by Corps of Engineers (COE), San Diego State University (SDSU), and Simons, Li & Associates (SLA), respectively. Among these three rivers, SLR is a channelized, stable, sand-bed river; SDR is characterized by an unstable, disturbed, sand-bed channel conditions; and SR is an unstable, gravel-bed river. Other characteristics of these rivers are as follows:

1. San Lorenzo River. The San Lorenzo River is located in Santa Cruz County in northern California, and meets the Pacific Ocean at the northern end of Monterey Bay in the City of Santa Cruz, as shown in figure 1. SLR historically has flooded frequently and caused substantial flood damage to the City of Santa Cruz before the COE's flood-control project, which included a leveed channel, was completed in 1959. Since completion of the project, sediment has accumulated in the channel, resulting in a loss of channel capacity. A photograph of the river supplied by COE, San Francisco District, taken upstream of the Water Street Bridge looking downstream, is shown in

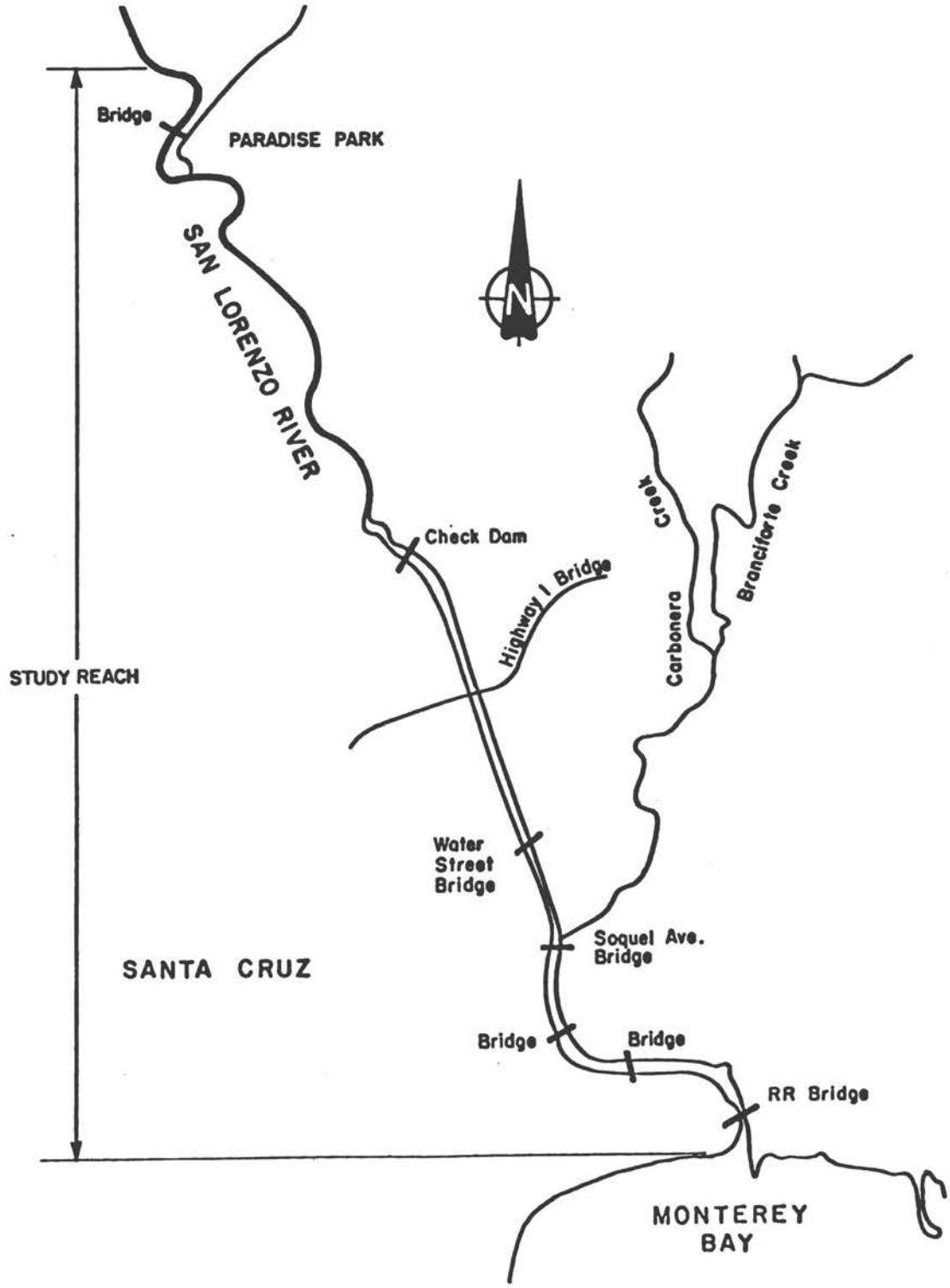

Figure 1 Map showing San Lorenzo River study reach

figure 2. The northern portion of the watershed has steep slopes and unstable rock structures with high landslide susceptibility. The southern portion has relatively low erosion potential, due to dense vegetation cover and stable granitic soils. The southeastern part is covered by loose, sandy soils with high erosion potential.

2. San Diequito River. The San Dieguito River flows through San Diego County in southern California, and flows through the City of Del Mar into the Pacific Ocean. The approximately 2-mi long study reach, delineated in figure 3, was innundated by recent floods, including those of March 1978 and February 1980. The reach shown in the figure is approximately 4 mi from the Pacific Ocean and 5 mi below Lake Hodges Dam, which was constructed in 1918. The drainage area above Lake Hodges is about 300 sq mi. During the 15 March 1978 flood, a peak flow of 4,400 cfs was recorded downstream from the reservoir. An estimated peak reservoir outflow of 22,000 cfs, corresponding to a 40-yr flood, was recorded during the 21 February 1980 flood. The SDR channel has a wide, flat cross section with highly erodible banks, as can be seen in figure 4, an aerial photograph taken above the Via de Santa Fe Road Bridge during the 21 February 1980 flood. This photograph was supplied by San Diego County Flood Control District through Dr. Howard Chang of SDSU. The river channel had been disturbed prior to the 1978 and 1980 floods by sand-mining activities and construction of the Via de Santa Fe Road and its SDR bridge. Several large borrow pits, with depths up to 25 ft, were produced by sand-mining operations. Although these borrows were partially refilled after the 1978 flood, major borrow-pit aggradation took place during the 1980 flood. The channel bed is composed of primarily sand-range materials.

3. Salt River. The Salt River is located in Maracopa County, Arizona, and flows from Granite Reef Dam to the confluence with the Gila River. A reach of the river through the City of Phoenix has drawn the most attention because recent development within the flood plain has resulted in recurrent damage to structures and facilities. SR experienced four major floods in three years between 1978 and 1980 (March 1978, peak flow = 99,000 cfs; December 1978, peak flow = 112,000 cfs; January 1979, peak flow = 73,500 cfs; and February 1980, peak flow = 185,000 cfs) which produced extensive damage to the Sky Harbor

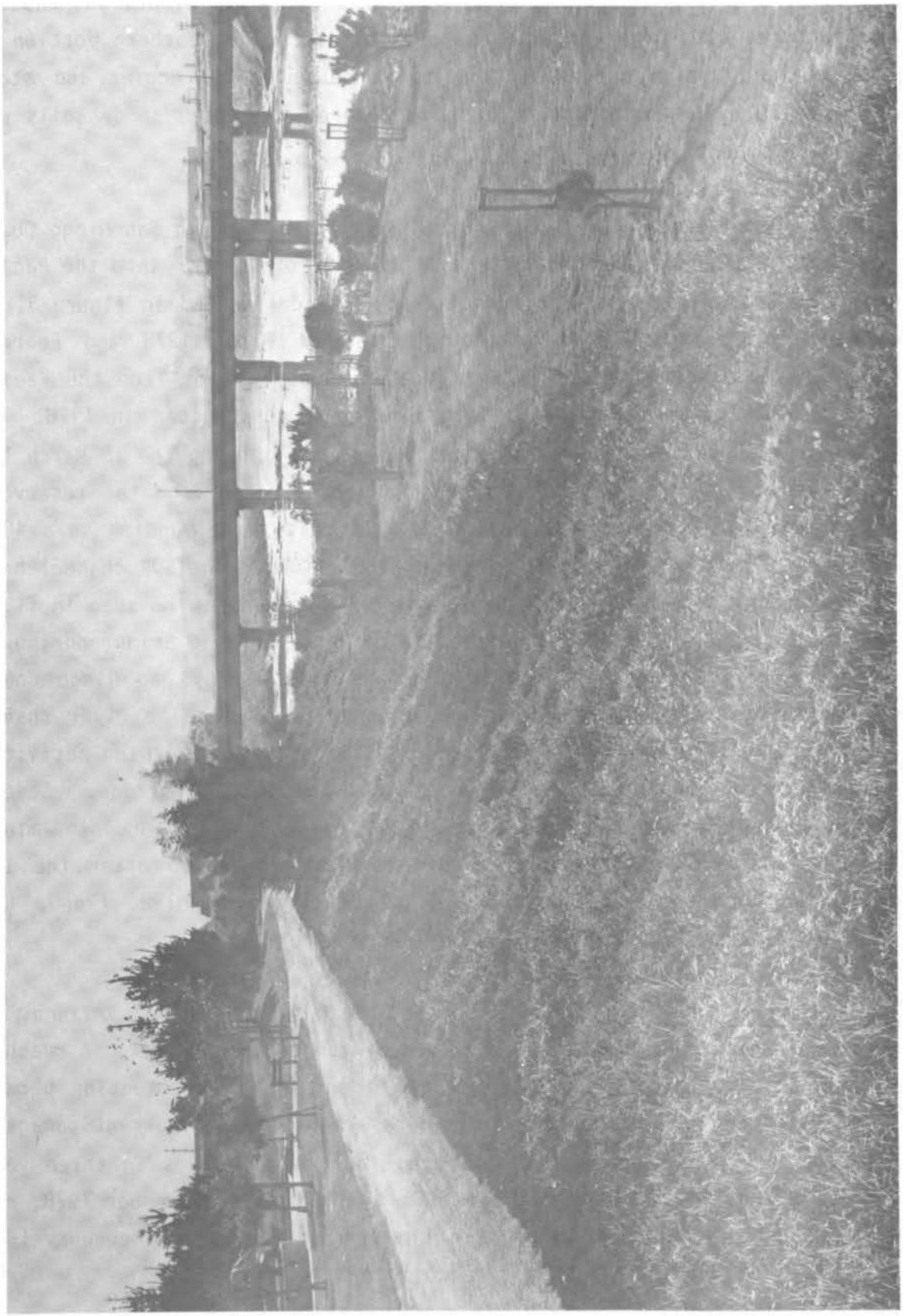

Figure 2 Photograph showing the San Lorenzo River

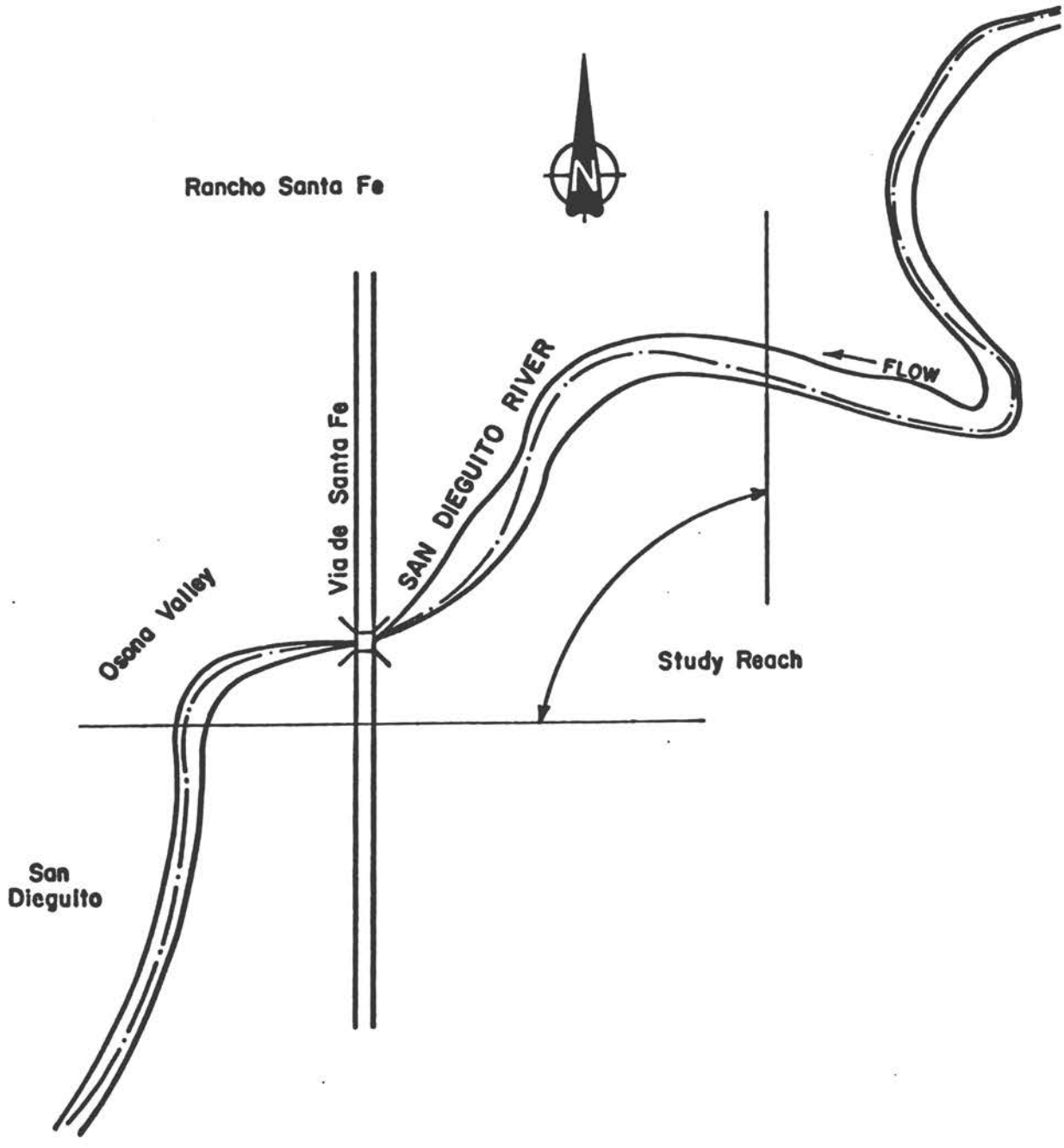

Figure 3 San Dieguito River study reach

Figure 4 Photograph showing the San Dieguito River

Airport facilities as well as to the streets and bridges in the vicinity. In order to mitigate future flood damage, and to become eligible for federal assistance to compensate for previous flood losses, the City of Phoenix proposed channelization of SR from just downstream of the I-10 Bridge to the Hohokam Expressway, as shown in figure 5. A photograph of SR taken near the Sky Harbor International Airport and supplied by SLA is shown in figure 6. The bed material is composed primarily of gravel with a median diameter of about 64 mm. There are many gravel-mining operations currently (1982) underway within the proposed channelization area.

B. Summaries of Input Data. A brief description of the input data utilized in this study is given in this section. Detailed input data are on file at the Iowa Institute of Hydraulic Research, The University of Iowa, Iowa City, Iowa, and are available through the Institute's library.

1. San Lorenzo River. Input data used previously by Jones-Tillson & Associates, et al. in 1980 were furnished by COE, San Francisco District, in HEC-6 format. The approximately 4.7-mi long study reach consists of two different subreaches: the upper half is approximately 2.3 mi long and is relatively steep; and the lower half, which is approximately 2.4 mi long, has a much smaller slope. Data on 38 cross sections with subreach length varying between 150 ft and 770 ft were supplied. Input hydrographs for the February 16-20, 1980 flood, with a peak flow of 12,800 cfs, are shown in figure 7, and the downstream boundary condition, which reflects tidal effects, is shown in figure 8. Pre-flood channel cross-section profiles were coded in HEC-6 format. Suspended-sediment discharge rating curves by particle sizes constructed from United States Geological Survey (USGS) data collected at Big Trees Gauging Station, which is 7 mi upstream of the study reach, were supplied to the modelers. Bed-material composition data were also coded in HEC-6 format. The median bed-material size in the study reach varied from 0.34 mm at the downstream end to 0.93 mm at the upstream end of the study reach.

2. San Dieguito River. Input data were provided by Dr. Howard Chang of SDSU and San Diego County, California. Twenty-one detailed cross sections based on

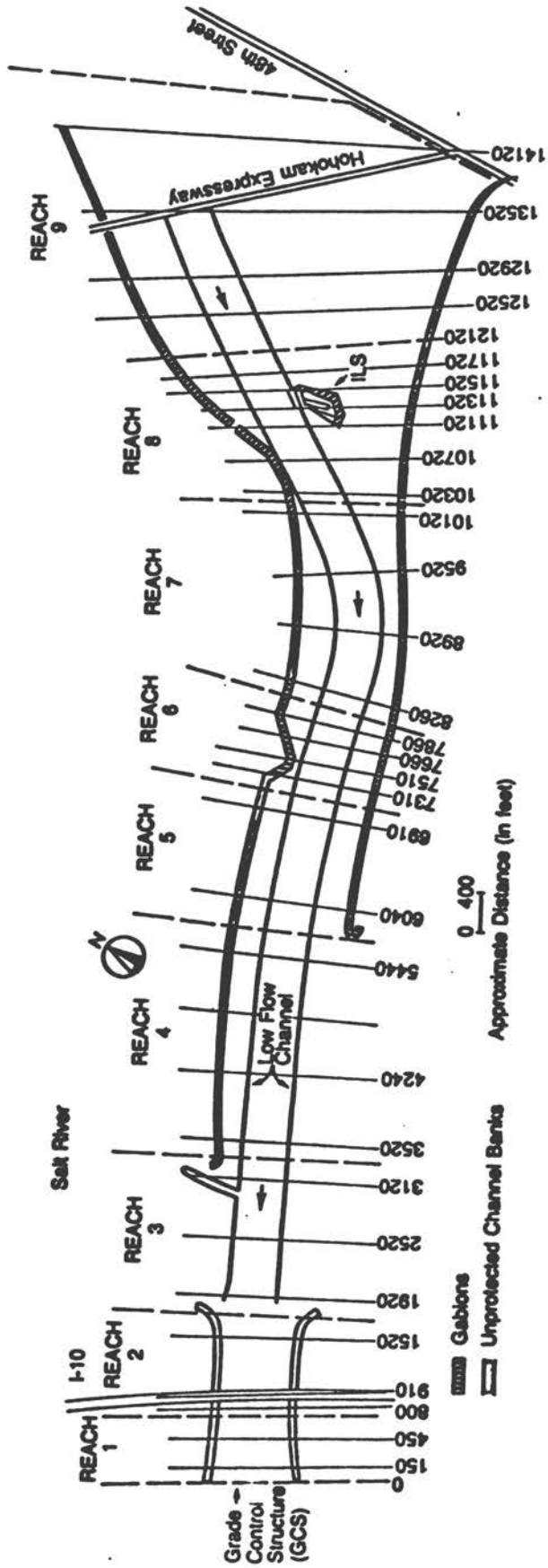

Figure 5 Salt River study reach

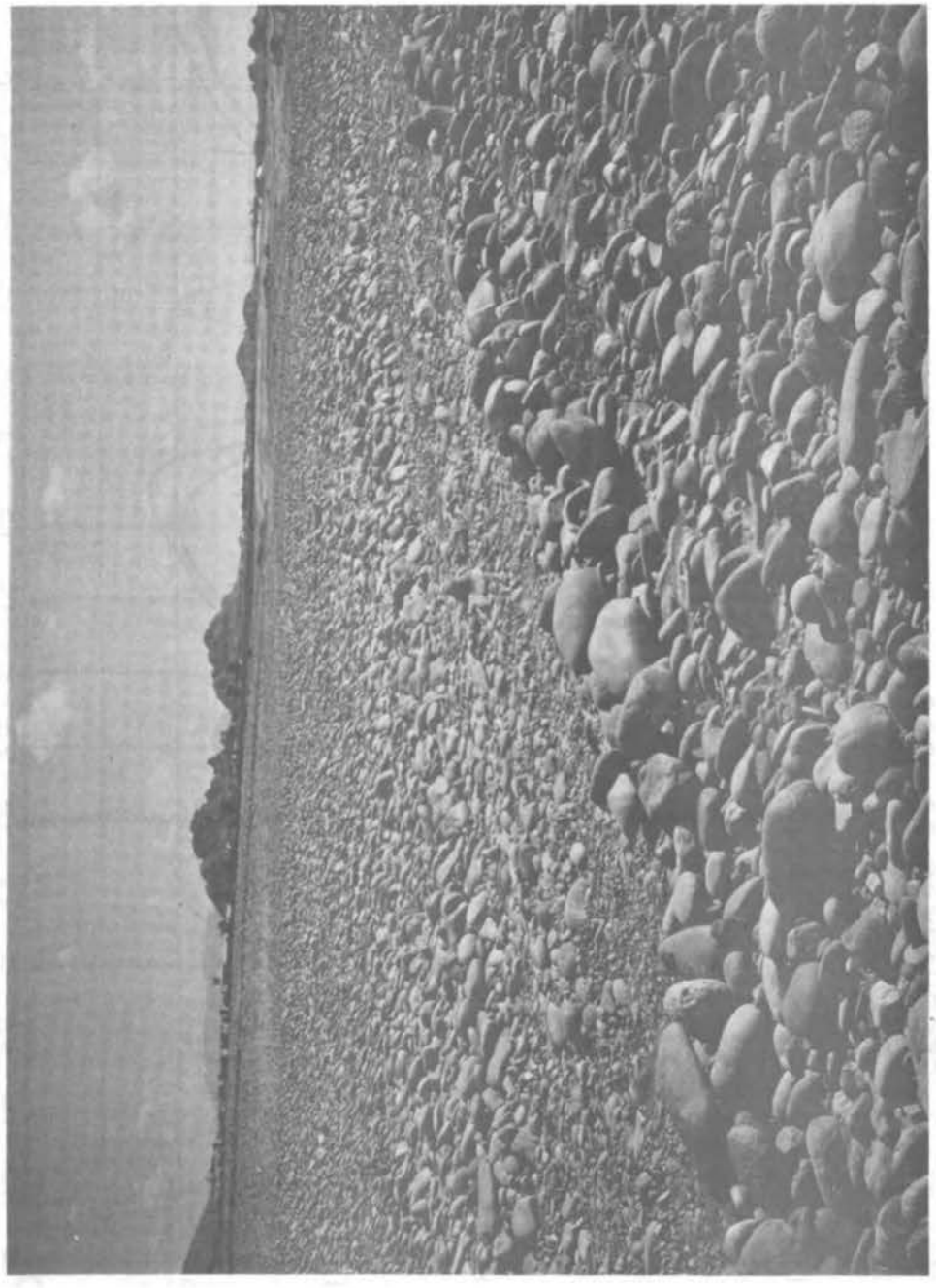

Figure 6 Photograph showing the Salt River

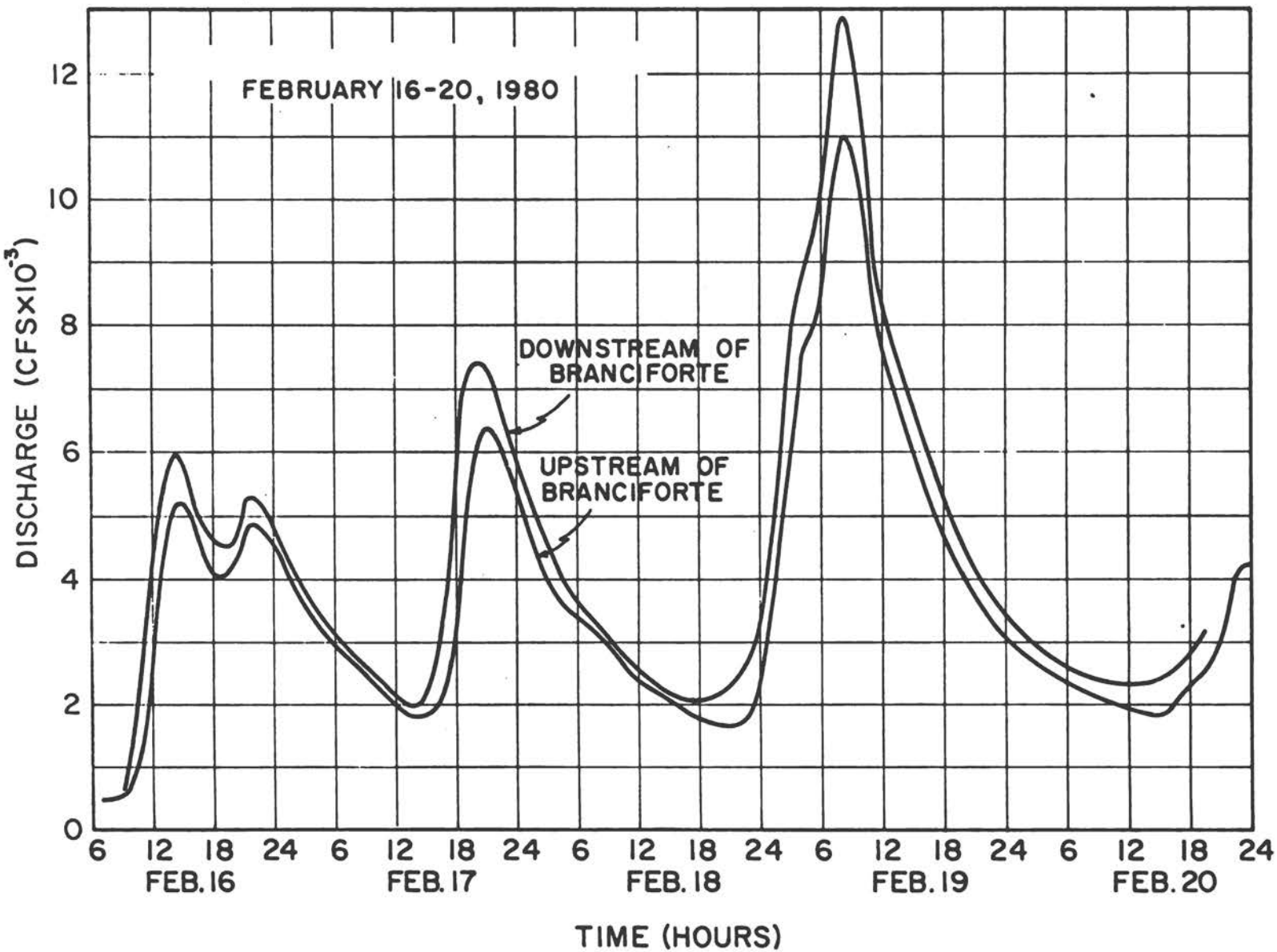

Figure 7 San Lorenzo River hydrographs

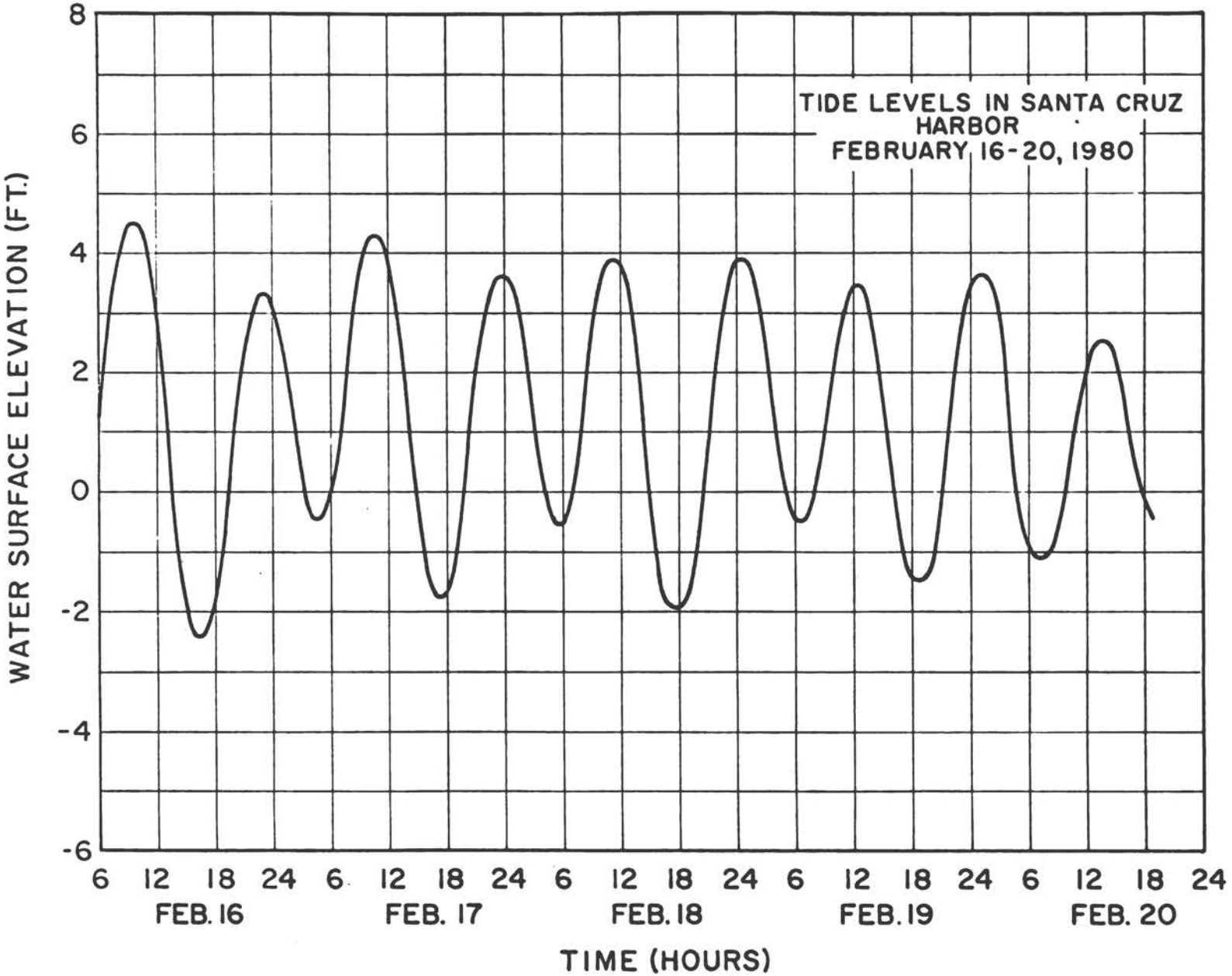

Figure 8 Stage hydrograph at the downstream boundary for the San Lorenzo River

the 1973 survey by San Diego County for the 1.9-mi long study reach were supplied in HEC-2 format. Input hydrographs at the upstream boundary, upstream from the Via de Santa Fe bridge, for the March 1978 and February 1980 floods with peak discharges of 4,400 cfs and 22,000 cfs, respectively, are shown in figure 9. The locations of the cross sections and pre-flood channel topography for the lower two-thirds of the study reach are presented in figure 10. No sediment-transport rating curve was available. Bed-material data were provided for only Sections 44 and 59; the median bed-material sizes for the main channel and south overbank area at Section 44 were 0.46 mm and 0.25 mm, respectively; and those at Section 59 were 0.70 mm and 0.36 mm, respectively.

3. Salt River. All input information was provided by SLA. Channel profiles for 41 designed cross sections were furnished in HEC-2 format. The total reach length was 4.34 mi, and each reach length varied from 150 ft to 1,100 ft. The projected 100-year-flood hydrograph, with a peak discharge of 176,000 cfs and a flood duration of 10 days, is shown in figure 11. The lower and upper limits of the geometric mean size of bed material were 0.22 mm and 185.0 mm, respectively, and the median diameter for all sections was 64.0 mm. Downstream boundary conditions were given in two different modes: one assuming the critical depth at the I-10 drop structure (see figure 5); and another with the assumed stage-discharge relationship at the I-10 bridge. Both conditions are possible, depending on the degradation below the I-10 drop structure. Initially, the area is backfilled and the second boundary condition is valid; however, if degradation removes this material, the first, critical-depth boundary condition is valid. The SR study reach was previously investigated by Colorado State University (CSU), in 1980, using fixed-bed and movable-bed physical models and SLA's HEC2SR numerical model (Anderson-Nichols, 1980).

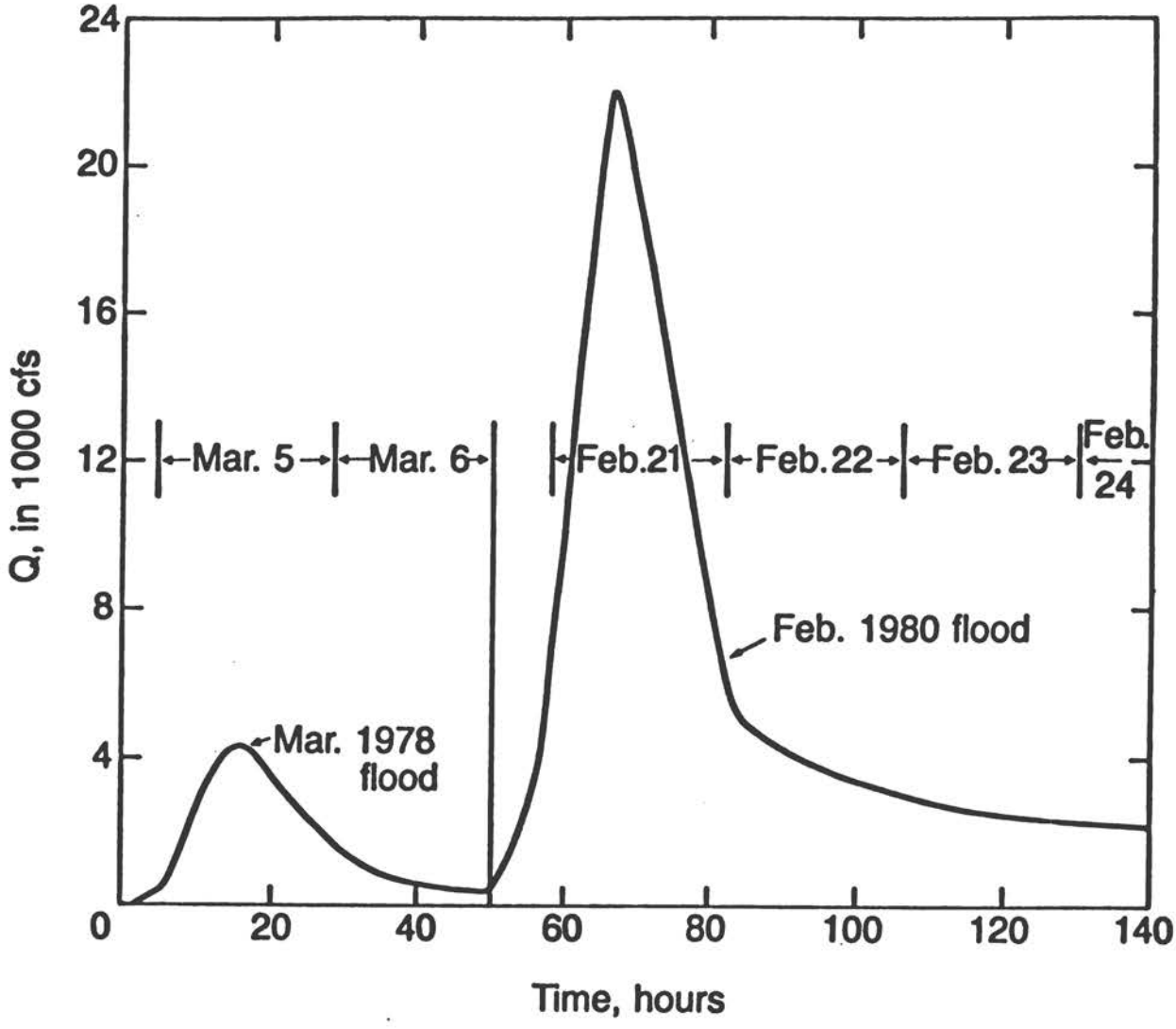

Figure 9 San Dieguito River hydrographs

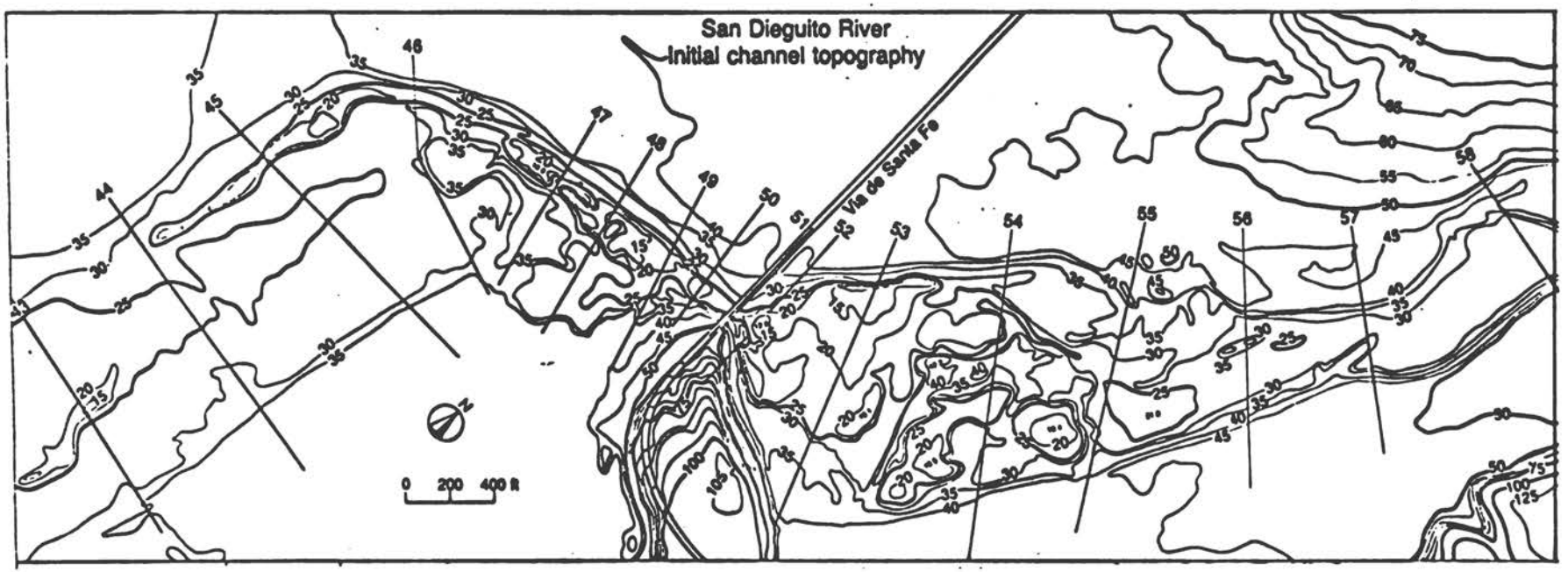

Figure 10 Topographic map of the San Dieguito River study reach

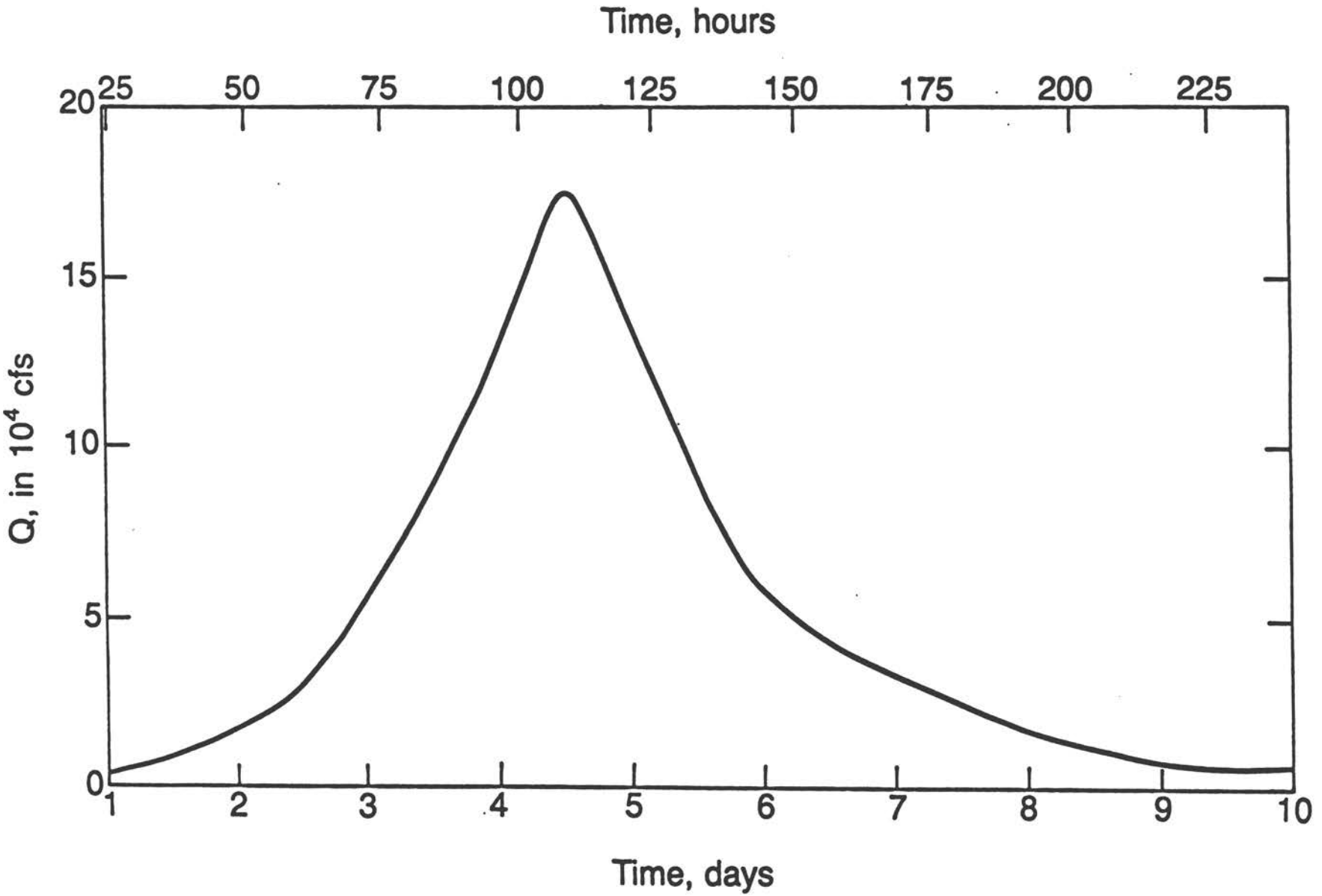

Figure 11 Salt River 100-year-flood hydrograph

IV. PRESENTATION AND DISCUSSION OF RESULTS

The input data summarized in Chapter III were sent to all modelers who participated in this project. A total of six models, the characteristics of which are summarized in Chapter II, was utilized. The models tested and the computational modes utilized for each of the three rivers (SLR, SDR, and SR) are summarized in table 1. It should be noted that the simulation of SR using HEC2SR was already developed in 1980 by SLA; these computational results were furnished to the Committee by SLA (SLA, 1980). All modelers submitted final reports describing their efforts and results (SLA, 1982; HEC, 1982; SDSU, 1982; and RMA, 1982), and also furnished computer outputs; these materials are on file at the Iowa Institute of Hydraulic Research Library. For this study, only the principal results were extracted from the vast computer-output listings, and were compiled in a uniform format to facilitate direct comparison. Each modeler was sent the summary tables based on his results to review for accuracy and correct interpretations. All numerical results presented in this chapter have been reviewed by the respective modelers. The figures included in this chapter were prepared on the basis of the reviewed output summaries. The principal results obtained from each simulation are summarized in the following sections.

1. San Lorenzo River. The principal results for a peak flow of 12,800 cfs computed using HEC2SR (SLA), HEC-6 (HEC), FLUVIAL-11 (SDSU), and SEDIMENT-4H (RMA) are tabulated in tables 2, 3, 4, and 5, respectively. In tables 4 and 5, the predicted water-surface elevations are shown for both movable-bed and fixed-bed simulations of FLUVIAL-11 and SEDIMENT-4H. Definitions of the symbols utilized are given in the individual tables. Thalweg and water-surface elevations at peak flow computed by the four movable-bed models are plotted together in figure 12, which also includes available field data on water-surface elevation between stations 1,150 ft and 10,150 ft (see table 6). The computed water-surface elevations are seen to agree with the measured values fairly well for all models over the lower half (roughly) of the study reach. However, computed elevations are seen to differ among the models over the upper part of the study reach. FLUVIAL-11 predictions are much higher than those of the other models; at a river distance of 18,258 ft, for example,

RIVER	MODEL	TESTED RIVER-BED CONDITIONS
SAN LORENZO (CALIFORNIA)	HEC2SR (SLA)	MOVABLE-BED & FIXED-BED*
	KUWASER (SLA)	MOVABLE-BED ONLY
	UUWSR (SLA)	MOVABLE-BED & FIXED-BED
	HEC-6 (HEC)	MOVABLE-BED & FIXED-BED**
	FLUVIAL-11 (SDSU)	MOVABLE-BED & FIXED-BED*
	SEDIMENT-4H (RMA)	MOVABLE-BED & FIXED-BED
SAN DIEGUITO (CALIFORNIA)	HEC2SR (SLA)	MOVABLE-BED & FIXED-BED*
	UUWSR (SLA)	MOVABLE-BED & FIXED-BED
	FLUVIAL-11 (SDSU)	MOVABLE-BED & FIXED-BED*
	SEDIMENT-4H (RMA)	MOVABLE-BED & FIXED-BED
SALT (ARIZONA)	HEC2SR (SLA)***	MOVABLE-BED & FIXED-BED*
	HEC-6 (HEC)	MOVABLE-BED & FIXED-BED**
	FLUVIAL-11 (SDSU)	MOVABLE-BED & FIXED-BED*
	SEDIMENT-4H (RMA)	MOVABLE-BED & FIXED-BED

* : HEC-2 (Fixed-bed model developed at HEC)
** : HEC-6 (Fixed-bed model) & HEC-2 (Fixed-bed model)
*** : Results were obtained from SLA's previous study in 1980.
SLA : Simons, Li & Associates, Inc.
HEC : Hydrologic Engineering Center
SDSU : San Diego State University
RMA : Resource Management Associates

Table 1 List of models and their computational modes

SAN LORENZO RIVER: HEC2SR

ID	X	Y0	YF	Y	H	W	Q	V	QB	QS	QT	D50
	FT	FT	FT	FT	FT	FT	CFS	FPS	T/D	T/D	T/D	MM
3	0	-4.5	-4.7	-4.7	1.6	246	12800	11.9	23160	221010	244170	0.47
4	558	-4.2	-4.4	-4.3	4.0	281	12800	8.1	23160	221010	244170	0.47
8	1183	-4.0	-4.2	-4.1	4.8	265	12800	7.9	23160	221010	244170	0.47
9	1700	-1.3	-1.4	-1.3	5.4	282	12800	7.3	23160	221010	244170	0.47
10	2200	-1.0	-1.6	-1.6	5.9	284	12800	6.6	17400	187810	205210	0.50
11	2600	-0.6	-1.2	-1.2	6.2	281	12800	6.8	17400	187810	205210	0.50
12	2800	-0.4	-1.1	-1.0	6.0	280	12800	9.2	17400	187810	205210	0.50
14	2950	-0.3	-1.1	-1.0	6.2	209	12800	9.2	17400	187810	205210	0.50
15	3575	0.2	-0.6	-0.5	7.6	235	12800	7.4	17400	187810	205210	0.50
19	4345	0.6	-0.2	-0.1	8.9	240	12800	6.6	17400	187810	205210	0.50
20	4955	1.4	1.9	1.8	9.6	237	12800	7.7	8160	145070	153230	0.58
21	5360	1.8	2.3	2.2	10.4	238	12800	7.3	8160	145070	153230	0.58
22	5610	2.0	2.3	2.3	11.3	340	12800	4.6	8160	145070	153230	0.58
25	6095	2.5	2.9	2.8	11.5	267	11000	5.2	8160	145070	153230	0.58
26	6745	3.0	4.1	3.9	11.9	226	11000	6.8	8160	160720	168880	0.41
27	7325	3.2	4.2	4.0	12.8	263	11000	5.9	8160	160720	168880	0.41
30	7575	3.4	4.4	4.2	13.1	237	11000	5.9	8160	160720	168880	0.41
31	8080	3.7	4.7	4.6	13.4	235	11000	6.0	8160	160720	168880	0.41
32	8585	4.1	6.2	5.9	13.6	229	11000	6.9	12610	195280	207890	0.35
33	9090	4.4	6.5	6.2	14.0	228	11000	6.9	12610	195280	207890	0.35
34	9595	4.8	6.9	6.6	14.4	226	11000	7.0	12610	195280	207890	0.35
35	9935	5.0	7.2	6.9	14.7	223	11000	7.1	12610	195280	207890	0.35
36	10140	5.2	5.5	5.4	14.7	172	11000	7.9	18020	252730	270750	0.64
38	10400	5.6	5.9	5.8	14.9	176	11000	8.1	18020	252730	270750	0.64
39	10780	6.4	6.7	6.6	15.4	175	11000	8.5	18020	252730	270750	0.64
40	11260	7.2	7.5	7.4	16.0	156	11000	9.5	18020	252730	270750	0.64
41	11800	8.2	10.4	10.0	17.0	171	11000	10.7	15910	256140	272050	0.51
42	12305	9.2	11.5	11.0	18.6	178	11000	9.5	15910	256140	272050	0.51
43	12645	9.8	12.3	11.8	19.1	153	11000	11.4	15910	256140	272050	0.51
46	14118	10.0	13.1	12.6	23.1	257	11000	6.7	15910	256140	272050	0.51
47	15308	12.8	12.4	12.5	24.3	221	11000	7.1	20600	314530	335130	1.50
48	16908	16.5	15.9	16.0	26.5	157	11000	13.2	20600	314530	335130	1.50
49	18258	20.6	20.1	20.2	32.2	204	11000	8.6	20600	314530	335130	1.50
50	19238	24.2	23.4	23.6	35.3	123	11000	14.2	20600	314530	335130	1.50
51	20578	29.8	30.8	30.8	41.7	107	11000	14.2	18130	301180	319310	0.64
52	21508	32.8	35.5	35.2	46.1	137	11000	10.8	18130	301180	319310	0.64
53	22968	35.7	35.7	35.7	49.1	145	11000	8.5	18260	306260	324520	1.25
54	24758	41.2	41.2	41.2	53.6	108	11000	15.0	18260	306260	324520	1.25

ID=SECTION I.D.
X =RIVER DISTANCE
Y0=INITIAL THALWEG EL
YF=FINAL THALWEG EL
Y =THALWEG EL AT PEAK FLOW
H =W.S. EL AT PEAK FLOW
W =TOP WIDTH AT PEAK FLOW

Q = WATER DISCHARGE AT PEAK FLOW
V = MEAN VELOCITY AT PEAK FLOW
QB = BED-LOAD DISCHARGE AT PEAK FLOW
QS = SUS-LOAD DISCHARGE AT PEAK FLOW
QT = TOTAL-LOAD DISCHARGE AT PEAK FLOW
D50= MEDIAN DIAMETER OF BED MATERIAL AT PEAK FLOW

Table 2 Principal results computed by HEC2SR for the San Lorenzo River

SAN LORENZO RIVER: HEC-6

ID	X	Y0	YF	Y	H	W	Q	V	QB	QS	QT	D50
	FT	FT	FT	FT	FT	FT	CFS	FPS	T/D	T/D	T/D	MM
3	0	-4.5	-4.6	-4.6	1.7	247	12800	12.0	74	46600	46680	0.71
4	558	-4.2	-3.7	-3.7	4.1	284	12800	8.4	203	41020	41230	0.70
8	1183	-4.0	-3.4	-3.4	5.0	258	12800	8.5	326	38630	38960	0.69
9	1700	-1.3	-0.7	-0.6	5.8	282	12800	7.7	489	38620	39110	0.66
10	2200	-1.0	-0.8	-0.7	6.4	284	12800	6.9	625	39730	40360	0.52
11	2600	-0.6	-0.7	-0.6	6.7	282	12800	7.0	197	41170	41370	0.56
12	2800	-0.4	-0.9	-0.8	6.7	202	12800	8.5	149	39390	39540	0.58
14	2950	-0.3	-1.3	-1.1	6.9	212	12800	8.2	115	37580	37700	0.60
15	3575	0.2	-0.9	-0.6	8.4	240	12800	6.7	69	36500	36570	0.61
19	4345	0.6	-0.7	-0.5	9.3	243	12800	6.1	92	30080	30180	0.65
20	4955	1.4	1.3	1.3	9.8	240	12800	7.0	72	17990	18060	1.17
21	5360	1.8	1.7	1.7	10.4	239	12800	6.9	52	16840	16890	1.18
22	5610	2.0	2.0	2.0	11.1	340	12800	4.5	74	16330	16400	1.23
25	6095	2.5	2.6	2.6	11.3	267	11000	5.2	112	13240	13350	1.08
26	6745	3.0	3.0	3.0	11.7	227	11000	6.3	84	12550	12640	1.21
27	7325	3.2	3.2	3.2	12.4	249	11000	5.7	91	11640	11730	1.34
30	7575	3.4	3.4	3.4	12.6	236	11000	5.7	176	10520	10700	1.30
31	8080	3.7	3.9	3.9	12.8	235	11000	5.9	293	9230	9520	1.48
32	8585	4.1	4.3	4.3	13.1	231	11000	6.1	280	9600	9880	1.44
33	9090	4.4	4.6	4.6	13.3	229	11000	6.2	259	9890	10150	1.43
34	9595	4.8	5.2	5.2	13.6	225	11000	6.6	244	10220	10460	1.38
35	9935	5.0	5.4	5.3	13.8	222	11000	6.6	44	9670	9720	1.37
36	10140	5.2	5.5	5.5	13.5	166	11000	9.4	41	10420	10460	1.73
38	10400	5.6	5.7	5.7	14.1	170	11000	9.1	46	9480	9520	1.76
39	10780	6.4	6.5	6.5	14.7	172	11000	9.1	43	9720	9770	1.75
40	11260	7.2	7.1	7.1	15.5	155	11000	9.7	47	9940	9980	1.86
41	11800	8.2	8.5	8.4	16.7	173	11000	8.9	43	9580	9630	1.72
42	12305	9.2	9.3	9.3	17.6	176	11000	8.7	42	10610	10650	1.77
43	12645	9.8	9.7	9.7	18.0	151	11000	10.1	43	11050	11100	1.86
46	14118	10.0	10.3	10.2	21.3	227	11000	7.7	33	10850	10880	1.66
47	15308	12.8	13.0	13.0	23.1	203	11000	8.9	31	14970	15000	1.74
48	16908	16.5	16.8	16.7	27.0	164	11000	12.3	29	17420	17450	1.76
49	18258	20.6	20.9	20.7	32.1	184	11000	9.8	23	20230	20260	1.77
50	19238	24.2	23.8	23.6	34.9	123	11000	14.2	27	20780	20810	2.02
51	20578	29.8	29.5	29.4	40.6	97	11000	13.4	24	18050	18070	1.93
52	21508	32.8	34.6	33.8	44.1	128	11000	11.1	18	18200	18210	1.45
53	22968	35.7	35.9	35.8	47.5	131	11000	10.3	20	34900	34920	1.75
54	24758	41.2	41.8	42.1	54.3	112	11000	14.6	15	51090	51110	1.54

ID=SECTION I.D.
X =RIVER DISTANCE
Y0=INITIAL THALWEG EL (T=0 HR)
YF=FINAL THALWEG EL (T=102 HR)
Y =THALWEG EL AT PEAK FLOW
H =W.S. EL AT PEAK FLOW
W =TOP WIDTH AT PEAK FLOW
Q =WATER DISCHARGE AT PEAK FLOW
V =MEAN VELOCITY AT PEAK FLOW
QB =BED-LOAD DIS. AT PEAK FLOW
QS =SUS-LOAD DIS. AT PEAK FLOW
QT =TOTAL-LOAD DIS. AT PEAK FLOW
D50=MEDIAN DIAMETER OF BED MATERIAL AT PEAK FLOW

Table 3 Principal results computed by HEC-6 for the San Lorenzo River

SAN LORENZO RIVER: FLUVIAL-11

ID	X	Y0	YF	Y	H	H1	W	Q	V	QB	QS	QT	D50
	FT	FT	FT	FT	FT	FT	FT	CFS	FPS	T/D	T/D	T/D	MM
3	0	-4.5	-7.5	-9.5	1.3	1.9	239	12870	9.0	-	-	158700	0.89
4	558	-4.2	-6.2	-7.8	2.0	4.1	239	12870	9.3	-	-	168380	0.97
8	1183	-4.0	-4.7	-6.2	3.0	4.8	232	12870	9.6	-	-	170590	0.98
9	1700	-1.3	-1.6	-1.6	4.0	5.6	274	12870	8.9	-	-	165180	1.02
10	2200	-1.0	-0.8	-0.8	4.8	6.0	274	12870	9.0	-	-	160760	1.20
11	2600	-0.6	-0.2	-0.2	5.5	6.3	274	12870	8.8	-	-	153930	1.09
12	2800	-0.4	-0.5	-2.0	5.7	6.1	201	12870	9.1	-	-	147460	0.89
14	2950	-0.3	-0.6	-0.6	5.5	6.4	206	12870	11.0	-	-	215140	1.68
15	3575	0.2	-0.1	-0.1	8.0	8.2	237	12870	7.4	-	-	141620	1.55
19	4345	0.6	0.3	0.3	9.4	9.6	243	12870	6.6	-	-	95720	1.08
20	4955	1.4	0.8	0.5	10.1	10.3	245	12870	6.2	-	-	86250	0.81
21	5360	1.8	1.2	1.0	10.4	10.8	243	12870	6.3	-	-	91380	0.96
22	5610	2.0	2.8	2.5	10.9	11.5	337	12870	5.0	-	-	80490	0.27
25	6095	2.5	2.9	2.9	11.2	11.7	265	10980	5.5	-	-	104050	0.30
26	6745	3.0	2.8	2.7	11.7	12.0	227	10980	6.1	-	-	116360	0.36
27	7325	3.2	3.6	3.2	12.3	12.6	247	10980	5.8	-	-	118490	0.31
30	7575	3.4	4.0	3.5	12.5	12.8	236	10980	5.8	-	-	116500	0.30
31	8080	3.7	5.3	5.2	12.8	13.1	228	10980	7.1	-	-	126680	0.31
32	8585	4.1	5.9	5.8	13.2	13.3	226	10980	7.4	-	-	145960	0.34
33	9090	4.4	6.5	6.5	13.6	13.5	224	10980	7.7	-	-	164040	0.39
34	9595	4.8	7.1	7.3	14.2	13.8	221	10980	8.1	-	-	181050	0.47
35	9935	5.0	7.5	7.8	14.6	13.9	218	10980	8.4	-	-	192720	0.56
36	10140	5.2	6.7	6.6	14.7	13.7	169	10980	9.2	-	-	198620	0.65
38	10480	5.6	6.0	5.7	15.7	14.0	181	10980	7.2	-	-	211080	0.91
39	10780	6.4	6.6	6.1	16.5	14.6	203	10980	6.9	-	-	202400	1.06
40	11260	7.2	7.0	6.4	17.4	15.4	166	10980	7.1	-	-	186100	1.10
41	11800	8.2	8.3	8.0	18.4	16.8	184	10980	6.8	-	-	174570	0.94
42	12305	9.2	9.3	8.6	19.3	17.6	187	10980	6.6	-	-	165460	0.85
43	12645	9.8	9.4	9.2	19.7	17.9	161	10980	7.6	-	-	198410	1.65
46	14118	10.0	13.9	14.1	23.2	21.1	263	10980	6.8	-	-	152940	0.37
47	15308	12.8	18.1	17.8	26.1	24.0	238	10980	7.4	-	-	199120	0.45
48	16908	16.5	20.6	20.1	30.8	28.0	221	10980	7.7	-	-	256410	0.59
49	18258	20.6	25.9	26.0	35.4	33.0	228	10980	8.1	-	-	291070	0.74
50	19238	24.2	25.6	23.6	39.0	37.0	160	10980	8.4	-	-	338320	1.39
51	20578	29.8	29.0	26.6	43.6	42.2	109	10980	8.7	-	-	363590	2.78
52	21508	32.8	33.7	33.6	46.4	44.5	142	10980	8.4	-	-	333840	1.01
53	22968	35.7	39.9	40.2	50.5	47.5	139	10980	9.1	-	-	348360	1.35
54	24758	41.2	41.2	41.2	57.3	53.9	144	10980	9.1	-	-	367860	3.15

ID=SECTION ID
X =RIVER DISTANCE
Y0=INITIAL THALWEG EL
YF=FINAL THALWEG EL
Y =THALWEG EL AT PEAK FLOW
H =W.S. EL AT PEAK FLOW
H1=W.S. EL AT PEAK FLOW (HEC-2)
W =TOP WIDTH AT PEAK FLOW
Q =WATER DISCHARGE AT PEAK FLOW
QB =BED-LOAD DIS. AT PEAK FLOW
QS =SUS-LOAD DIS. AT PEAK FLOW
QT =TOTAL-LOAD DIS. AT PEAK FLOW
D50=MEDIAN SIZE OF BED MATERIAL AT PEAK FLOW
NOTE: QB & QS WERE NOT COMPUTED WITH FLUVIAL-11

Table 4 Principal results computed by FLUVIAL-11 for the San Lorenzo River

SAN LORENZO RIVER: SEDIMENT-4H

ID	X	Y0	YF	Y	H	H1	W	Q	V	QT	D50
	FT	FT	FT	FT	FT	FT	FT	CFS	FPS	T/D	MM
3	0	-4.8	-5.3	-5.3	1.9	2.2	264	12701	9.3	1580	0.50
4	558	-4.3	-4.5	-4.3	3.3	3.8	260	12704	8.9	1070	0.50
8	1183	-3.8	-4.2	-4.0	4.2	4.6	233	12706	8.4	1170	0.50
9	1700	-2.5	-2.5	-2.5	4.8	5.1	282	12707	6.7	224	0.50
10	2200	-1.3	-1.6	-1.5	5.2	5.5	280	12708	7.3	849	0.50
11	2600	-0.8	-1.2	-1.0	5.6	5.9	277	12709	7.4	863	0.50
14	2750	-0.3	-1.5	-1.1	6.1	6.5	206	12710	9.1	1830	0.50
15	3375	0.2	-0.4	-0.2	7.3	7.8	220	12711	8.2	1610	0.50
19	4145	0.6	0.4	0.5	8.9	9.3	238	12712	7.1	833	0.50
20	4755	1.2	1.1	1.2	9.9	10.1	241	12713	6.8	417	0.50
21	5160	1.7	1.5	1.6	10.4	10.7	242	12713	6.6	190	0.50
22	5410	1.9	1.9	1.9	10.7	10.9	337	12714	4.6	11	0.50
25	5895	2.3	2.3	2.3	11.0	11.2	270	10895	5.1	24	0.50
26	6545	2.8	2.8	2.8	11.6	11.8	226	10895	6.2	93	0.50
27	7125	3.1	3.1	3.1	11.9	12.0	235	10896	5.9	29	0.50
30	7375	3.3	3.3	3.3	11.9	12.1	233	10896	6.1	25	0.50
31	7880	3.6	3.6	3.6	12.2	12.3	231	10897	6.2	30	0.50
32	8385	4.0	4.0	4.0	12.5	12.6	229	10897	6.3	26	0.50
33	8890	4.4	4.4	4.4	12.8	12.9	228	10898	6.4	24	0.50
34	9395	4.8	4.8	4.8	13.1	13.2	224	10898	6.6	20	0.50
35	9735	5.0	5.0	5.0	13.4	13.4	222	10899	6.6	14	0.50
36	9940	5.2	5.1	5.1	13.6	13.7	169	10899	8.6	79	0.50
38	10200	5.6	5.5	5.6	14.2	14.2	176	10899	8.5	99	0.50
39	10580	6.1	6.1	6.1	14.9	14.9	173	10899	8.5	91	0.50
40	11060	7.0	6.9	7.0	15.8	15.8	157	10899	9.2	144	0.50
41	11600	8.1	8.1	8.1	16.8	16.8	168	10899	8.6	96	0.50
42	12105	9.1	8.9	9.0	17.8	17.9	144	10899	10.1	179	0.50
43	12445	9.7	9.7	9.7	19.1	19.2	158	10900	8.6	140	0.50
46	13918	10.7	10.7	10.7	21.2	21.2	222	10900	7.9	113	0.50
47	15108	13.0	13.0	13.0	23.8	23.8	198	10900	8.2	51	0.50
48	16708	16.6	16.6	16.6	27.0	27.0	200	10900	8.7	93	0.50
49	18058	20.6	20.6	20.6	31.5	31.5	182	10900	9.9	135	0.50
50	19038	24.7	24.7	24.7	37.2	37.2	139	10900	11.3	198	0.50
51	20378	29.1	29.1	29.1	41.6	41.6	114	10900	10.4	54	0.50
52	21308	32.7	32.7	32.7	44.0	44.0	130	10900	9.8	26	0.50
53	22768	36.3	36.3	36.3	47.1	47.1	131	10900	10.0	37	0.50
54	24558	40.2	40.1	40.1	54.5	54.6	103	10900	12.9	350	0.50

ID=SECTION ID
X =RIVER DISTANCE
Y0=INITIAL THALWEG EL
YF=FINAL THALWEG EL
Y =THALWEG EL AT PEAK FLOW
H =W.S. EL AT PEAK FLOW
H1=W.S. EL AT PEAK FLOW
COMPUTED USING FIXED-BED FLOOD-ROUTING MODEL

W =TOP WIDTH AT PEAK FLOW
Q =WATER DISCHARGE AT PEAK FLOW
V =MEAN VELOCITY AT PEAK FLOW
QT =TOTAL-LOAD DISCHARGE AT PEAK FLOW
D50=MEDIAN DIAMETER OF BED MATERIAL AT PEAK FLOW

Table 5 Principal results computed by SEDIMENT-4H for the San Lorenzo River

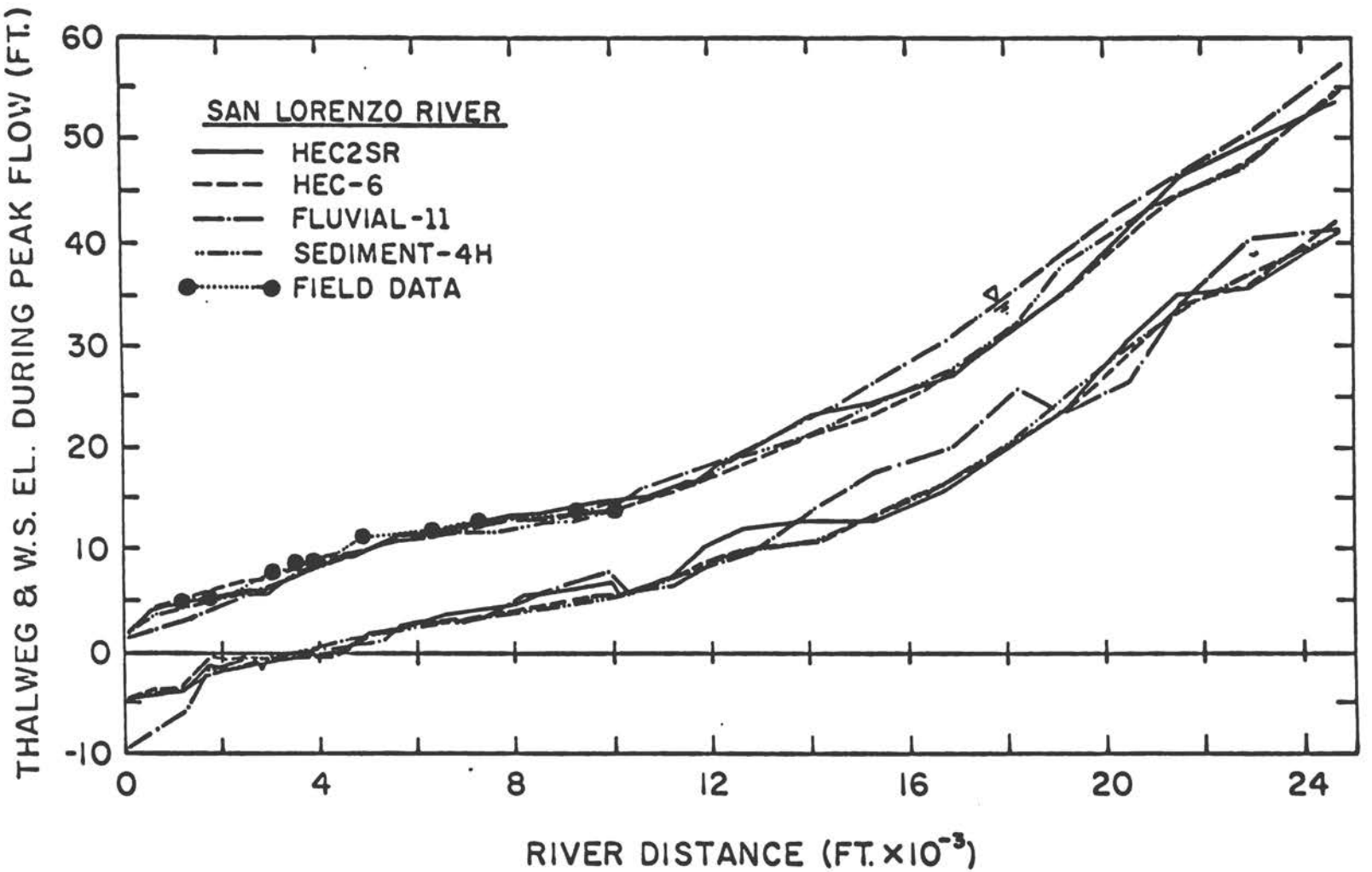

Figure 12 Comparison of thalweg and water-surface profiles at peak flow computed using the HEC2SR, HEC-6, FLUVIAL-11, and SEDIMENT-4H movable-bed models for the San Lorenzo River

SAN LORENZO RIVER

GAGE NO	RIVER DISTANCE	OBSERVED W.S. EL
	FT	FT
2	1150	5.0
3	1950	4.9
4	3070	7.6
5	3650	8.3
6	3950	8.3
7	4950	11.2
8	6400	11.8
9	7250	12.9
10	9300	13.5
11	10150	13.5

NOTE: THESE VALUES WERE RECORDED AT 8 A.M., 19 FEBRUARY 1980 DURING THE FLOOD-PEAK DISCHARGE OF 12,800 CFS

DATA SOURCE: "WATER SURFACE ELEVATION PLOTS"---SAN LORENZO RIVER STUDY, STAGE II, FIELD AND SIMULATION STUDIES, FINAL REPORT PREPARED BY JONES-TILLSON & ASSOCIATES, WATER RESOURCES ENGINEERS, H. ESMAILI & ASSOCIATES, SEPTEMBER 1980.

Table 6 Water-surface elevations observed during 19 February 1980 flood for the San Lorenzo River

the deviation amounts to over 3 ft in the water-surface elevation (see tables 2 through 5). Predictions of thalweg elevations also differ quite widely along the upper portion of the study reach, as seen in figure 12. Table 7 lists the water-surface and thalweg elevations at a peak flow of 12,800 cfs computed by SLA using three different movable-bed models (HEC2SR, KUWASER, and UUWSR). The results are depicted in figure 13. Among these three models, HEC2SR is seen to predict greater water-surface elevations for the lower reach, and smaller values for the upper reach. At a river distance of 19,238 ft, the prediction gap between HEC2SR and UUWSR is 3.6 ft (see table 7).

Table 8 summarizes the water-surface elevations predicted by HEC using the HEC-6 movable-bed model, HEC-6 fixed-bed model, and HEC-2 fixed-bed model. As seen in the table, there are no significant differences among these three models. According to the HEC report, the computed water-surface profiles rarely differed by more than 0.5 ft at any cross section, although thalweg-elevation changes of more than a foot occurred at some cross sections during the simulations. The report also stated that local scour or deposition does not translate directly into water-surface changes at a cross section because sediment movement is often limited to only a portion of the channel by specifying movable-bed limits. Figure 14 shows the water-surface elevations predicted by SDSU using the FLUVIAL-11 movable-bed model (comparison of H and H1 given in table 4). FLUVIAL-11 is seen to predict much smaller water-surface elevations in the upper reach than the HEC-2 fixed-bed model simulation. SEDIMENT-4H movable-bed model predicts a water-surface profile that is almost identical to that yielded by SEDIMENT-4H fixed-bed model, as seen in figure 15 (comparison of H and H1 in table 5).

The final post-flood thalweg profile predicted by HEC2SR is shown in figure 16, together with the initial thalweg profile (YF and YO in table 2). The largest thalweg deposition, 3.1 ft, was predicted to occur at a river distance of 14,118 ft. As stated earlier, HEC-6 did not predict significant changes in thalweg elevation. As can be seen in table 4 (YO and YF), FLUVIAL-11 predicted significant changes in thalweg elevation; as much as 5.3 ft of deposition was computed at river distance of 15,308 ft and 18,258 ft. On the other hand, SEDIMENT-4H predicted practically no change (see YO and YF in table 5). Typical longitudinal mean flow-velocity distributions at peak flow

SAN LORENZO RIVER: HEC2SR, KUWASER, & UUWSR

ID	X	Y0	Y1	H1	Y1F	Y2	H2	Y2F	Y3	H3	Y3F
	FT	FT	FT	FT	FT	FT	FT	FT	FT	FT	FT
3	0	-4.5	-4.7	1.6	-4.7	-4.5	1.2	-4.5	-4.5	1.2	-4.5
4	558	-4.2	-4.3	4.0	-4.4	-6.1	4.6	-6.0	-4.0	2.0	-4.4
8	1183	-4.0	-4.1	4.8	-4.2	-4.4	4.7	-3.7	-4.4	3.7	-4.2
9	1700	-1.3	-1.3	5.4	-1.4	-1.7	5.6	-1.7	-1.3	4.5	-1.8
10	2200	-1.0	-1.6	5.9	-1.6	-0.6	5.8	-1.0	-1.3	5.1	-2.0
11	2600	-0.6	-1.2	6.2	-1.2	0.2	6.3	-1.2	-1.3	5.5	-2.0
12	2800	-0.4	-1.0	6.0	-1.1	-1.0	6.3	-2.5	-2.5	5.7	-3.0
14	2950	-0.3	-1.0	6.2	-1.1	-2.0	6.3	-2.0	-2.9	5.8	-3.3
15	3575	0.2	-0.5	7.6	-0.6	-0.8	7.3	-1.3	-2.1	6.5	-2.7
19	4345	0.6	-0.1	8.9	-0.2	0.2	8.5	-0.5	-1.7	7.5	-2.1
20	4955	1.4	1.8	9.6	1.9	0.0	9.5	-0.3	-0.1	8.3	-0.4
21	5360	1.8	2.2	10.4	2.3	0.0	10.2	0.4	-0.1	8.8	0.6
22	5610	2.0	2.3	11.3	2.3	2.4	10.6	2.9	2.0	9.1	2.1
25	6095	2.5	2.8	11.5	2.9	2.9	10.8	2.7	3.0	9.7	2.5
26	6745	3.0	3.9	11.9	4.1	2.6	11.4	3.9	2.3	10.5	2.7
27	7325	3.2	4.0	12.8	4.2	3.8	11.9	5.0	3.6	11.3	4.0
30	7575	3.4	4.2	13.1	4.4	5.2	12.2	5.4	4.1	11.6	4.6
31	8080	3.7	4.6	13.4	4.7	6.1	12.6	6.6	4.9	12.1	5.4
32	8585	4.1	5.9	13.6	6.2	7.1	13.1	7.6	5.5	12.6	6.1
33	9090	4.4	6.2	14.0	6.5	8.0	13.6	7.7	6.4	13.1	6.7
34	9595	4.8	6.6	14.4	6.9	8.1	14.0	8.5	7.0	13.6	7.1
35	9935	5.0	6.9	14.7	7.2	9.0	15.7	9.2	7.6	14.0	7.5
36	10140	5.2	5.4	14.7	5.5	6.5	15.9	7.4	6.4	14.3	7.1
38	10480	5.6	5.8	14.9	5.9	6.6	16.1	7.5	7.0	14.7	7.4
39	10780	6.4	6.6	15.4	6.7	8.7	16.5	8.2	7.7	15.5	8.1
40	11260	7.2	7.4	16.0	7.5	8.2	17.1	9.1	8.2	16.4	8.8
41	11800	8.2	10.0	17.0	10.4	9.6	18.1	10.1	10.0	17.5	10.0
42	12305	9.2	11.0	18.6	11.5	9.9	18.8	11.1	10.9	18.5	11.0
43	12645	9.8	11.8	19.1	12.3	10.8	19.3	11.5	10.9	19.2	11.4
46	14118	10.0	12.6	23.1	13.1	13.1	21.5	13.3	13.3	22.1	13.9
47	15308	12.8	12.5	24.3	12.4	14.9	23.3	16.2	16.7	24.9	17.6
48	16908	16.5	16.0	26.5	15.9	17.2	28.6	16.6	19.7	29.9	20.9
49	18258	20.6	20.2	32.2	20.1	24.1	34.6	24.0	27.8	35.3	27.5
50	19238	24.2	23.6	35.3	23.4	27.4	37.1	27.6	27.9	38.9	30.3
51	20578	29.8	30.8	41.7	30.8	31.8	42.5	33.0	32.2	42.8	33.8
52	21508	32.8	35.2	46.1	35.5	34.0	44.0	34.4	36.1	45.8	36.1
53	22968	35.7	35.7	49.1	35.7	41.2	51.9	40.5	40.7	50.0	41.1
54	24758	41.2	41.2	53.6	41.2	41.2	53.6	41.2	41.2	54.5	41.2

ID = SECTION I.D.
X = RIVER DISTANCE
Y0 = INITIAL THALWEG EL
Y1 = THALWEG EL AT PEAK FLOW: (HEC2SR)
H1 = W.S. EL AT PEAK FLOW: (HEC2SR)
Y1F= FINAL THALWEG EL: (HEC2SR)
Y2 = THALWEG EL AT PEAK FLOW: (KUWASER)
H2 = W.S. EL AT PEAK FLOW: (KUWASER)
Y2F= FINAL THALWEG EL: (KUWASER)
Y3 = THALWEG EL AT PEAK FLOW: (UUWSR)
H3 = W.S. EL AT PEAK FLOW: (UUWSR)
Y3F= FINAL THALWEG EL: (UUWSR)
NOTE: PEAK-FLOW DISCHARGE = 12,800 CFS

Table 7 Comparison of thalweg and water-surface elevations computed by SLA using HEC2SR, KUWASER, and UUWSR for the San Lorenzo River

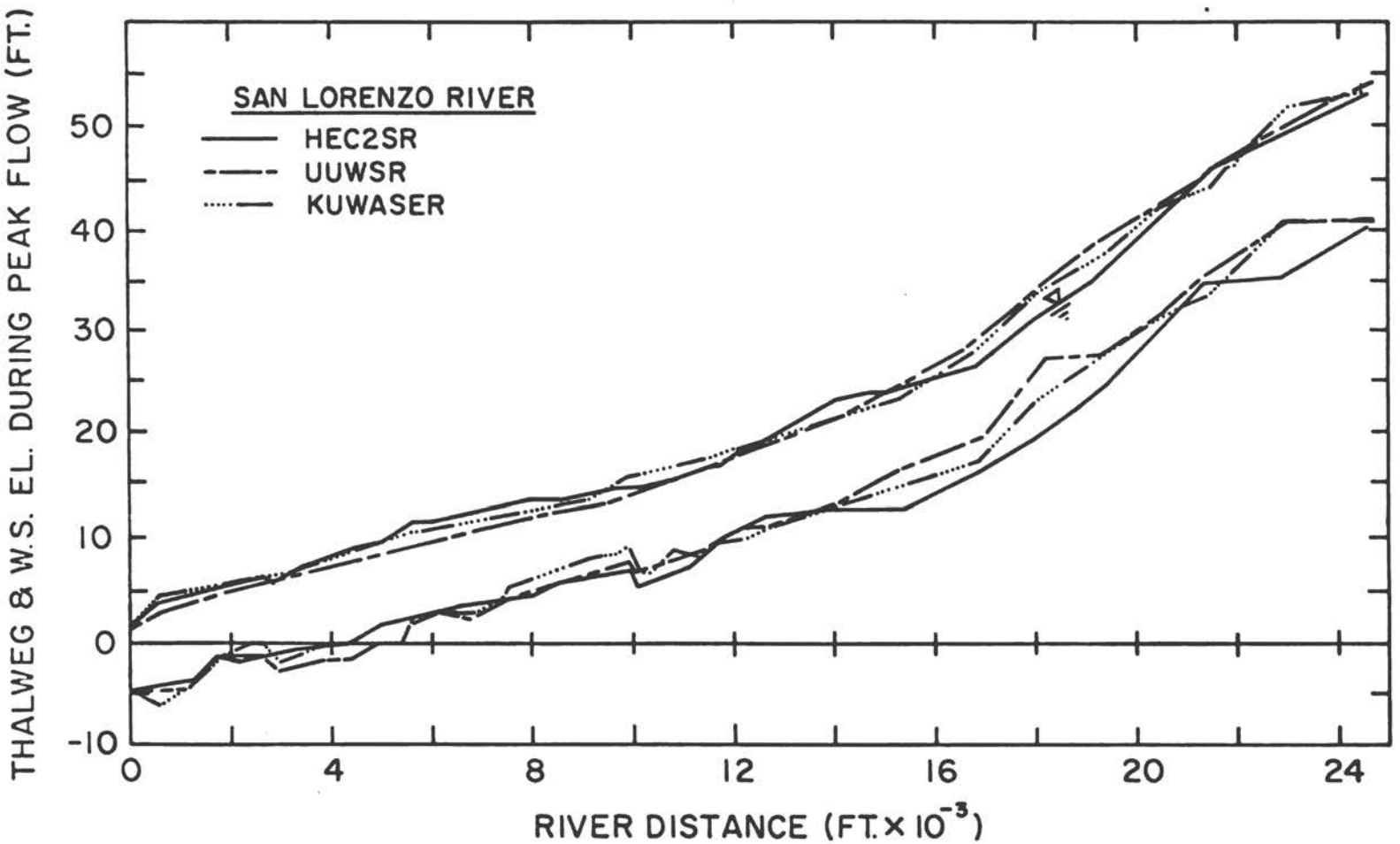

Figure 13 Comparison of thalweg and water-surface profiles at peak flow computed using the three SLA movable-bed models for the San Lorenzo River

SAN LORENZO RIVER: HEC-6

ID	X	H1	H2	H3	Q
	FT	FT	FT	FT	CFS
3	0	1.67	1.67	1.66	12800
4	558	4.14	4.17	4.07	12800
8	1183	4.97	4.88	4.82	12800
9	1700	5.80	5.51	5.47	12800
10	2200	6.41	5.94	5.90	12800
11	2600	6.69	6.20	6.17	12800
12	2800	6.67	6.14	6.11	12800
14	2950	6.92	6.34	6.31	12800
15	3575	8.36	8.71	8.17	12800
19	4345	9.26	9.76	9.52	12800
20	4955	9.80	10.41	10.23	12800
21	5360	10.37	10.87	10.72	12800
22	5610	11.11	11.52	11.41	12800
25	6095	11.31	11.68	11.62	11000
26	6745	11.74	12.04	11.98	11000
27	7325	12.39	12.62	12.58	11000
30	7575	12.60	12.82	12.77	11000
31	8080	12.82	13.02	13.05	11000
32	8585	13.05	13.21	13.25	11000
33	9090	13.32	13.45	13.48	11000
34	9595	13.57	13.69	13.72	11000
35	9935	13.79	13.86	13.89	11000
36	10140	13.51	13.60	13.63	11000
38	10400	14.05	14.00	13.96	11000
39	10780	14.72	14.62	14.60	11000
40	11260	15.49	15.38	15.37	11000
41	11800	16.72	16.79	16.80	11000
42	12305	17.62	17.54	17.54	11000
43	12645	17.95	17.84	17.86	11000
46	14118	21.26	21.29	21.31	11000
47	15308	23.08	22.94	22.94	11000
48	16908	27.02	26.84	26.85	11000
49	18258	32.14	32.00	32.01	11000
50	19238	34.94	35.50	35.36	11000
51	20578	40.64	41.13	41.25	11000
52	21508	44.13	44.44	44.47	11000
53	22968	47.46	46.94	46.93	11000
54	24758	54.26	53.73	53.64	11000

ID=SECTION I.D.
X =RIVER DISTANCE
H1=W.S. EL BY HEC-6 (MOVABLE BED)
H2=W.S. EL BY HEC-6 (FIXED BED)
H3=W.S. EL BY HEC-2 (FIXED BED)
Q =PEAK FLOW WATER DISCHARGE

Table 8 Comparison of water-surface elevations computed by the HEC-6 movable-bed and fixed-bed models and HEC-2 for the San Lorenzo River

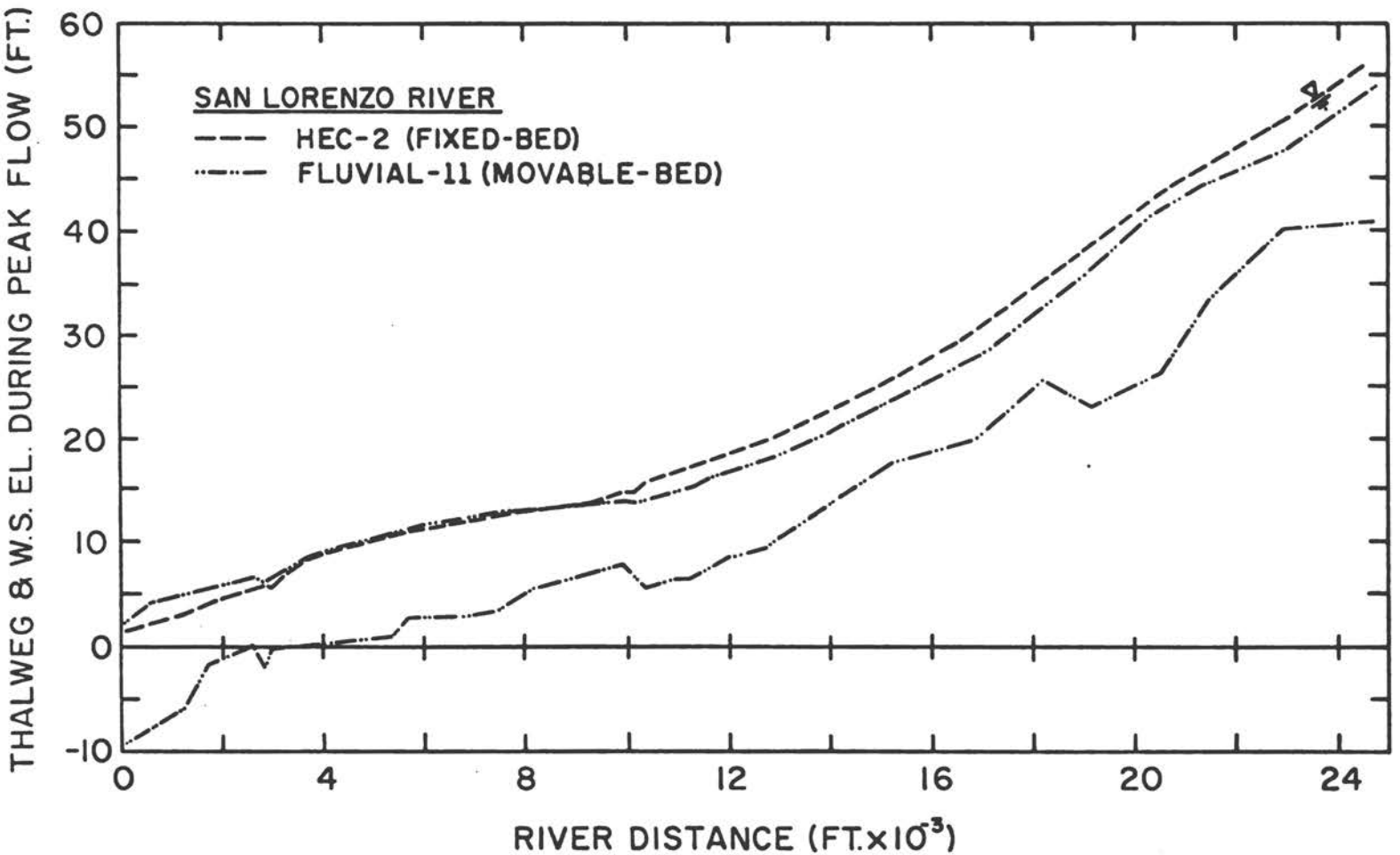

Figure 14 Comparison of thalweg and water-surface profiles computed by SDSU using HEC-2 and FLUVIAL-11 for the San Lorenzo River

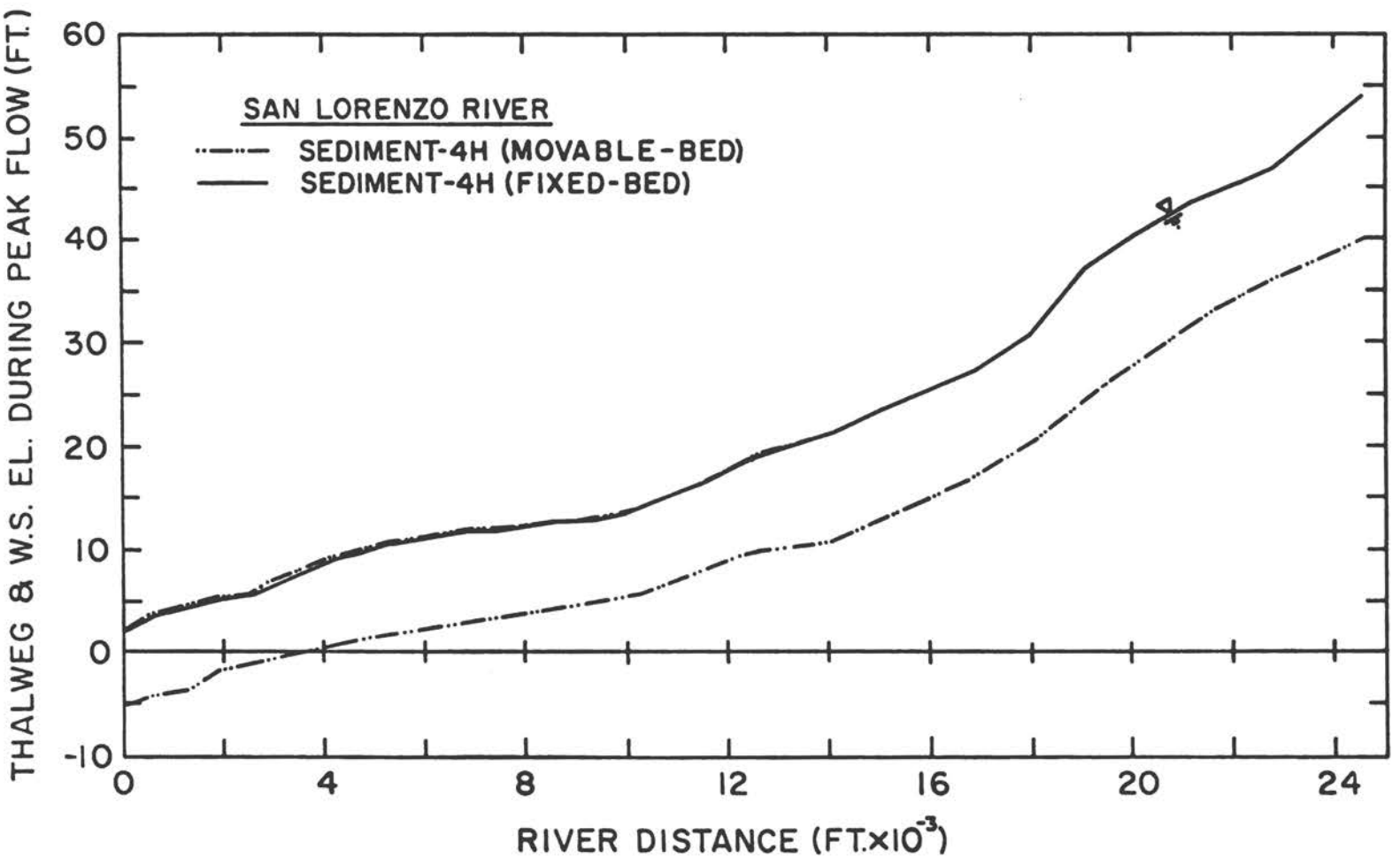

Figure 15 Comparison of thalweg and water-surface profiles at peak flow computed by RMA using the SEDIMENT-4H movable-bed and fixed-bed models for the San Lorenzo River

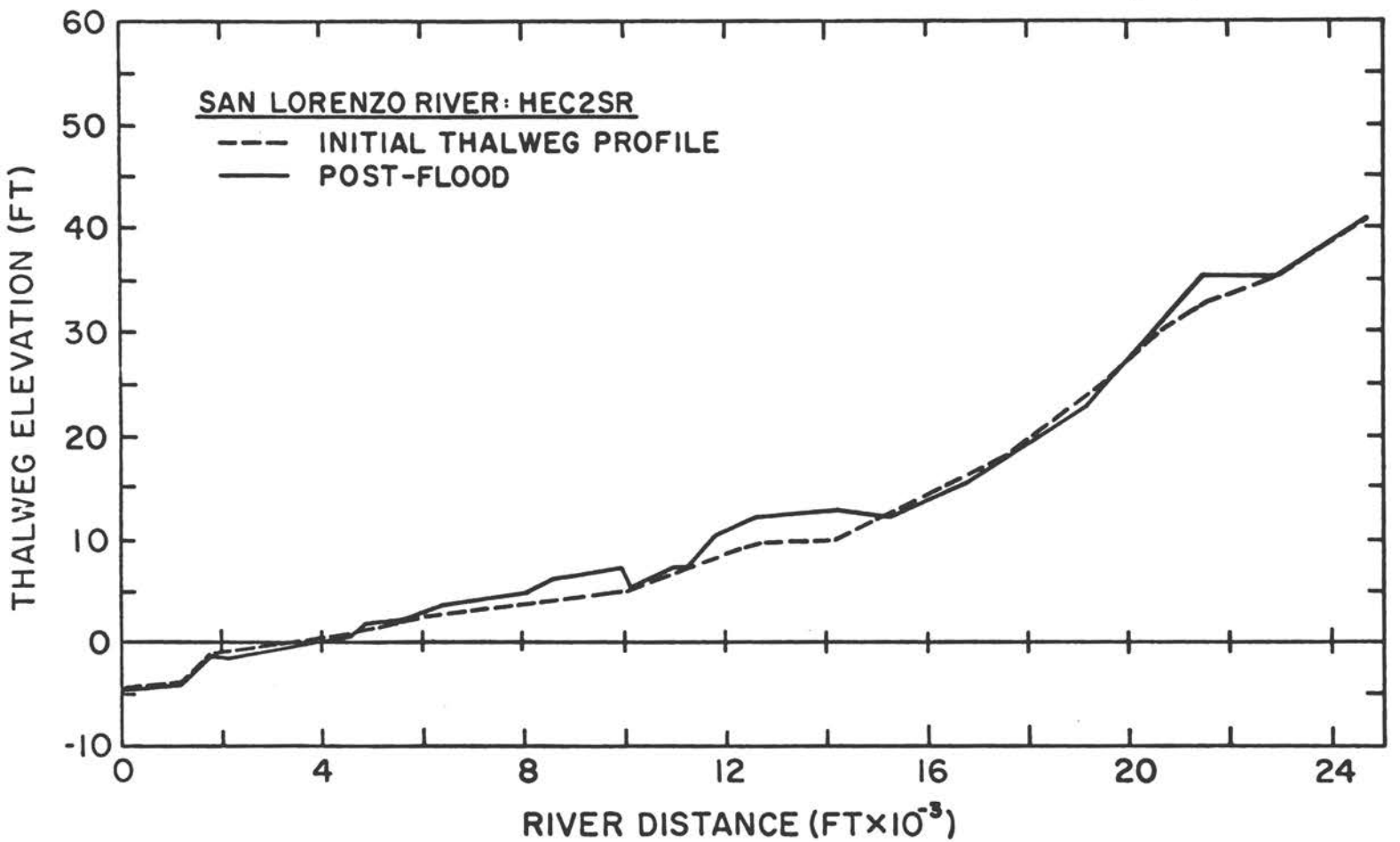

Figure 16 Comparison of initial and post-flood thalweg profiles computed using HEC2SR for the San Lorenzo River

are shown in figure 17 for HEC-6 and FLUVIAL-11; mean velocities predicted by HEC-6 are seen to be much higher than those of FLUVIAL-11 in the upper part of the study reach. Mean velocities predicted by HEC2SR and SEDIMENT-4H are closer to those computed by HEC-6, as can be seen in tables 2,3, and 5.

The total-load discharges at peak flow and the post-flood median bed-material sizes that were predicted by HEC2SR, HEC-6, FLUVIAL-11, and SEDIMENT-4H are summarized in table 9. Longitudinal distributions of the total-load discharge computed by these four models are plotted in figure 18. HEC2SR predictions are seen to be very high compared with those of HEC-6, in spite of the fact that both models predicted very similar mean velocities, as mentioned earlier. SEDIENT-4H predicted extremely low total-load sediment-transport rates, as is shown in table 9 (its predicted total-load discharges are too small to plot visibly in figure 18). Total-load discharges and mean flow velocities computed by the three SLA models (HEC2SR, KUWASER, and UUWSR) are tabulated in table 10 and plotted in figure 19. Although KUWASER and UUWSR used the same sediment-transport function, as mentioned in Chapter II, their predictions are seen to differ substantially because their predicted mean-flow-velocity predictions were quite different. Post-flood median bed-material sizes predicted by HEC2SR, HEC-6, FLUVIAL-11 are plotted in figure 20, together with the pre-flood values (see table 9 also). Note that SEDIMENT-4H does not account for sediment sorting processes. HEC-6 predicted significant coarsening of the river-bed material over the entire study reach.

In order to demonstrate model prediction of thalweg and water-surface elevations during both rising and falling stages of the hydrograph, numerical values predicted by HEC2SR, HEC-6, FLUVIAL-11, and SEDIMENT-4H are summarized in tables 11, 12, 13, and 14, respectively. Direct comparisons of these results are not possible because time-discretization intervals of the hydrograph differed from model to model, resulting in the modelers' computer outputs being prepared for different water discharges. However, approximate comparisons can be made. For example, thalweg and water-surface elevations predicted by FLUVIAL-11 and SEDIMENT-4H during the rising stage can be compared because water discharges of 7,690 cfs and 7,960 cfs used by the two models, respectively, are nearly equal. As seen in tables 13 and 14 (YR and HR), their predictions of the thalweg elevation differed considerably,

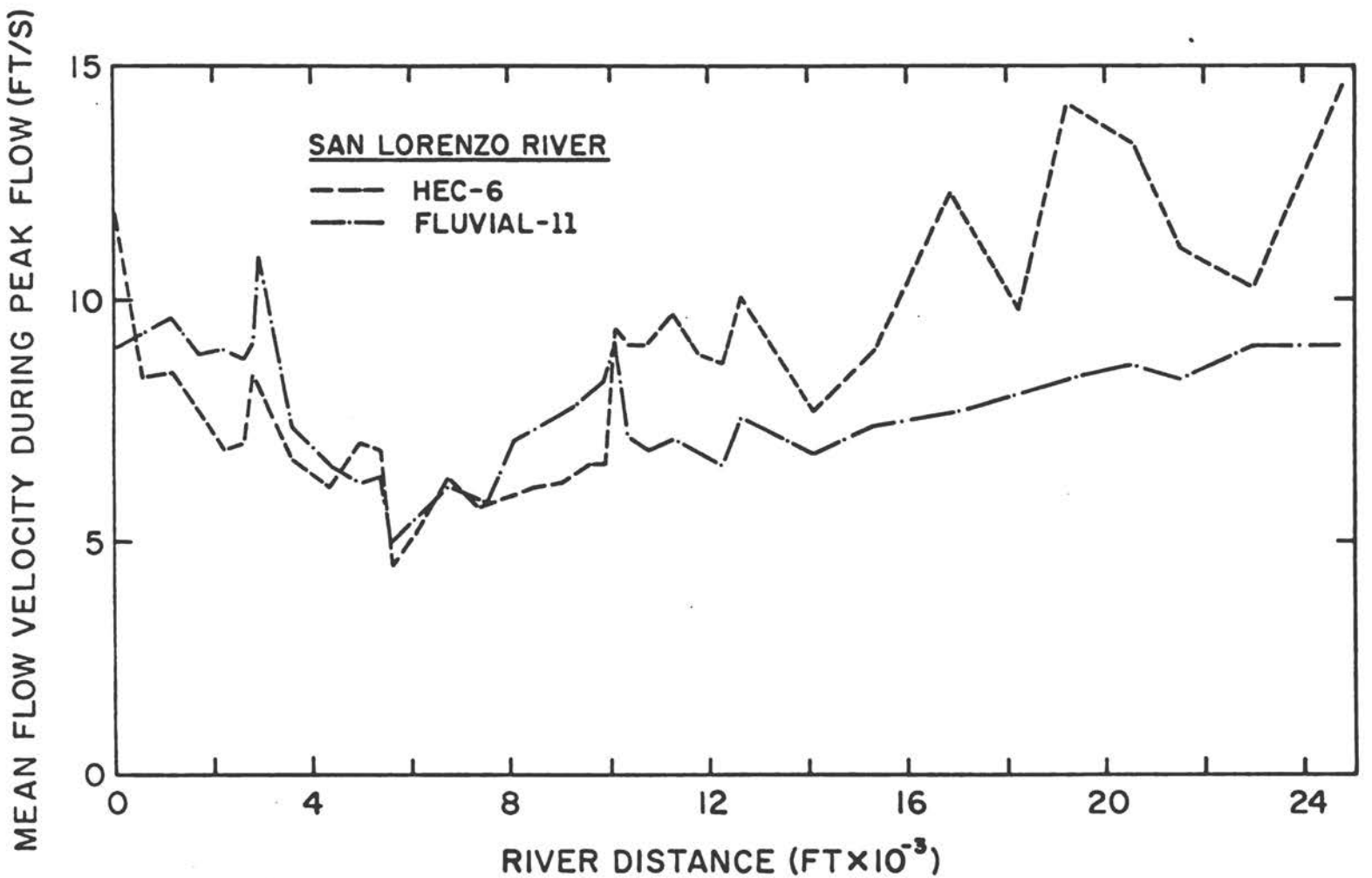

Figure 17 Longitudinal distributions of mean flow velocity at peak flow computed using the HEC-6 and FLUVIAL-11 movable-bed models for the San Lorenzo River

SAN LORENZO RIVER			(HEC-6)		(FLUVIAL-11)		(HEC2SR)		(SEDIMENT-4H)	
ID	X	D50I	QT	D50F	QT	D50F	QT	D50F	QT	D50F
	FT	MM	T/D	MM	T/D	MM	T/D	MM	T/D	MM
3	0	0.34	46670	0.71	158700	0.57	244170	0.47	1580	0.50
4	558	0.34	41230	0.70	168380	0.59	244170	0.47	1070	0.50
8	1183	0.34	38960	0.69	170590	0.65	244170	0.47	1170	0.50
9	1700	0.34	39110	0.68	165180	0.77	244170	0.47	224	0.50
10	2200	0.27	40360	0.54	160760	1.13	205210	0.50	849	0.50
11	2600	0.27	41370	0.58	153930	1.25	205210	0.50	863	0.50
12	2800	0.27	39540	0.59	147460	1.31	205210	0.50	1830	0.50
14	2950	0.27	37700	0.65	215140	1.15	205210	0.50	1830	0.50
15	3575	0.27	36570	0.67	141620	1.28	205210	0.50	1610	0.50
19	4345	0.27	30180	0.72	95720	0.50	205210	0.50	833	0.50
20	4955	0.53	18060	1.14	86250	0.39	153230	0.53	417	0.50
21	5360	0.53	16890	1.37	91380	0.37	153230	0.53	190	0.50
22	5610	0.53	16400	1.05	80490	0.35	153230	0.53	11	0.50
25	6065	0.53	13350	1.10	104050	0.37	153230	0.53	24	0.50
26	6745	0.53	12640	1.16	116360	0.39	168880	0.37	93	0.50
27	7325	0.53	11730	1.21	118490	0.32	168880	0.37	29	0.50
30	7575	0.53	10700	1.06	116500	0.35	168880	0.37	25	0.50
31	8080	0.93	9520	0.93	126680	0.42	168880	0.37	30	0.50
32	8585	0.93	9880	1.06	145960	0.46	207890	0.34	26	0.50
33	9090	0.93	10150	1.24	164040	0.51	207890	0.34	24	0.50
34	9595	0.93	10460	1.15	181050	0.56	207890	0.34	20	0.50
35	9935	0.93	9720	0.98	192720	0.55	207890	0.34	14	0.50
36	10140	0.93	10460	1.68	198620	0.41	270750	0.58	79	0.50
38	10400	0.93	9520	1.75	211080	0.40	270750	0.58	99	0.50
39	10780	0.93	9770	1.72	202400	0.44	270750	0.58	91	0.50
40	11260	0.93	9980	1.83	186100	0.51	270750	0.58	144	0.50
41	11800	0.93	9620	1.66	174570	0.46	272050	0.50	96	0.50
42	12305	0.93	10650	1.75	165460	0.53	272050	0.50	179	0.50
43	12645	0.93	11090	1.84	198410	0.59	272050	0.50	140	0.50
46	14118	0.93	10880	1.55	152940	0.51	272050	0.50	113	0.50
47	15308	0.93	15000	1.68	199120	0.50	335130	1.62	51	0.50
48	16908	0.93	17450	1.71	256410	0.61	335130	1.62	93	0.50
49	18258	0.93	20260	1.64	291070	1.03	335130	1.62	135	0.50
50	19238	0.93	20810	1.93	338320	0.83	335130	1.62	198	0.50
51	20578	0.93	18070	1.93	363590	1.19	319310	0.64	54	0.50
52	21508	0.93	18210	0.98	333840	1.53	319310	0.64	26	0.50
53	22968	0.93	34920	1.80	348360	2.37	324520	1.25	37	0.50
54	24758	0.93	51110	1.68	367860	3.15	324520	1.25	350	0.50

ID = SECTION I.D.
X = RIVER DISTANCE
D50I = INITIAL MEDIAN SIZE OF BED MATERIAL (PRE-FLOOD)
D50F = FINAL MEDIAN SIZE OF BED MATERIAL (POST-FLOOD)
QT = TOTAL-LOAD DISCHARGE AT PEAK-FLOW DISCHARGE OF 12,800 CFS

Table 9 Comparison of total-load discharges computed by HEC2SR, HEC-6, FLUVIAL-11, and SEDIMENT-4H for the San Lorenzo River

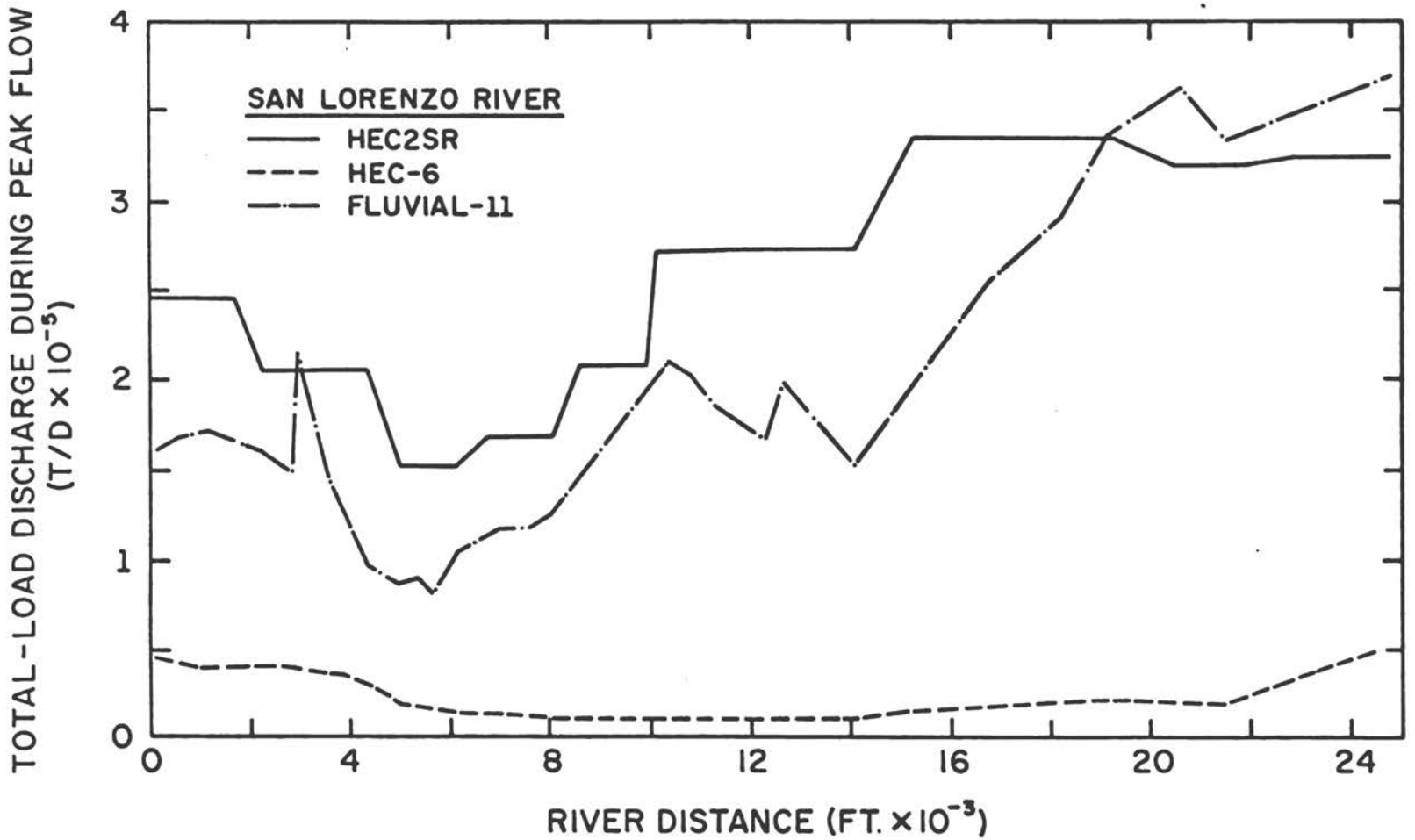

Figure 18 Total-load discharges at peak flow computed using HEC2SR, HEC-6, and FLUVIAL-11 for the San Lorenzo River

SAN LORENZO RIVER		THREE SLA MODELS					
		⟨HEC2SR⟩		⟨KUWASER⟩		⟨UUWSR⟩	
ID	X	QT	V	QT	V	QT	V
	FT	T/D	FPS	T/D	FPS	T/D	FPS
3	0	244170	11.9	555200	13.5	1287340	13.2
4	558	244170	8.1	60420	6.6	321070	9.2
8	1183	244170	7.9	151730	8.5	304990	9.1
9	1700	244170	7.3	70750	6.7	285810	8.7
10	2200	205210	6.6	114940	7.8	255480	7.5
11	2600	205210	6.8	88220	7.3	243420	7.4
12	2800	205210	9.2	158590	8.9	234260	7.7
14	2950	205210	9.2	134010	8.5	226080	7.5
15	3575	205210	7.4	84720	7.4	184530	7.0
19	4345	205210	6.6	73440	7.2	125610	6.4
20	4955	153230	7.7	50500	6.6	87100	7.1
21	5360	153230	7.3	41210	6.1	69250	6.7
22	5610	153230	4.6	25120	5.1	51840	6.0
25	6095	153230	5.2	31670	5.7	54460	6.4
26	6745	168880	6.8	25400	5.5	59430	6.7
27	7325	168880	5.9	38320	6.0	60410	6.8
30	7575	168880	5.9	66830	6.9	68370	6.9
31	8080	168880	6.0	90650	7.5	76190	7.2
32	8585	207890	6.9	173520	7.7	94430	7.6
33	9090	207890	6.9	300240	9.9	110410	7.9
34	9595	207890	7.0	189300	8.9	134960	8.2
35	9935	207890	7.1	102510	7.7	143090	8.4
36	10140	270750	7.9	159160	7.5	151710	9.3
38	10400	270750	8.1	164450	7.6	159140	9.4
39	10780	270750	8.5	179380	7.8	166600	9.4
40	11260	270750	9.5	279530	8.8	170190	9.6
41	11800	272050	10.7	252600	8.4	174060	9.6
42	12305	272050	9.5	272380	8.6	183110	9.7
43	12645	272050	11.4	222590	8.1	188660	9.9
46	14118	272050	6.7	204450	7.9	186720	9.4
47	15308	335130	7.1	378890	10.9	226690	9.7
48	16908	335130	13.2	268030	10.6	269100	10.2
49	18258	335130	8.6	292460	8.2	259530	10.7
50	19238	335130	14.2	527770	13.1	441080	11.8
51	20578	319310	14.2	566560	10.9	429780	12.7
52	21508	319310	10.8	738640	15.1	420910	12.4
53	22968	324520	8.5	306820	9.0	459860	12.3
54	24758	324520	15.0	683280	14.5	497220	13.1

ID = SECTION I.D.
X = RIVER DISTANCE
QT = TOTAL-LOAD DISCHARGE AT PEAK FLOW
V = MEAN FLOW VELOCITY AT PEAK FLOW
NOTE: PEAK-FLOW DISCHARGE = 12,800 CFS

Table 10 Comparison of total-load discharges and mean flow velocities computed by SLA using HEC2SR, KUWASER, and UUWSR for the San Lorenzo River

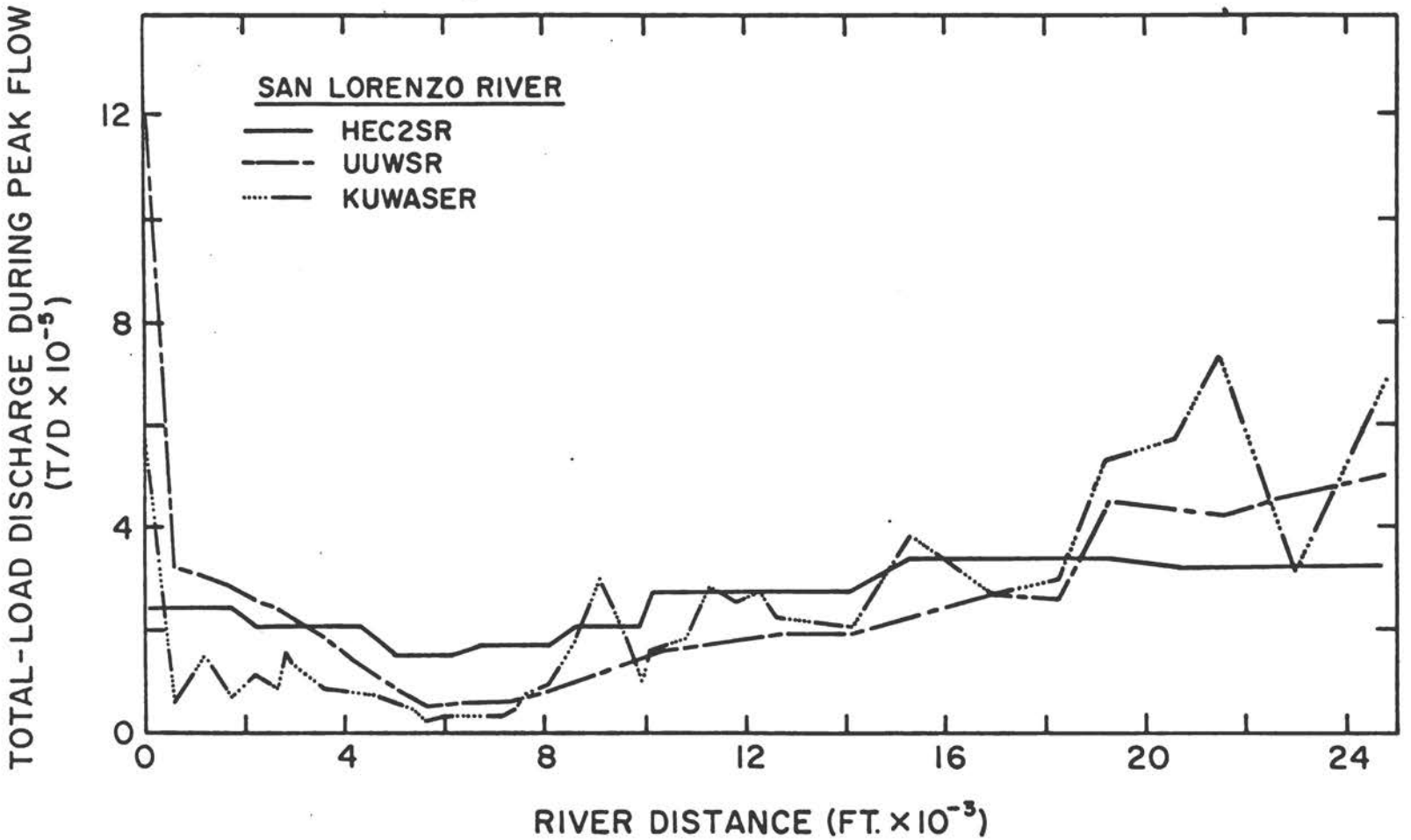

Figure 19 Total-load discharges at peak flow computed by SLA using the three SLA models for the San Lorenzo River

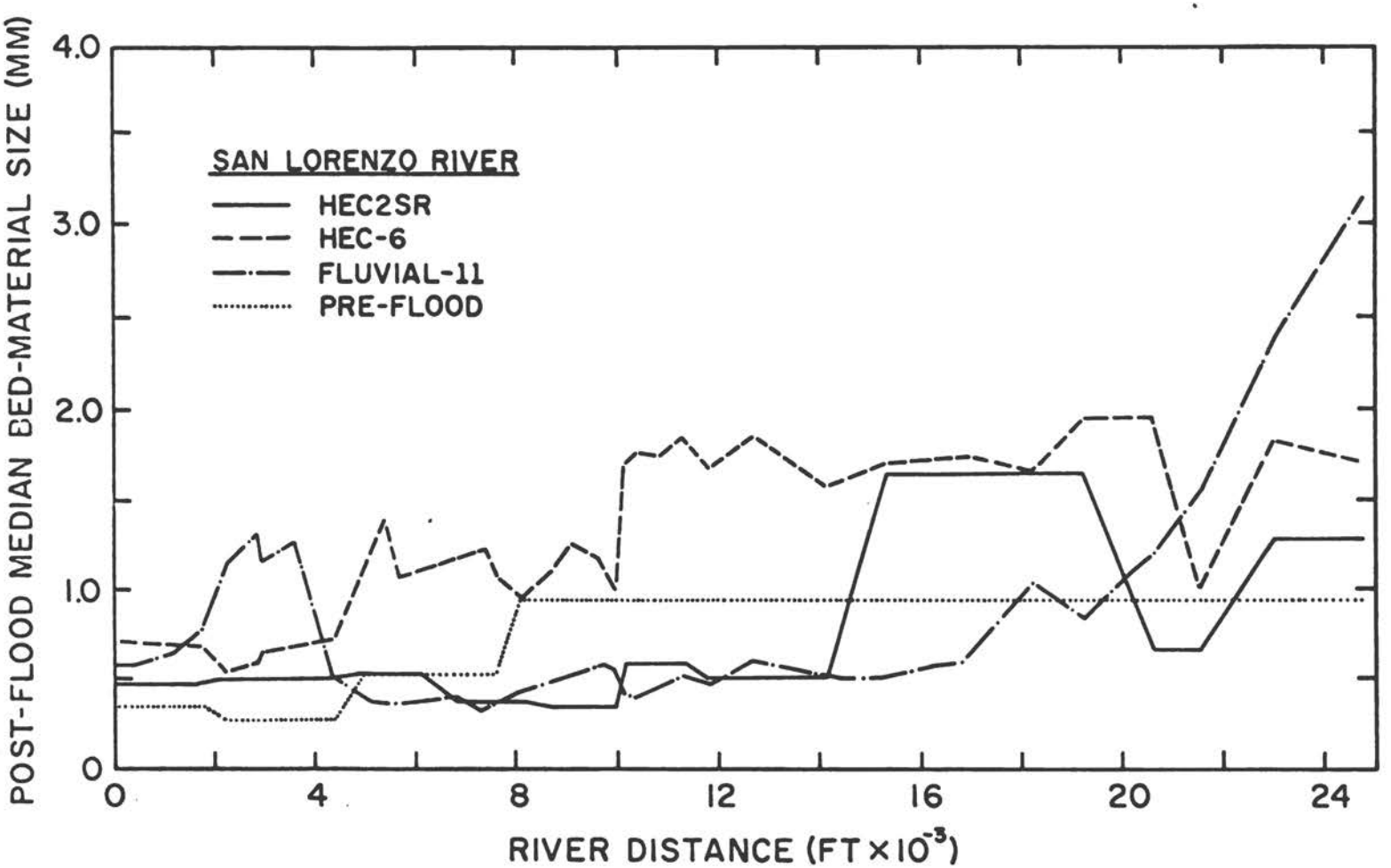

Figure 20 Longitudinal distributions of post-flood median bed-material size computed using HEC2SR, HEC-6, FLUVIAL-11, and SEDIMENT-4H for the San Lorenzo River

SAN LORENZO RIVER: HEC2SR

ID	X	YR	HR	YFA	HFA
	FT	FT	FT	FT	FT
3	0	-4.4	2.3	-4.6	3.4
4	558	-4.1	2.8	-4.3	3.7
8	1183	-3.7	3.3	-4.1	4.1
9	1700	-1.2	3.7	-1.3	4.4
10	2200	-1.4	4.2	-1.6	4.8
11	2600	-1.0	4.4	-1.2	5.0
12	2800	-0.9	4.4	-1.1	4.9
14	2950	-0.8	4.5	-1.1	5.1
15	3575	-0.3	5.6	-0.6	6.1
19	4345	0.1	6.8	-0.1	7.2
20	4955	1.7	7.4	1.9	7.9
21	5360	2.1	8.1	2.3	8.7
22	5610	2.2	8.7	2.3	9.4
25	6095	2.8	9.0	2.9	9.7
26	6745	3.7	9.4	4.0	10.2
27	7325	3.9	10.2	4.1	11.1
30	7575	4.0	10.4	4.3	11.4
31	8080	4.4	10.8	4.6	11.7
32	8585	5.5	11.0	6.0	11.9
33	9090	5.8	11.4	6.3	12.5
34	9595	6.3	11.8	6.8	12.9
35	9935	6.5	12.0	7.0	13.2
36	10140	5.4	12.1	5.4	13.3
38	10400	5.8	12.3	5.8	13.5
39	10780	6.6	12.8	6.6	13.9
40	11260	7.4	13.5	7.4	14.5
41	11800	9.8	14.6	10.2	15.4
42	12305	10.8	16.2	11.2	17.4
43	12645	11.5	16.8	12.0	17.9
46	14118	12.4	20.3	12.8	21.6
47	15308	12.5	21.6	12.5	22.8
48	16908	16.1	24.2	16.0	25.0
49	18258	20.2	29.7	20.1	30.6
50	19238	23.7	32.6	23.5	33.5
51	20578	30.8	39.4	30.8	40.3
52	21500	35.2	43.0	35.3	44.1
53	22968	35.7	46.1	35.7	47.2
54	24758	41.2	50.5	41.2	51.7

ID =SECTION I.D.
X =RIVER DISTANCE
YR =THALWEG EL AT Q=7,250 CFS (RISING STAGE)
HR =W.S. EL AT Q=7,250 CFS (RISING STAGE)
YFA=THALWEG EL AT Q=8,570 CFS (FALLING STAGE)
HFA=W.S. EL AT Q=8,570 CFS (FALLING STAGE)

Table 11 Thalweg and water-surface elevations during rising and falling stages computed by HEC2SR for the San Lorenzo River

SAN LORENZO RIVER: HEC-6

ID	X	YR	HR	YFA	HFA
	FT	FT	FT	FT	FT
3	0	-4.2	1.6	-4.6	3.5
4	558	-3.7	2.7	-3.7	3.7
8	1183	-3.4	3.5	-3.4	4.1
9	1700	-0.7	4.2	-0.6	4.6
10	2200	-0.7	4.8	-0.7	5.1
11	2600	-0.5	5.0	-0.7	5.3
12	2800	-0.6	5.1	-0.8	5.3
14	2950	-1.0	5.4	-1.1	5.5
15	3575	-0.5	6.6	-0.8	6.5
19	4345	-0.2	7.4	-0.7	7.2
20	4955	1.4	8.0	1.3	7.7
21	5360	1.7	8.5	1.7	8.3
22	5610	2.0	9.1	2.0	8.9
25	6095	2.6	9.3	2.5	9.1
26	6745	3.0	9.7	3.0	9.7
27	7325	3.2	10.4	3.2	10.4
30	7575	3.5	10.5	3.4	10.6
31	8080	3.9	10.8	3.9	10.8
32	8585	4.3	11.0	4.3	11.0
33	9090	4.5	11.3	4.6	11.3
34	9595	5.2	11.5	5.2	11.6
35	9935	5.3	11.8	5.4	11.9
36	10140	5.6	11.6	5.5	11.7
38	10400	5.7	12.2	5.7	12.2
39	10780	6.5	12.8	6.5	12.9
40	11260	7.1	13.6	7.1	13.8
41	11800	8.4	14.7	8.4	14.9
42	12305	9.2	15.6	9.3	15.8
43	12645	9.7	16.0	9.7	16.3
46	14118	10.2	19.1	10.3	19.4
47	15308	12.9	21.2	13.0	21.4
48	16908	16.7	25.3	16.7	25.6
49	18258	20.7	30.2	20.8	30.5
50	19238	23.7	32.9	23.6	33.0
51	20578	27.5	38.6	29.5	38.8
52	21508	33.4	41.4	34.2	41.7
53	22968	35.5	44.9	36.0	45.9
54	24758	40.8	50.7	42.4	52.7

ID =SECTION I.D.
X =RIVER DISTANCE
YR =THALWEG EL AT Q=8,200 CFS (RISING STAGE)
HR =W.S. EL AT Q=8,200 CFS (RISING STAGE)
YFA=THALWEG EL AT Q=8,100 CFS (FALLING STAGE)
HFA=W.S. EL AT Q=8,100 CFS (FALLING STAGE)

Table 12 Thalweg and water-surface elevations during rising and falling stages computed by HEC-6 for the San Lorenzo River

SAN LORENZO RIVER: FLUVIAL-11

ID	X	YR	HR	YFA	HFA
	FT	FT	FT	FT	FT
3	0	-6.8	2.7	-8.3	3.0
4	550	-5.3	2.9	-6.8	3.2
8	1183	-3.9	3.2	-5.3	3.5
9	1700	-1.5	3.8	-1.5	3.9
10	2200	-0.7	4.1	-0.8	4.4
11	2600	0.1	4.4	-0.3	4.8
12	2800	-0.4	4.5	-1.3	4.9
14	2950	-0.6	4.8	-0.6	4.9
15	3575	-0.1	6.1	-0.1	6.7
19	4345	0.3	7.2	0.3	8.0
20	4955	0.5	7.8	0.5	8.6
21	5360	1.0	8.1	1.0	9.0
22	5610	2.1	8.5	2.7	9.4
25	6095	2.6	8.8	2.9	9.7
26	6745	2.7	9.2	2.7	10.3
27	7325	3.2	9.7	3.4	10.9
30	7575	3.4	9.9	3.7	11.1
31	8080	4.6	10.1	5.3	11.4
32	8585	5.2	10.5	5.9	12.0
33	9090	5.8	10.9	6.6	12.5
34	9595	6.5	11.4	7.3	13.1
35	9935	7.0	11.7	7.7	13.5
36	10140	6.3	11.9	6.7	13.7
38	10400	5.7	12.6	5.7	14.6
39	10780	6.4	13.2	6.2	15.2
40	11260	6.9	13.9	6.3	15.9
41	11800	8.2	14.9	8.0	16.8
42	12305	9.3	15.7	8.8	17.6
43	12645	9.4	16.3	9.2	18.1
46	14110	13.4	19.6	14.3	21.6
47	15308	17.2	22.6	18.1	25.0
48	16908	19.9	27.5	20.3	30.0
49	18258	24.5	31.8	26.2	34.2
50	19238	22.9	34.9	24.5	37.7
51	20578	28.7	39.1	26.6	41.7
52	21508	33.2	41.8	33.6	44.1
53	22968	39.2	46.0	40.2	48.6
54	24758	41.2	52.9	41.2	55.6

ID =SECTION I.D.
X =RIVER DISTANCE
YR =THALWEG EL AT Q=7,690 CFS (RISING STAGE)
HR =W.S. EL AT Q=7,690 CFS (RISING STAGE)
YFA=THALWEG EL AT Q=9,440 CFS (FALLING STAGE)
HFA=W.S. EL AT Q=9,440 CFS (FALLING STAGE)

Table 13 Thalweg and water-surface elevations during rising and falling stages computed by FLUVIAL-11 for the San Lorenzo River

SAN LORENZO RIVER:SEDIMENT-4H

ID	X	YR	HR	YFA	HFA
	FT	FT	FT	FT	FT
3	0	-5.0	1.4	-5.3	3.5
4	558	-4.4	2.1	-4.4	3.7
8	1183	-4.0	2.7	-4.2	3.9
9	1700	-2.5	3.2	-2.5	4.2
10	2200	-1.5	3.6	-1.6	4.4
11	2600	-1.0	4.0	-1.1	4.6
14	2750	-0.9	4.5	-1.3	4.9
15	3375	0.0	5.7	-0.3	5.8
19	4145	0.5	7.1	0.4	7.1
20	4755	1.2	8.0	1.1	8.0
21	5160	1.7	8.5	1.6	8.5
22	5410	1.9	8.8	1.9	8.8
25	5895	2.3	9.0	2.3	9.1
26	6545	2.8	9.6	2.8	9.7
27	7125	3.1	9.9	3.1	10.1
30	7375	3.3	10.0	3.3	10.2
31	7880	3.6	10.3	3.6	10.5
32	8385	4.0	10.6	4.0	10.8
33	8890	4.4	10.9	4.4	11.1
34	9395	4.8	11.2	4.8	11.4
35	9735	5.0	11.4	5.0	11.6
36	9940	5.2	11.7	5.1	11.9
38	10200	5.6	12.2	5.5	12.4
39	10580	6.1	12.9	6.0	13.1
40	11060	7.0	13.7	6.9	14.0
41	11600	8.1	14.7	8.1	14.9
42	12105	9.0	15.8	9.0	16.0
43	12445	9.7	17.0	9.7	17.3
46	13918	10.7	19.1	10.7	19.4
47	15108	13.0	21.7	13.0	22.0
48	16708	16.6	25.0	16.6	25.2
49	18058	20.6	29.5	20.6	29.8
50	19038	24.7	35.0	24.6	35.3
51	20378	29.1	39.0	29.1	39.3
52	21308	32.7	41.4	32.7	41.7
53	22768	36.3	44.6	36.3	45.0
54	24558	40.1	51.3	40.1	51.8

ID =SECTION I.D.
X =RIVER DISTANCE
YR =THALWEG EL AT Q=7,960 CFS (RISING STAGE)
HR =W.S. EL AT Q=7,960 CFS (RISING STAGE)
YFA=THALWEG EL AT Q=8,260 CFS (FALLING STAGE)
HFA=W.S. EL AT Q=8,260 CFS (FALLING STAGE)

Table 14 Thalweg and water-surface elevations during rising and falling stages computed by SEDIMENT-4H for the San Lorenzo River

although the predicted water-surface elevations are in relatively good agreement.

2. San Dieguito River. The principal hydraulic and sediment-transport characteristics at a peak flow of 22,000 cfs computed by HEC2SR, FLUVIAL-11, and SEDIMENT-4H are shown in tables 15, 16, and 17, respectively. Water-surface elevations computed using the fixed-bed models (FLUVIAL-11 and SEDIMENT-4H) are also listed in tables 16 and 17 (see H1). Thalweg and water-surface elvations during the peak flow predicted by these three movable-bed models are presented in figure 21, in which the three models are seen to predict widely differing elevations. HEC2SR predicted the backwater profile upstream of the Via de Santa Fe bridge located at a river distance of 3,780 ft; however, both FLUVIAL-11 and SEDIMENT-11 predicted smooth water-surface profiles in the vicinity of the bridge. Figure 22 shows two different water-surface profiles obtained by SDSU using the HEC-2 fixed-bed and FLUVIAL-11 movable-bed models. At a river distance of 3,925 ft, immediately upstream of the bridge, the HEC-2 fixed-bed model is seen to predict a water-surface elevation 5.8 ft higher than that of FLUVIAL-11. According to the SDSU report, the river channel in the vicinity of the bridge was predicted by FLUVIAL-11 to be scoured and widened extensively during the peak flow, resulting in much lower water-surface elevations than those predicted by the fixed-bed model. The results obtained by SLA using the UUWSR fixed-bed and movable-bed models are compared with the SLA's HEC-2 simulation in figure 23. The UUWSR fixed-bed model predicted much lower water-surface elevation upstream of the Via de Santa Fe bridge than HEC-2. The SLA report states that as much as 20 ft of scour was predicted by the UUWSR movable-bed model at the bridge section during the peak flow, lowering the water-surface elevation considerably, as seen in figure 23.

Thalweg elevations predicted by HEC2SR are shown in figure 24 together with field data acquired by the County of San Diego, California, in June 1981 (see table 18). The field data indicate that sand-mining pits were completely filled during the 1980 flood. HEC2SR predicted scour along the lower part of the study reach, downstream from the bridge, and stable river-bed patterns for the upper reach. On the other hand, UUWSR predicted a generally aggrading

SAN DIEGUITO RIVER: HEC2SR

ID	X	Y0	YF	Y	H	W	Q	V	QB	QS	QT	D50
	FT	FT	FT	FT	FT	FT	CFS	FPS	T/D	T/D	T/D	MM
43	0	14.5	11.1	12.0	26.1	601	22000	10.6	20070	183930	204000	0.58
44	800	23.6	22.6	22.9	30.0	736	22000	6.5	20070	183930	204000	0.58
45	1610	16.8	13.7	14.5	31.4	1009	22000	4.6	20070	183930	204000	0.58
46	2310	23.6	18.8	20.0	32.2	563	22000	10.3	20070	183930	204000	0.58
47	2790	19.7	15.5	16.7	33.6	326	22000	9.7	20070	183930	204000	0.58
48	3190	13.7	11.9	12.6	35.9	765	22000	2.8	5660	48280	53940	0.86
49	3440	18.2	15.1	16.3	35.9	467	22000	5.4	5660	48280	53940	0.86
50	3600	18.8	12.4	14.7	35.7	170	22000	11.6	5660	48280	53940	0.86
50.1	3780	25.0	15.1	17.5	38.4	317	22000	5.5	2680	21190	23870	0.91
51.1	3805	25.0	14.5	17.2	38.4	307	22000	5.8	2680	21190	23870	0.91
52	3930	10.9	16.5	11.8	39.0	474	22000	3.0	250	3570	3820	0.38
53	4350	13.3	14.8	13.5	39.2	1143	22000	1.2	250	3570	3820	0.38
54	4950	17.5	18.4	18.6	39.2	940	22000	2.2	4200	38700	42900	0.50
55	5460	22.7	24.9	25.0	39.1	616	22000	5.3	4200	38700	42900	0.50
56	6060	25.7	27.2	27.0	39.7	438	22000	5.2	4200	38700	42900	0.50
57	6590	27.2	27.6	27.5	40.0	294	22000	7.7	15560	164950	180510	0.57
58	7260	27.0	27.4	27.3	41.3	551	22000	4.0	15560	164950	180510	0.57
59	7770	27.8	28.5	28.3	41.2	230	22000	10.5	15560	164950	180510	0.57
60	8290	33.4	33.4	33.4	44.5	516	22000	11.3	14480	179730	194210	0.59
61	8870	37.3	37.3	37.3	50.8	493	22000	6.4	14480	179730	194210	0.59
62	9370	40.5	40.5	40.5	52.2	493	22000	5.0	14480	179730	194210	0.59
63	9820	40.9	40.9	40.9	52.9	507	22000	5.1	14480	179730	194210	0.59

ID=SECTION I.D.
X =RIVER DISTANCE
Y0=INITIAL THALWEG EL
YF=FINAL THALWEG EL
Y =THALWEG EL AT PEAK FLOW
H =W.S. EL AT PEAK FLOW
W =TOP WIDTH AT PEAK FLOW

Q =WATER DISCHARGE AT PEAK FLOW
V =MEAN VELOCITY AT PEAK FLOW
QB =BED-LOAD DISCHARGE AT PEAK FLOW
QS =SUS-LOAD DISCHARGE AT PEAK FLOW
QT =TOTAL-LOAD DISCHARGE AT PEAK FLOW
D50=MEDIAN DIAMETER OF BED MATERIAL AT PEAK FLOW

Table 15 Principal results computed by HEC2SR for the San Dieguito River

SAN DIEGUITO RIVER: FLUVIAL-11

ID	X	Y0	YF	Y	H	Hi	W	Q	V	QB	QS	QT	D50
	FT	FT	FT	FT	FT	FT	FT	CFS	FPS	T/D	T/D	T/D	MM
43	0	18.0	18.0	18.0	31.1	31.2	963	22000	4.0	-	-	366360	0.25
44	800	23.6	20.6	18.4	31.7	31.6	787	22000	4.3	-	-	373270	0.25
45	1610	16.8	23.5	26.3	32.5	32.4	1166	22000	3.8	-	-	396320	0.24
46	2310	23.6	25.6	22.5	33.1	32.9	857	22000	4.4	-	-	518590	0.25
47	2790	19.7	26.2	20.5	33.5	36.4	491	22000	5.5	-	-	637080	0.28
48	3190	13.7	26.4	24.7	33.9	36.8	482	22000	5.5	-	-	645830	0.25
49	3440	18.2	26.4	23.2	34.0	36.8	359	22000	6.2	-	-	719270	0.27
50	3600	18.0	26.5	21.1	34.1	36.8	266	22000	6.9	-	-	811580	0.27
51	3780	25.0	27.1	23.1	34.5	37.2	345	22000	5.8	-	-	902600	0.27
52	3925	10.9	26.9	24.9	34.7	40.5	439	22000	6.0	-	-	896690	0.27
53	4345	13.3	27.3	29.8	35.4	40.8	829	22000	5.1	-	-	960950	0.28
54	4945	17.5	29.3	30.3	36.5	40.9	758	22000	5.5	-	-	1189820	0.33
55	5455	22.7	30.4	27.7	37.4	41.0	644	22000	6.1	-	-	1377560	0.37
56	6055	25.7	31.6	31.1	38.4	41.2	452	22000	7.0	-	-	1491140	0.43
57	6585	27.2	32.4	30.9	39.4	41.4	346	22000	7.8	-	-	1502080	0.47
58	7255	27.0	33.4	34.4	41.0	42.3	451	22000	7.6	-	-	1820820	0.53
59	7765	27.8	35.5	34.8	42.5	42.4	501	22000	7.5	-	-	1860140	0.58
60	8285	33.4	37.7	37.1	44.1	44.5	536	22000	7.4	-	-	1861060	0.64
61	8865	37.3	39.2	40.4	46.0	49.6	517	22000	7.9	-	-	2251690	0.74
62	9365	40.5	41.2	40.9	47.7	51.0	442	22000	8.3	-	-	2088720	0.79
63	9815	40.9	40.9	40.9	49.4	51.7	444	22000	8.5	-	-	2344990	0.85

ID=SECTION I.D.
X =RIVER DISTANCE
Y0=INITIAL THALWEG EL
YF=FINAL THALWEG EL
Y =THALWEG EL AT PEAK FLOW
H =W.S. EL AT PEAK FLOW
Hi=W.S. EL AT PEAK FLOW (HEC-2)
W =TOP WIDTH AT PEAK FLOW
NOTE: QB & QS WERE NOT COMPUTED WITH FLUVIAL-11

Q = WATER DISCHARGE AT PEAK FLOW
V = MEAN VELOCITY AT PEAK FLOW
QB = BED-LOAD DISCHARGE AT PEAK FLOW
QS = SUS-LOAD DISCHARGE AT PEAK FLOW
QT = TOTAL-LOAD DISCHARGE AT PEAK FLOW
D50= MEDIAN DIAMETER OF BED MATERIAL AT PEAK FLOW

Table 16 Principal results computed by FLUVIAL-11 for the San Dieguito River

SAN DIEGUITO RIVER: SEDIMENT-4H

ID	X	Y0	YF	Y	H	H1	W	Q	V	QT	D50
	FT	FT	FT	FT	FT	FT	FT	CFS	FPS	T/D	MM
43	600	21.9	21.7	21.8	29.9	29.9	846	22100	5.1	2670	0.46
44	1400	24.1	24.0	24.1	30.6	30.6	818	22100	5.5	2760	0.46
45	2210	25.0	24.8	25.0	31.4	31.4	1165	22100	5.1	3100	0.46
46	2910	25.0	23.8	24.6	32.7	32.8	488	22100	8.7	4150	0.46
47	3390	23.0	23.8	23.1	33.7	34.0	693	22100	4.7	3670	0.46
48	3790	21.6	21.2	21.9	33.8	34.1	690	22100	3.2	3130	0.46
49	4040	22.9	22.4	22.8	33.9	34.2	415	22100	7.1	3430	0.46
50	4200	24.4	22.9	24.1	34.2	34.5	237	22100	9.0	3940	0.46
51	4380	24.4	20.2	22.4	34.6	35.3	283	22100	9.6	4290	0.46
52	4530	20.6	21.0	20.9	34.8	35.9	523	22100	3.8	3140	0.46
53	4950	18.2	19.0	18.7	34.8	35.9	944	22099	1.8	1543	0.46
54	5550	21.2	22.7	21.2	34.8	36.0	1066	22099	3.0	2550	0.46
55	6060	24.9	20.3	24.6	35.3	36.3	313	22100	8.6	3920	0.46
56	6600	26.9	28.9	27.0	35.9	36.7	544	22099	5.6	3790	0.46
57	7190	27.2	27.2	27.1	36.8	37.3	325	22100	9.3	3700	0.46
58	7860	27.8	30.5	28.1	37.7	38.1	470	22100	6.1	3980	0.46
59	8370	28.9	31.1	28.3	38.8	39.3	193	22100	12.2	4260	0.70
60	8890	34.1	33.0	34.0	45.9	46.1	495	22100	10.6	4680	0.70
61	9470	39.6	40.6	40.1	52.2	52.0	625	22100	4.9	5130	0.70
62	9920	41.0	41.9	41.6	52.5	52.2	544	22100	5.2	7460	0.70
63	10420	41.1	41.3	41.2	52.7	52.4	542	22100	5.0	9780	0.70

ID=SECTION ID
X =RIVER DISTANCE
Y0=INITIAL THALWEG EL
YF=FINAL THALWEG EL
Y =THALWEG EL AT PEAK FLOW
H =W.S. EL AT PEAK FLOW
H1=W.S. EL AT PEAK FLOW COMPUTED USING FIXED-BED FLOOD-ROUTING MODEL
W = TOP WIDTH AT PEAK FLOW
Q = WATER DISCHARGE AT PEAK FLOW
V = MEAN VELOCITY AT PEAK FLOW
QT = TOTAL-LOAD DISCHARGE AT PEAK FLOW
D50= MEDIAN SIZE OF BED MATERIAL AT PEAK FLOW
NOTE: RESULTS SHOWN ARE FOR ENTIRE CROSS-SECTION OF MAIN AND OVERBANK CHANNELS

Table 17 Principal results computed by SEDIMENT-4H for the San Dieguito River

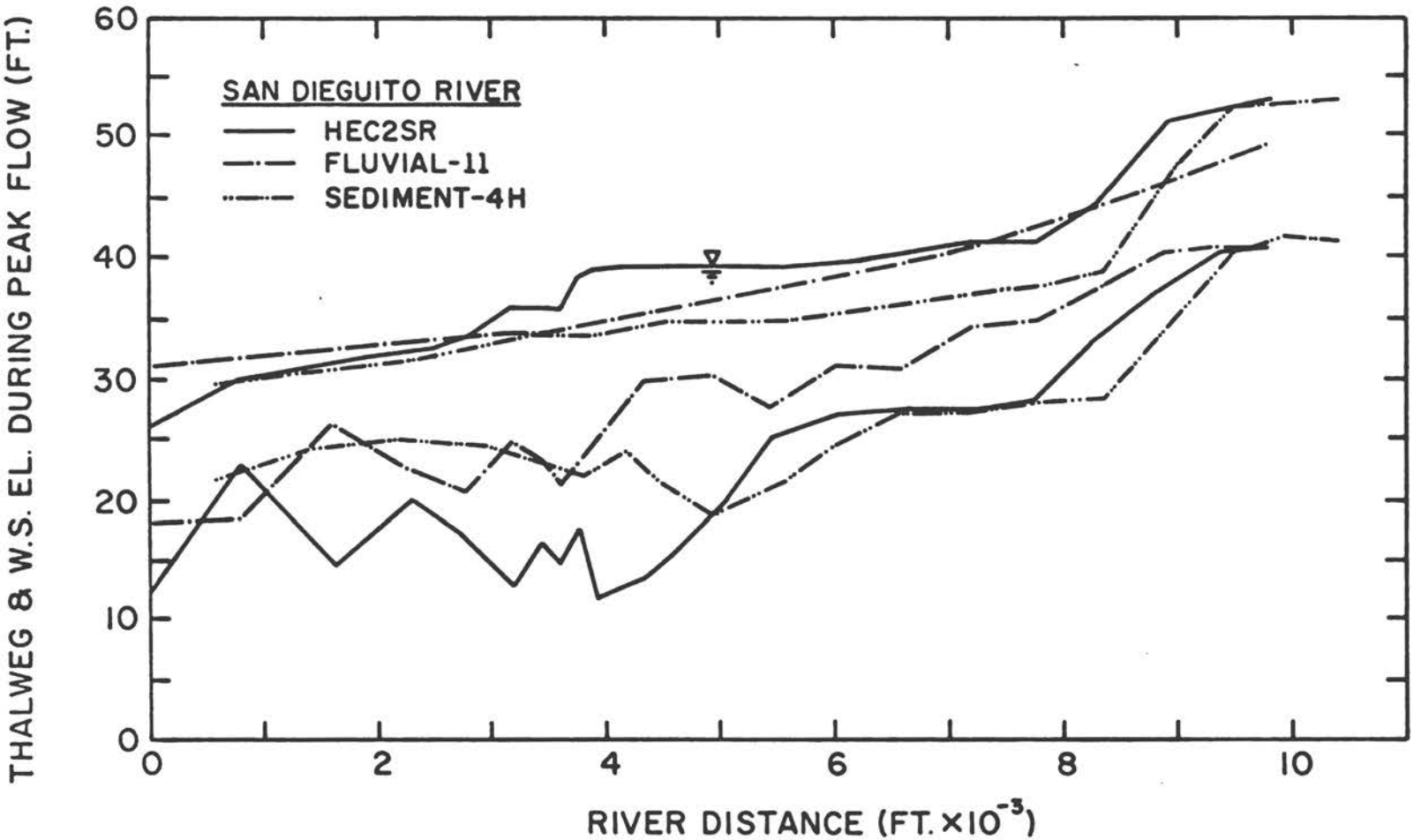

Figure 21 Comparison of thalweg and water-surface profiles at peak flow computed using the HEC2SR, FLUVIAL-11, and SEDIMENT-4H movable-bed models for the San Dieguito River

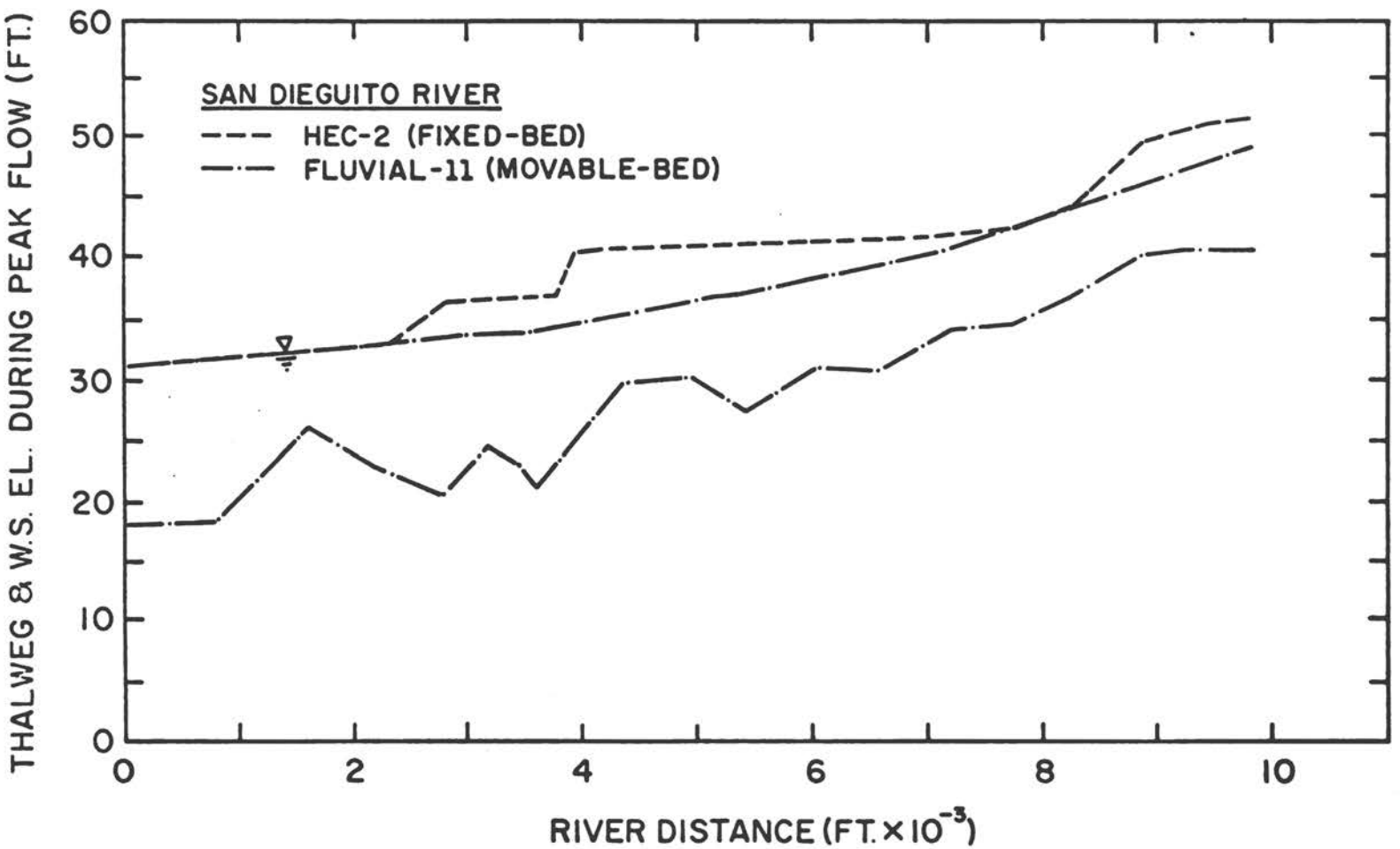

Figure 22 Comparison of water-surface profiles at peak flow computed by SDSU using HEC-2 and FLUVIAL-11 for the San Dieguito River

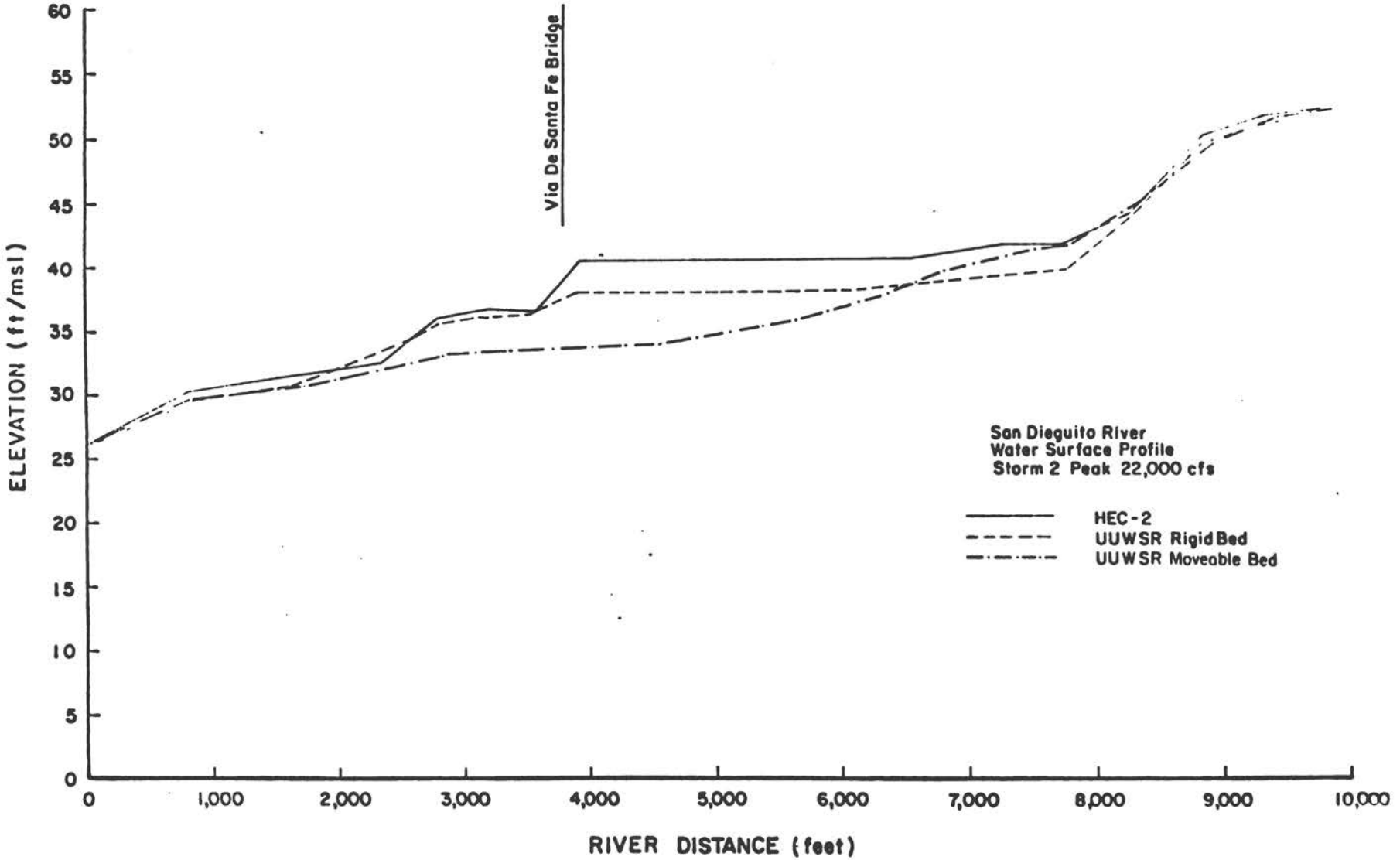

Figure 23 Comparison of water-surface profiles at peak flow computed by SLA using HEC-2, and the UUWSR fixed-bed and movable-bed models for the San Dieguito River

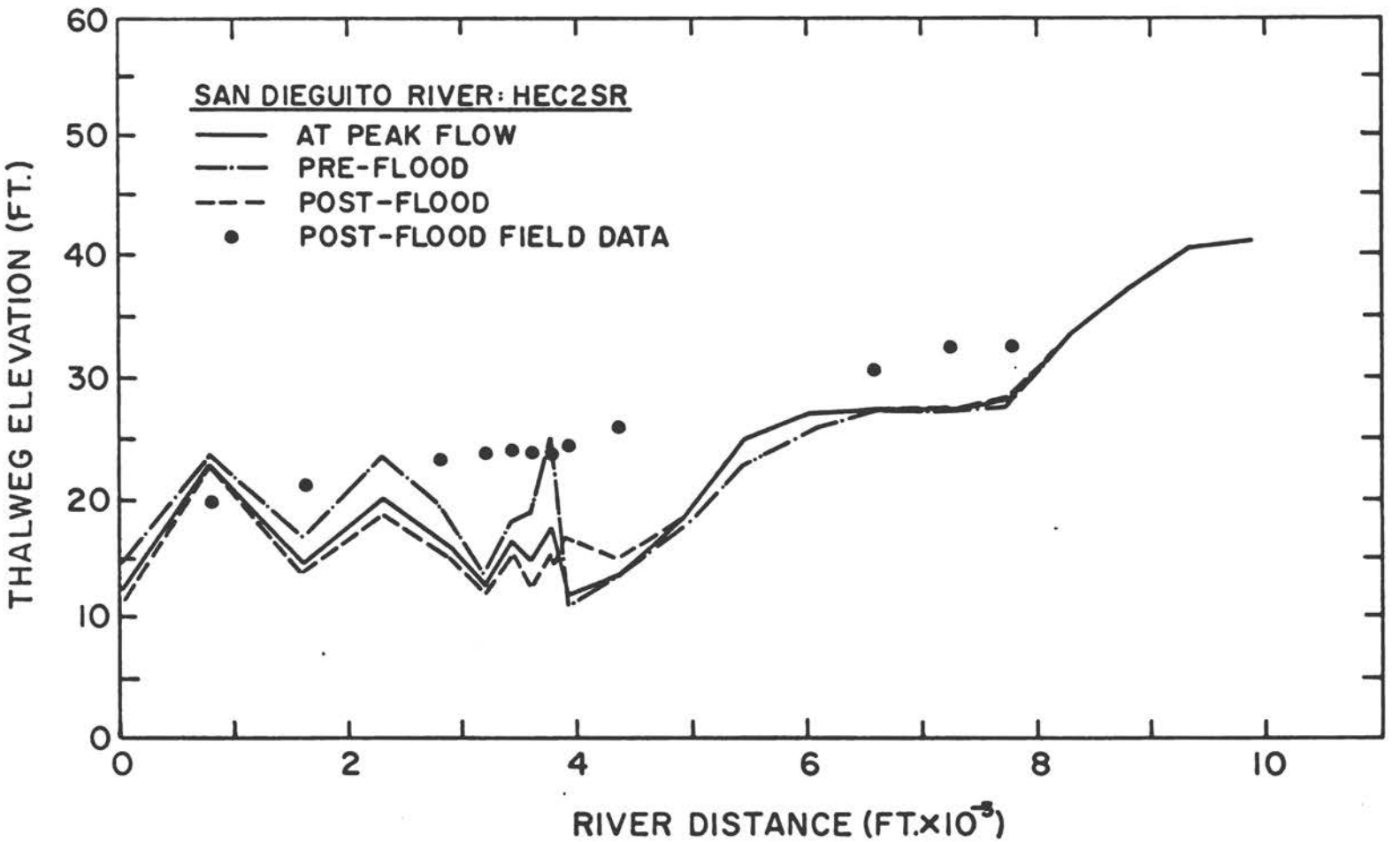

Figure 24 Thalweg profiles predicted by SLA using HEC2SR for the San Dieguito River

SAN DIEGUITO RIVER

X-SECTION ID	RIVER DISTANCE	OBSERVED THALWEG ELEVATION
	FT	FT
44	800	19.9
45	1610	21.4
47	2790	23.3
48	3190	23.8
49	3440	24.1
50	3600	23.8
50.1	3780	23.9
52	3930	24.4
53	4350	26.0
57	6590	30.4
58	7260	32.4
59	7770	32.4

NOTE: CROSS-SECTION DATA SHOWN WERE OBTAINED IN JUNE 1981 BY DEPARTMENT OF PUBLIC WORKS, COUNTY OF SAN DIEGO, CALIFORNIA.

THE HIGHEST WATER-SURFACE ELEVATION OBSERVED AT SECTION 52 (X = 3,930 FT) OF THE SAN DIEGUITO RIVER WAS APPROXIMATELY 36 FT ABOVE MSL.

Table 18 Thalweg elevations measured in June 1981 for the San Dieguito River

channel over the entire study reach, as seen in figure 25. FLUVIAL-11 predictions, shown in figure 26, indicate general deposition throughout the reach. It should be pointed out that FLUVIAL-11 allows for bank erosion, so variable river width is incorporated into the model, while UUWSR considers changes in cross-section profile for a fixed river width. Figure 27 shows the thalweg elevations predicted by SEDIMENT-4H. These profiles were plotted using output-summary tables submitted by RMA. As seen in the figure, the pre-flood, initial thalweg profile does not conform to the input data supplied to RMA (compare figure 27 with figure 24 or 26, for example, for the initial thalweg profile). It must be pointed out that because of RMA's failure to respond to requests for clarification, the results from SEDIMENT-4H presented in this report are based entirely on RMA's output summaries submitted to the Committee, and no modification or adjustment of their tabulated values could be made in spite of the fact that inconsistencies between the summarized values and computer output listings were detected and brought to their attention.

Longitudinal distributions of the mean flow velocity predicted by the HEC2SR, FLUVIAL-11, and SEDIMENT-4H movable-bed models are shown in figue 28. FLUVIAL-11 predicted gradual changes in the mean flow velocity between 3.8 ft/s and 8.5 ft/s; however, HEC2SR's predictions are seen to vary abruptly from cross section to cross section, with a variation range of 1.2 ft/s to 11.6 ft/s (see tables 15 and 16). The range of variation predicted by SEDIMENT-4H is seen to be between 1.8 ft/s and 12.2 ft/s (see table 17). Longitudinal variations of the water-surface width during the flood peak are presented in figure 29, in which the three models are seen to yield quite different results.

Table 19 lists total-load discharges during the peak flow and post-flood median bed-material sizes predicted by HEC2SR, FLUVIAL-11, and SEDIMENT-4H. The total-load predictions differ widely among these three models, as seen in figure 30. RMA's results were not included in the figure because of their small values. FLUVIAL-11 predicted extremely high total-load discharges with an almost linearly increase along the study reach. At a river distance of 9,815 ft, the total-load discharges predicted by HEC2SR, FLUVIAL-11, and SEDIMENt-4H were approximately 194,000 tons/day, 2,345,000 tons/day, and 7,000

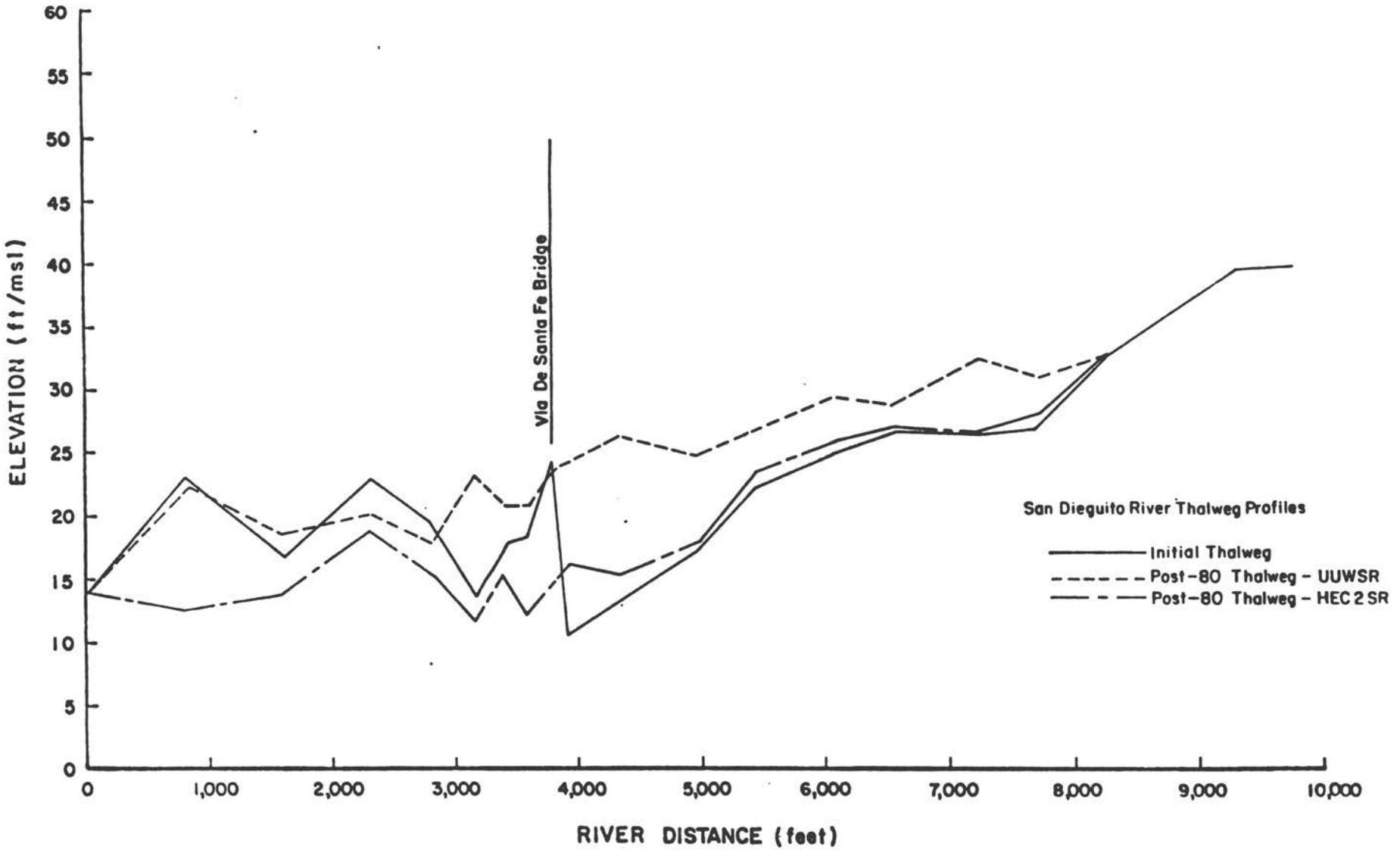

Figure 25 Comparison of post-flood thalweg profiles computed by SLA using UUWSR and HEC2SR for the San Dieguito River

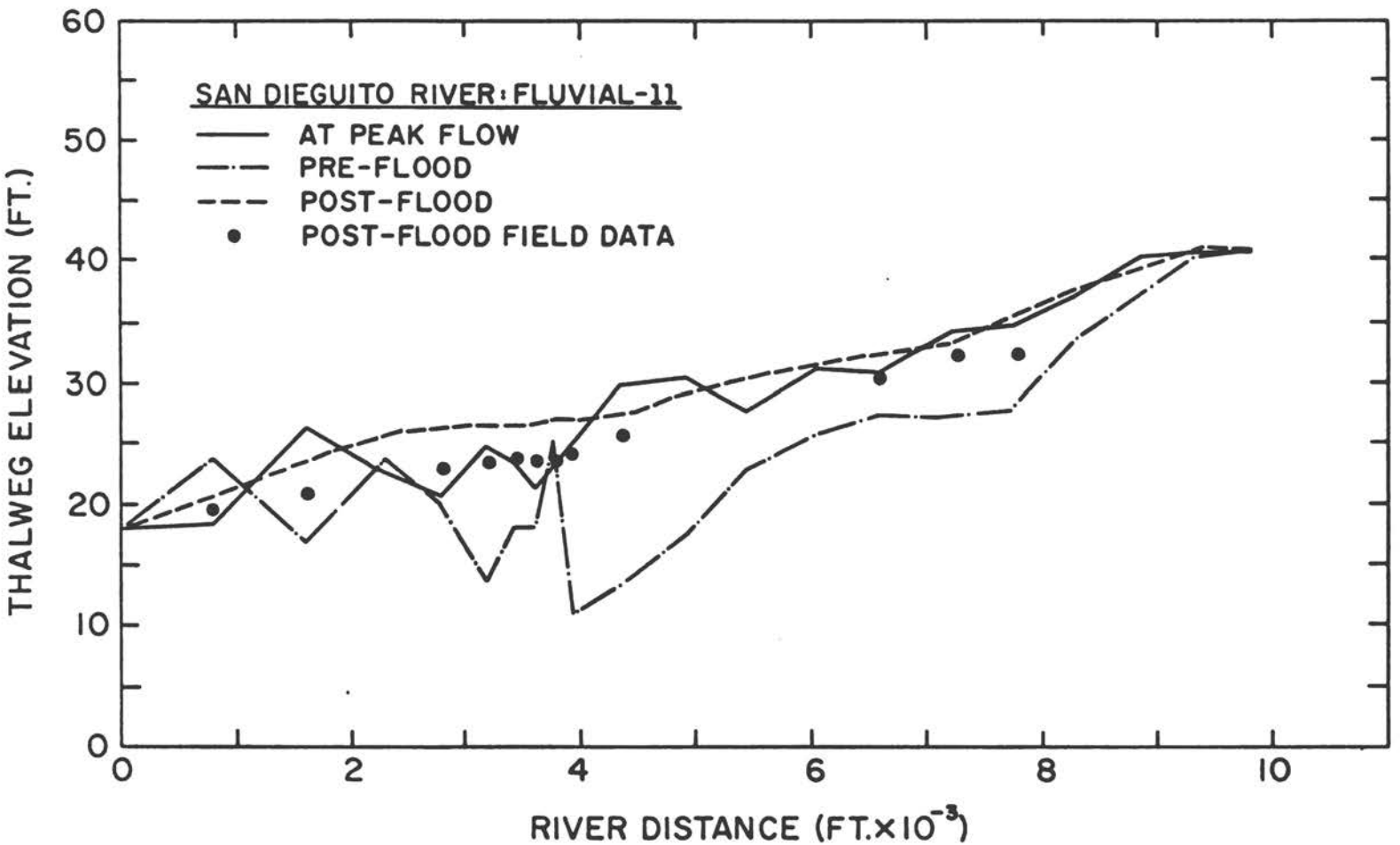

Figure 26 Thalweg profiles predicted by SDSU using FLUVIAL-11 for the San Dieguito River

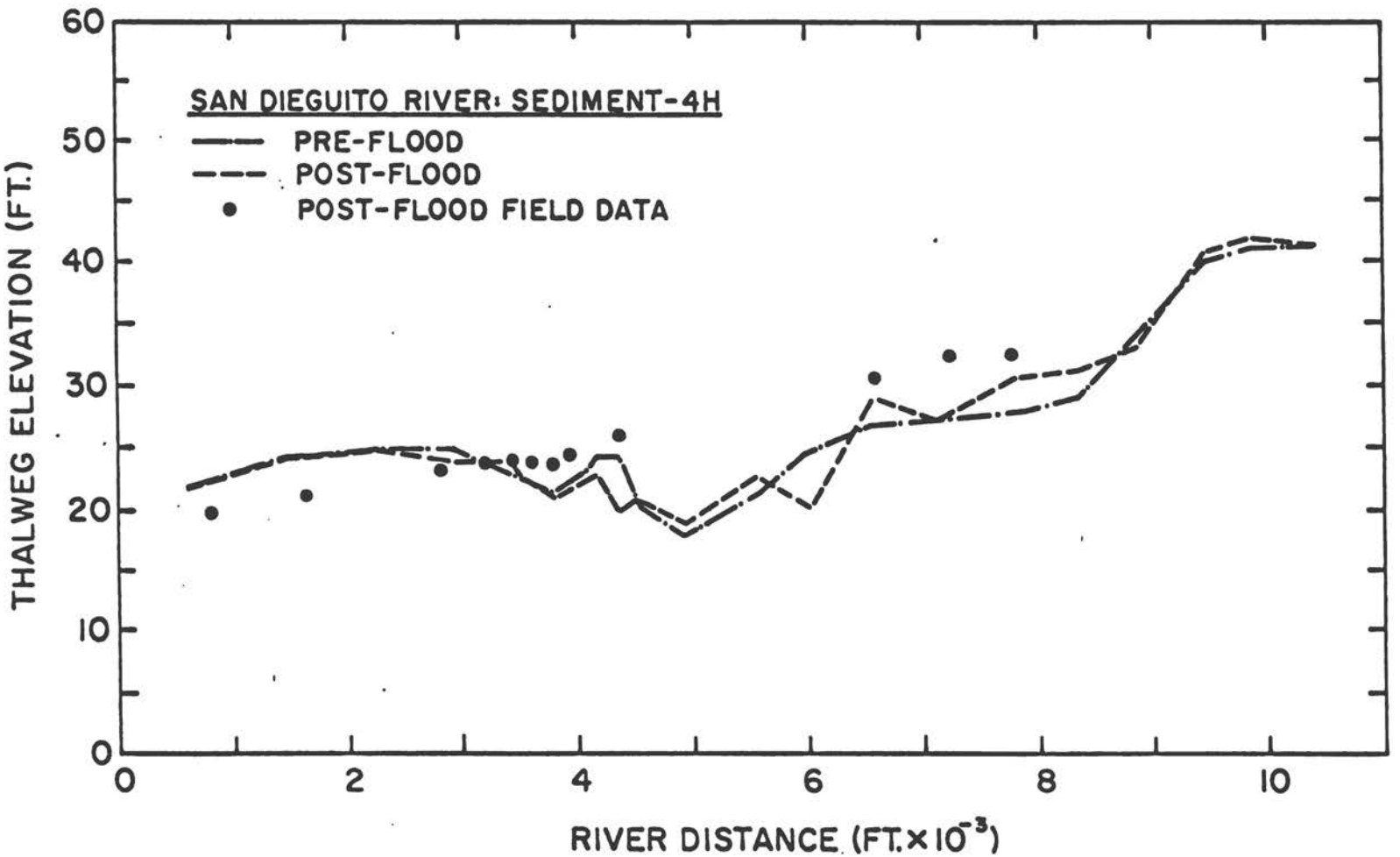

Figure 27 Thalweg profiles predicted by RMA using SEDIMENT-4H for the San Dieguito River

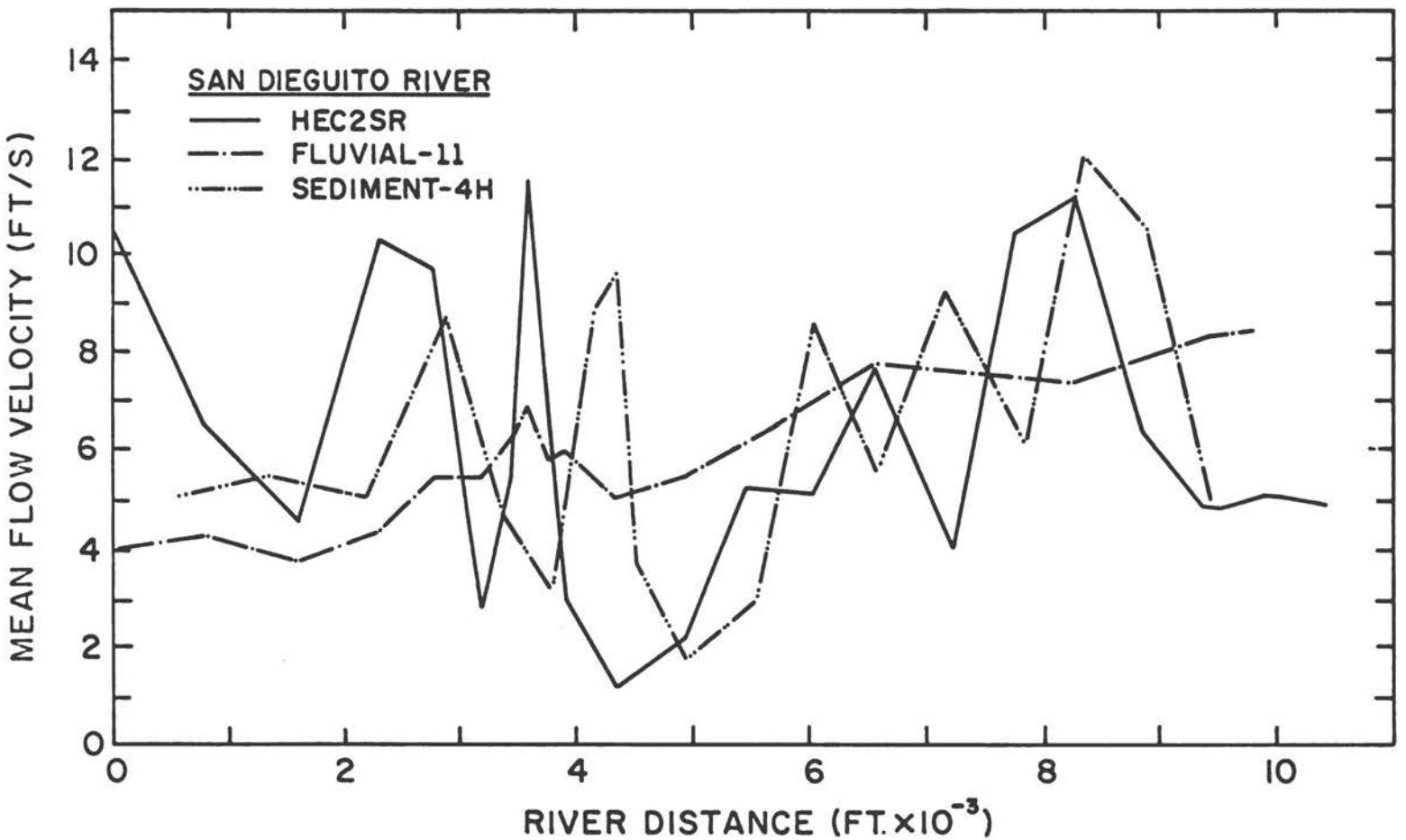

Figure 28 Longitudinal distributions of mean flow velocity at peak flow computed using the HEC2SR, FLUVIAL-11, and SEDIMENT-4H movable-bed models for the San Dieguito River

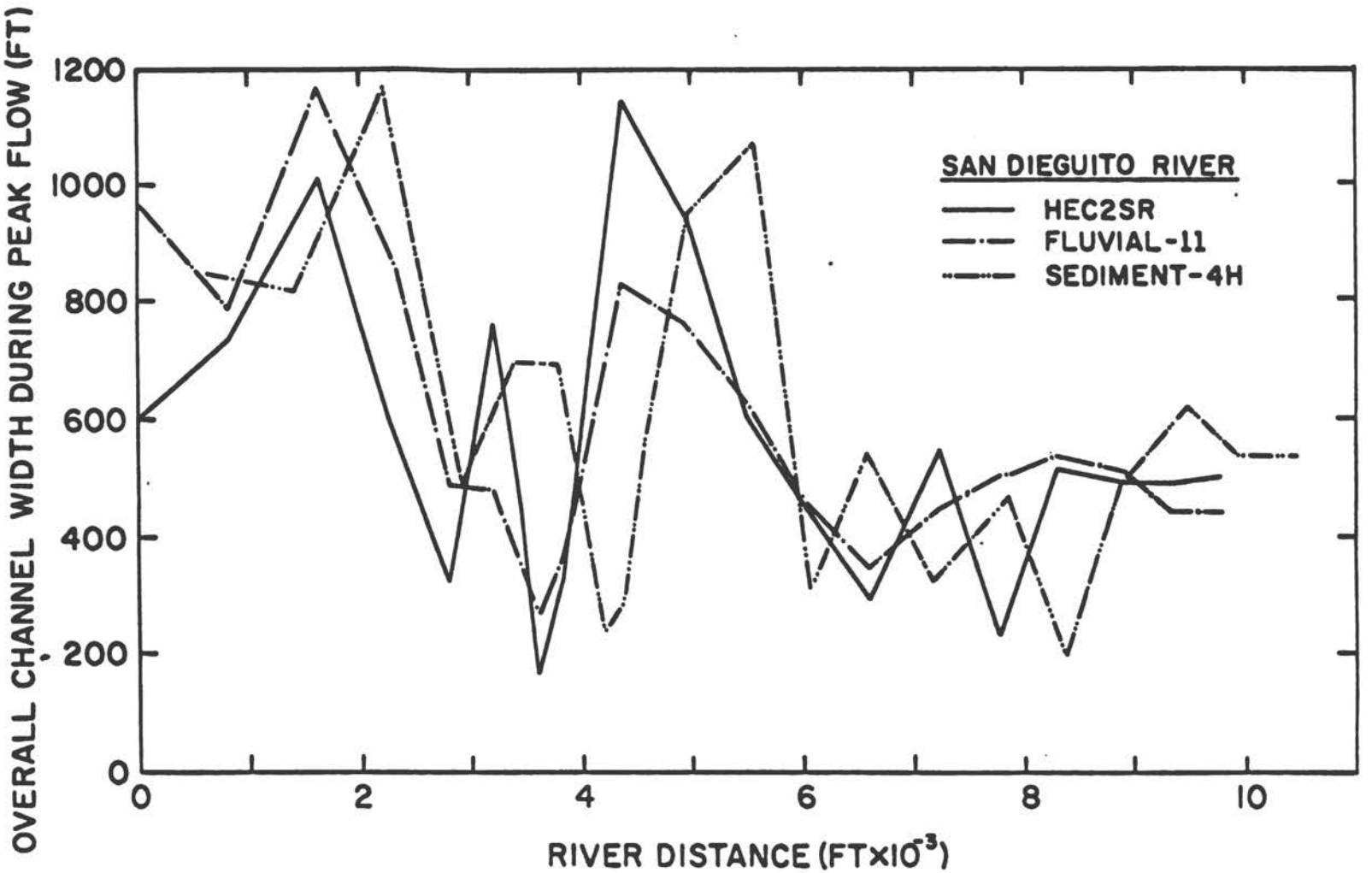

Figure 29 Water-surface widths at peak flow predicted by the HEC2SR, FLUVIAL-11, and SEDIMENT-4H movable-bed models for the San Dieguito River

SAN DIEGUITO RIVER			(FLUVIAL-11)		(HEC2SR)		(SEDIMENT-4H)		
ID	X	D50I	QT	D50F	QT	D50F	X	QT	D50F
	FT	MM	T/D	MM	T/D	MM	FT	T/D	MM
43	0	--	366360	0.23	204000	0.87	600	2670	0.46
44	800	0.46	373270	0.25	204000	0.87	1400	2760	0.46
45	1610	-	396320	0.25	204000	0.87	2210	3100	0.46
46	2310	-	518590	0.25	204000	0.87	2910	4150	0.46
47	2790	-	637080	0.25	204000	0.87	3390	3670	0.46
48	3190	-	645830	0.26	53940	0.92	3790	3130	0.46
49	3440	-	719270	0.27	53940	0.92	4040	3430	0.46
50	3600	--	811580	0.28	53940	0.92	4200	3940	0.46
51	3780	-	902600	0.28	23870	1.04	4380	4290	0.46
52	3925	--	896690	0.28	3820	0.30	4530	3140	0.46
53	4345	--	960950	0.30	3820	0.30	4950	1543	0.46
54	4945	-	1189820	0.33	42900	0.53	5550	2550	0.46
55	5455	--	1377560	0.36	42900	0.53	6060	3920	0.46
56	6055	--	1491140	0.40	42900	0.53	6600	3790	0.46
57	6585	-	1502880	0.46	180510	0.55	7190	3700	0.46
58	7255	--	1828820	0.54	180510	0.55	7860	3980	0.46
59	7765	0.70	1860140	0.58	180510	0.55	8370	4260	0.70
60	8285	--	1861060	0.58	194210	0.59	8890	4680	0.70
61	8065	-	2251690	0.67	194210	0.59	9470	5130	0.70
62	9365	-	2088720	0.81	194210	0.59	9920	7460	0.70
63	9815	-	2344990	0.85	194210	0.59	10420	9780	0.70

ID = SECTION I.D.
X = RIVER DISTANCE
D50I = INITIAL MEDIAN SIZE OF BED MATERIAL (PRE-FLOOD)
D50F = FINAL MEDIAN SIZE OF BED MATERIAL (POST-FLOOD)
QT = TOTAL-LOAD DISCHARGE AT PEAK-FLOW DISCHARGE OF 22,000 CFS

Table 19 Total-load discharges at peak flow and final median bed-material sizes computed by HEC2SR, FLUVIAL-11, and SEDIMENT-4H for the San Dieguito River

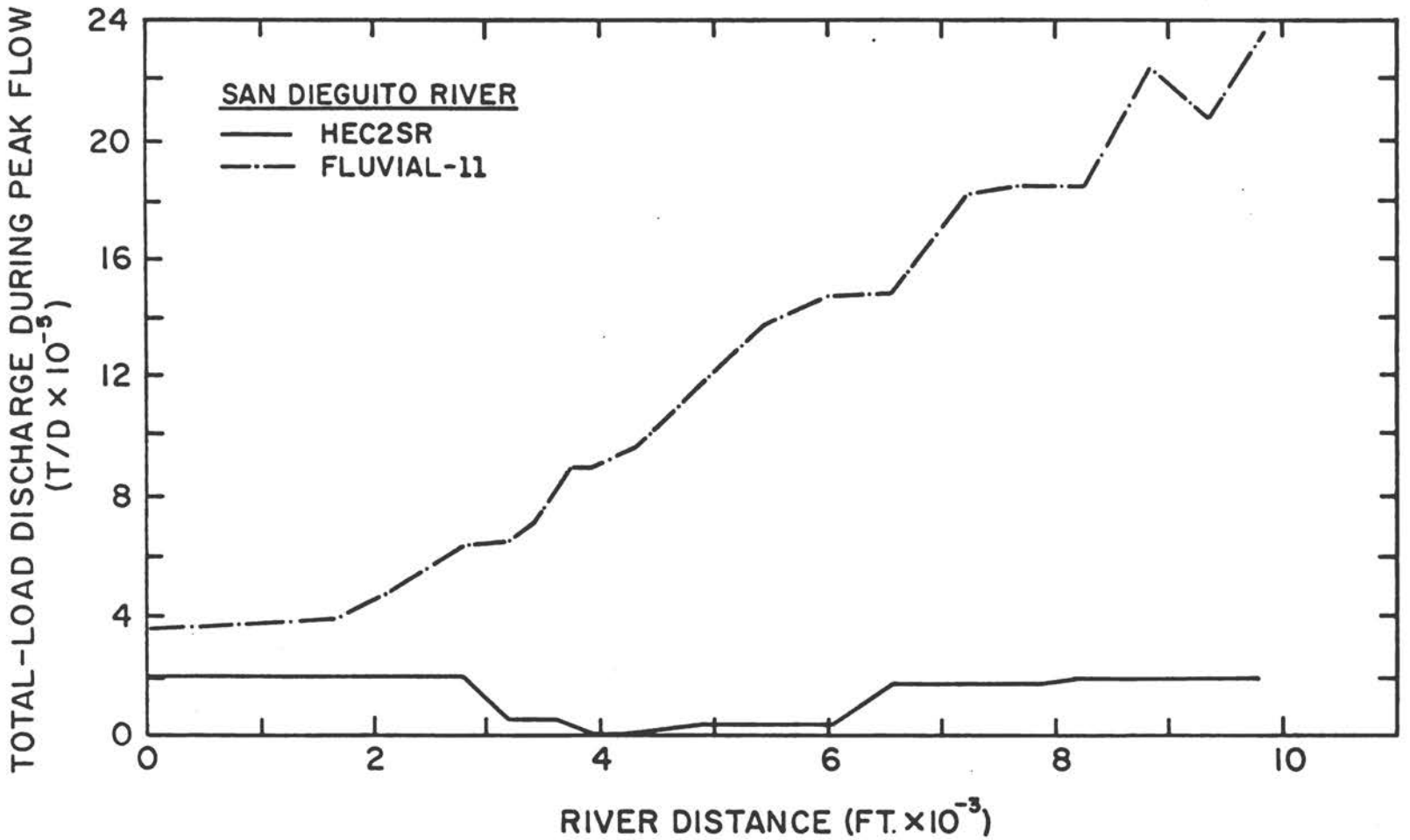

Figure 30 Total-load discharges at peak flow predicted by HEC2SR and FLUVIAL-11 for the San Dieguito River

tons/day, respectively; these values for a peak discharge of 22,000 cfs correspond to sediment concentrations of approximately 3,270 mg/l, 39,480 mg/l, and 120 mg/l, respectively. Longitudinal distributions of the median bed-material size at peak flow are shown in figure 31. Thalweg and water-surface elevations predicted by these three movable-bed models for the rising and falling limbs of the hydrograph are tabulated in tables 20, 21, and 22. During the falling stage, at a discharge of approximately 12,000 cfs, HEC2SR predicted generally much higher water-surface elevations, as seen in tables 20 and 21.

3. Salt River. Four movable-bed models, HEC2SR, HEC-6, FLUVIAL-11, and SEDIMENT-4H, were used to simulate a 100-yr flood with a peak discharge of 176,000 cfs; the principal hydraulic and sediment-transport parameters computed are summarized in tables 23, 24, 25, and 26, respectively. Note that additional water-surface elevations predicted by SDSU and RMA using the HEC-2 and SEDIMENT-4H fixed-bed models are also listed in tables 25 and 26, respectively. The peak-flow thalweg and water-surface elevations predicted by these four models are presented in figure 32. HEC2SR is seen to predict somewhat lower water-surface elevations in the middle reach than the other three models. At a river distance of 10,120 ft, the difference of the water-surface elevations between HEC2SR and FLUVIAL-11 amounts to 2.2 ft. Water-surface profiles predicted by HEC-6, FLUVIAL-11, and SEDIMENT-4H are seen to be similar to each other, while their thalweg-elevation predictions are quite different. As seen in tables 23 and 25, HEC2SR predicted a general trend of scour over the entire reach, while FLUVIAL-11 predicted deposition. Thalweg elevations predicted by HEC-6 and SEDIMENT-4H seem to fall between those of HEC2SR and FLUVIAL-11. At a river distance of 12,150 ft, FLUVIAL-11 predicted a thalweg elevation 9 ft higher than that of HEC2SR; however, the water-surface elevation predicted by FLUVIAL-11 was higher by only 1.8 ft. Similarly, at a river distance of 15,500 ft, the thalweg elevation obtained from FLUVIAL-11 was 11 ft higher than that computed by HEC2SR, but the water-surface elevations predicted by those models were almost identical (see tables 23 and 25). It should be pointed out that overall changes in thalweg elevations predicted by HEC2SR conformed quite well to those observed in the CSU movable-bed physical model (Anderson-Nichols, 1980) at a prototype discharge of 210,000 cfs.

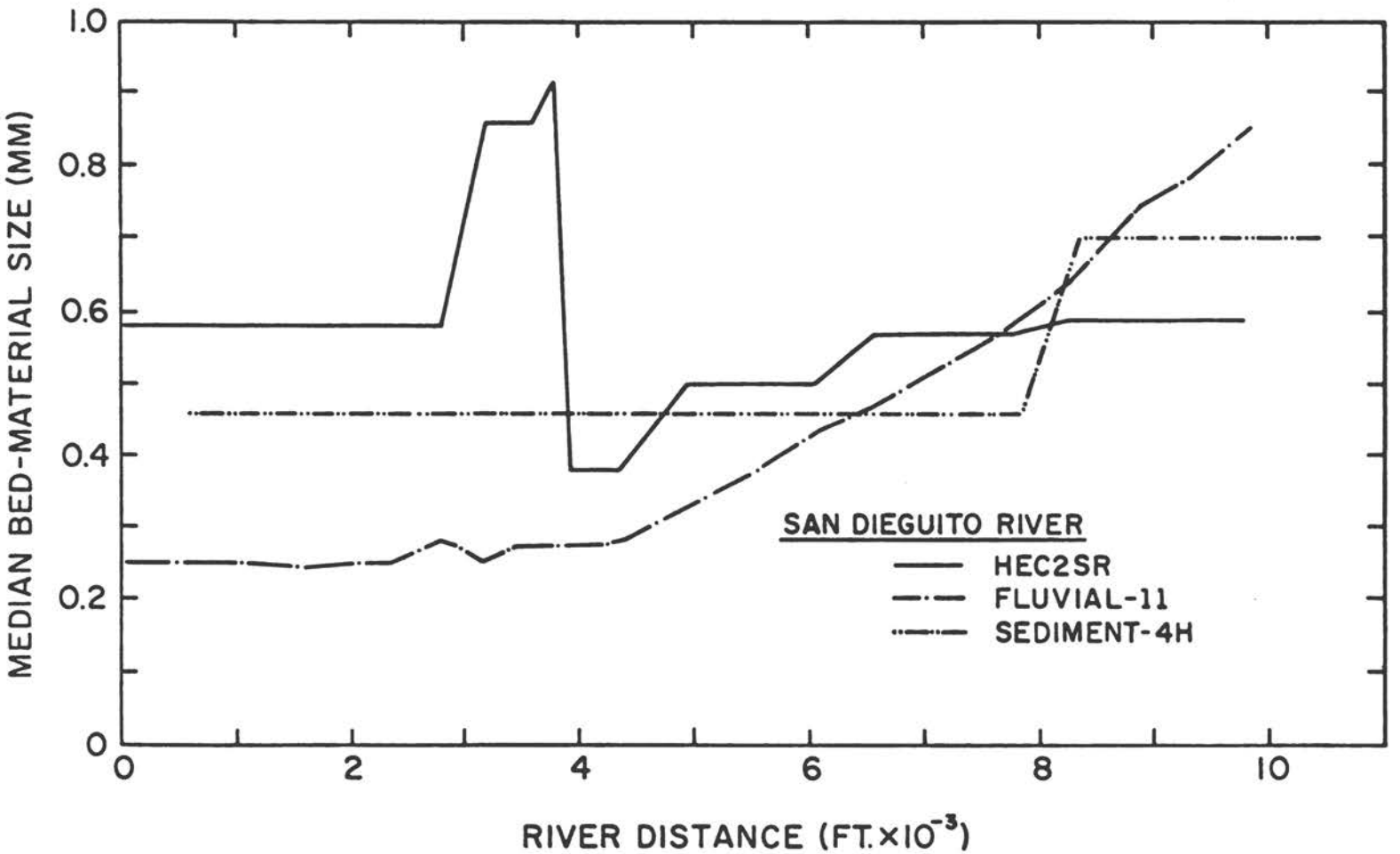

Figure 31 Longitudinal distributions of median bed-material size at peak flow computed using HEC2SR, FLUVIAL-11, and SEDIMENT-4H for the San Dieguito River

SAN DIEGUITO RIVER: HEC2SR

ID	X	YR	HR	YFA	HFA
	FT	FT	FT	FT	FT
43	0	13.6	23.2	11.2	24.3
44	800	23.4	27.1	22.6	28.1
45	1610	15.8	28.1	13.9	29.4
46	2310	22.1	29.0	19.0	30.2
47	2790	18.8	30.3	15.7	31.4
48	3190	13.9	30.7	11.9	32.3
49	3440	18.7	30.7	15.1	32.3
50	3600	19.6	30.7	12.5	32.3
50.1	3780	21.8	31.3	15.2	33.4
51.1	3805	21.8	31.3	14.6	33.4
52	3930	11.1	31.9	14.9	33.7
53	4350	13.4	31.9	14.4	33.9
54	4950	17.8	31.9	18.9	33.9
55	5460	23.2	31.9	25.7	34.2
56	6060	25.9	32.7	27.5	37.1
57	6590	27.3	33.1	27.6	37.4
58	7260	27.1	33.9	27.4	38.2
59	7770	27.9	34.0	28.4	38.2
60	8290	33.4	41.9	33.4	43.2
61	8070	37.3	46.6	37.3	48.7
62	9370	40.5	47.4	40.5	49.8
63	9820	40.9	47.7	40.9	50.3

ID =SECTION I.D.
X =RIVER DISTANCE
YR =THALWEG EL AT Q=5,000 CFS (RISING STAGE)
HR =W.S. EL AT Q=5,000 CFS (RISING STAGE)
YFA=THALWEG EL AT Q=12,000 CFS (FALLING STAGE)
HFA=W.S. EL AT Q=12,000 CFS (FALLING STAGE)

Table 20 Thalweg and water-surface elevations during rising and falling stages computed by HEC2SR for the San Dieguito River

SAN DIEGUITO RIVER: FLUVIAL-11

ID	X	YR	HR	YFA	HFA
	FT	FT	FT	FT	FT
43	0	18.0	25.7	18.0	27.8
44	800	19.2	26.8	20.5	28.9
45	1610	20.1	27.8	26.1	30.2
46	2310	20.1	28.5	24.6	31.2
47	2790	19.7	29.0	25.8	31.7
48	3190	19.0	29.2	25.5	32.2
49	3440	18.5	29.2	25.6	32.4
50	3600	18.5	29.3	25.6	32.6
51	3780	18.6	29.5	26.2	32.9
52	3925	10.9	29.7	26.6	33.0
53	4345	23.0	29.8	28.9	33.8
54	4945	24.6	29.8	29.6	34.9
55	5455	23.8	30.4	30.8	35.8
56	6055	27.9	31.7	31.3	36.9
57	6585	28.9	32.9	32.5	37.9
58	7255	29.9	34.9	34.7	39.5
59	7765	33.1	36.5	36.4	40.8
60	8285	35.6	38.5	37.8	42.2
61	8865	37.4	40.8	38.8	43.7
62	9365	39.5	43.1	41.3	45.5
63	9815	40.9	45.3	40.9	47.4

ID=SECTION I.D.
X =RIVER DISTANCE
YR =THALWEG EL AT Q=4,695 CFS (RISING STAGE)
HR =W.S. EL AT Q=4,695 CFS (RISING STAGE)
YFA=THALWEG EL AT Q=12,180 CFS (FALLING STAGE)
HFA=W.S. EL AT Q=12,180 CFS (FALLING STAGE)

Table 21 Thalweg and water-surface elevations during rising and falling stages computed by FLUVIAL-11 for the San Dieguito River

SAN DIEGUITO RIVER:SEDIMENT-4H

ID	X	YR	HR	YFA	HFA
	FT	FT	FT	FT	FT
43	600	20.0	26.1	19.9	28.2
44	1400	22.7	27.0	22.7	29.0
45	2210	23.6	28.0	23.5	29.9
46	2910	23.3	28.9	22.0	30.9
47	3390	20.1	29.6	20.2	31.6
48	3790	17.7	29.6	17.9	31.7
49	4040	18.8	29.7	18.3	31.8
50	4200	20.9	29.7	19.1	31.9
51	4380	20.9	30.1	16.4	32.0
52	4530	16.4	30.4	15.9	32.1
53	4950	14.2	30.4	14.6	32.2
54	5550	19.5	30.4	19.3	32.2
55	6060	24.9	30.7	24.2	32.6
56	6600	26.9	31.1	27.1	33.3
57	7190	27.2	32.0	26.9	34.4
58	7860	27.8	32.7	28.5	35.4
59	8370	29.1	33.3	27.6	36.1
60	8890	34.1	42.1	33.7	43.9
61	9470	39.9	50.4	40.3	51.4
62	9920	41.7	50.4	41.6	51.5
63	10420	41.4	50.4	40.8	51.6

ID =SECTION ID
X =RIVER DISTANCE
YR =THALWEG EL AT Q=4,360 CFS (RISING STAGE)
HR =W.S. EL AT Q=4,360 CFS (RISING STAGE)
YFA=THALWEG EL AT Q=12,940 CFS (FALLING STAGE)
HFA=W.S. EL AT Q=12,940 CFS (FALLING STAGE)

Table 22 Thalweg and water-surface elevations during rising and falling stages computed by SEDIMENT-4H for the San Dieguito River

SALT RIVER: HEC2SR

X	Y0	YF	Y	H	W	Q	V	QB	QS	QT	D50
FT	FT	FT	FT	FT	FT	CFS	FPS	T/D	T/D	T/D	MM
0	1079.2	1079.2	1079.2	1089.3	934	166320	17.8	-	-	2306010	49.0
150	1079.3	1079.3	1079.3	1091.4	912	166320	15.2	-	-	2306010	49.0
450	1079.6	1079.6	1079.6	1092.2	828	166320	16.2	-	-	2306010	49.0
800	1080.0	1080.2	1078.0	1094.0	749	166320	14.8	-	-	2306010	56.0
910	1080.0	1080.2	1078.0	1094.6	751	166320	13.5	-	-	2306010	56.0
1520	1080.7	1080.9	1078.6	1096.3	746	166320	12.8	-	-	2306010	56.0
1920	1081.1	1080.6	1082.7	1097.7	1122	166320	11.1	-	-	2321440	52.0
2520	1081.7	1081.2	1083.8	1098.5	1064	166320	12.6	-	-	2321440	52.0
3120	1084.5	1084.2	1086.5	1100.0	1176	166320	12.4	-	-	2321440	52.0
3520	1085.5	1084.4	1085.4	1100.9	1054	166320	12.4	-	-	2284790	79.0
4240	1087.3	1086.3	1087.3	1102.3	1025	166320	13.2	-	-	2284790	79.0
4840	1088.8	1087.8	1088.7	1104.1	1075	166320	12.3	-	-	2284790	79.0
5440	1090.4	1089.5	1090.4	1105.3	994	166320	13.7	-	-	2284790	79.0
6040	1092.0	1089.5	1089.1	1106.7	833	166320	13.8	-	-	2264580	106.0
6910	1094.2	1091.7	1091.3	1108.6	825	166320	14.2	-	-	2264580	106.0
7310	1095.3	1092.1	1090.3	1110.0	791	166320	13.0	-	-	2202860	126.0
7510	1095.8	1092.2	1090.3	1109.6	645	166320	15.6	-	-	2202860	126.0
7660	1096.2	1092.7	1090.8	1110.1	657	166320	15.4	-	-	2202860	126.0
7860	1096.7	1093.6	1091.7	1111.4	759	166320	13.4	-	-	2202860	126.0
8260	1097.7	1094.1	1095.0	1112.0	831	166320	14.3	-	-	2151420	154.0
8920	1099.4	1095.8	1096.7	1113.6	829	166320	14.4	-	-	2151420	154.0
9520	1101.0	1097.4	1098.3	1115.1	827	166320	14.5	-	-	2151420	154.0
10120	1102.6	1099.1	1099.9	1116.7	826	166320	14.4	-	-	2151420	154.0
10320	1103.1	1098.1	1099.6	1117.4	801	166320	14.8	-	-	2050060	120.0
10720	1104.6	1099.6	1101.1	1118.5	864	166320	13.5	-	-	2050060	120.0
11120	1106.0	1100.7	1102.5	1120.1	1060	166320	11.6	-	-	2050060	120.0
11320	1106.8	1101.6	1103.2	1120.3	1051	166320	12.1	-	-	2050060	120.0
11520	1107.5	1102.2	1103.8	1120.3	984	166320	13.4	-	-	2050060	120.0
11730	1108.3	1103.5	1104.9	1122.3	1415	166320	9.5	-	-	2050060	120.0
12150	1109.7	1104.6	1107.6	1122.8	1624	166320	9.7	-	-	1963050	108.0
12570	1111.2	1106.1	1109.0	1123.4	1574	166320	10.8	-	-	1963050	108.0
12990	1112.7	1107.6	1110.5	1124.6	1551	166320	11.3	-	-	1963050	108.0
13640	1117.7	1112.3	1115.5	1129.8	1513	166320	12.3	-	-	1963050	108.0
14440	1117.8	1113.9	1116.2	1132.9	2342	166320	7.6	-	-	1963050	108.0
15500	1118.5	1117.8	1118.0	1134.2	3529	166320	5.7	-	-	1940900	86.0
16620	1121.3	1120.5	1120.8	1135.1	2176	166320	10.0	-	-	1940900	86.0
17880	1126.3	1125.4	1125.7	1139.0	1623	166320	11.5	-	-	1940900	86.0
19520	1131.3	1132.6	1134.0	1143.8	2926	166320	7.9	-	-	1940190	6.6
20820	1129.7	1131.2	1132.5	1145.7	2968	166320	6.5	-	-	1940190	6.6
21820	1131.2	1131.2	1131.2	1146.6	1787	166320	8.1	-	-	2271650	49.0
22920	1129.0	1129.0	1129.0	1146.8	803	166320	14.5	-	-	2271650	49.0

ID=SECTION I.D.
X =RIVER DISTANCE
Y0=INITIAL THALWEG EL
YF=FINAL THALWEG EL
Y =THALWEG EL AT PEAK FLOW
H =W.S. EL AT PEAK FLOW
W =TOP WIDTH AT PEAK FLOW
Q = WATER DISCHARGE AT PEAK FLOW
V = MEAN VELOCITY AT PEAK FLOW
QB = BED-LOAD DISCHARGE AT PEAK FLOW
QS = SUS-LOAD DISCHARGE AT PEAK FLOW
QT = TOTAL-LOAD DISCHARGE AT PEAK FLOW
D50= MEDIAN DIAMETER OF BED MATERIAL AT PEAK FLOW
NOTE: VALUES OF QS & QB ARE NOT LISTED BECAUSE OF THE LIMITED SPACE.

Table 23 Principal results computed by HEC2SR for the Salt River

SALT RIVER: HEC-6

X	Y0	YF	Y	H	W	Q	V	QS	QT	D50
FT	FT	FT	FT	FT	FT	CFS	FPS	T/D	T/D	MM
0	1079.2	1079.4	1079.3	1089.8	962	176000	18.1	579310	581320	15.5
150	1079.3	1078.6	1078.6	1092.8	955	176000	13.7	574560	575880	24.8
450	1079.6	1078.8	1078.9	1093.2	874	176000	14.9	486510	487680	20.4
800	1080.0	1078.8	1078.9	1093.9	785	176000	15.9	453570	454710	21.0
910	1080.0	1079.1	1079.2	1094.2	787	176000	15.8	419020	420080	20.4
1520	1080.7	1080.3	1080.3	1096.4	782	176000	14.7	347750	348690	23.8
1920	1081.1	1082.7	1082.8	1099.0	1187	176000	10.9	323080	323210	0.7
2520	1081.7	1084.2	1083.0	1099.7	1276	176000	11.9	326760	326930	0.7
3120	1084.5	1084.7	1084.5	1101.0	1377	176000	11.4	371560	372330	7.5
3520	1085.5	1085.4	1085.4	1101.4	1230	176000	11.9	384790	385960	16.5
4240	1087.3	1086.9	1087.0	1102.8	1264	176000	13.0	394720	396040	16.1
4840	1088.8	1088.7	1088.7	1104.5	1274	176000	12.1	411890	413210	12.6
5440	1090.4	1090.1	1090.0	1105.7	1189	176000	13.0	426360	427590	20.5
6040	1092.0	1090.5	1090.6	1106.2	1033	176000	19.0	350640	351480	20.7
6910	1094.2	1093.5	1093.9	1110.3	1040	176000	16.7	344520	345010	10.1
7310	1095.3	1094.2	1094.1	1111.5	1030	176000	16.2	374540	375020	19.1
7510	1095.8	1094.6	1094.0	1110.9	850	176000	19.3	379670	380180	24.8
7660	1096.2	1095.0	1094.7	1111.9	865	176000	18.5	333010	333550	21.7
7860	1096.7	1095.8	1095.7	1114.1	982	176000	15.4	329410	329860	17.3
8260	1097.7	1097.2	1097.7	1115.1	1046	176000	15.2	322510	322850	6.9
8920	1099.4	1098.8	1099.2	1116.4	1044	176000	15.4	326940	327330	8.9
9520	1101.0	1100.4	1100.7	1117.7	1043	176000	15.7	330790	331200	9.8
10120	1102.6	1101.8	1102.0	1119.1	1042	176000	15.7	334950	335420	12.6
10320	1103.1	1102.8	1103.1	1119.6	1042	176000	15.9	334650	335050	7.9
10720	1104.6	1103.0	1103.5	1121.2	1180	176000	14.1	335610	336380	17.8
11120	1106.0	1108.3	1106.8	1122.7	1533	176000	10.2	334360	334550	1.1
11320	1106.8	1105.9	1105.3	1122.9	1618	176000	12.6	336960	337640	21.2
11520	1107.5	1108.0	1106.9	1123.0	1630	176000	14.0	343880	344260	13.4
11730	1108.3	1107.2	1107.6	1124.4	2204	176000	10.8	369770	370610	13.0
12150	1109.7	1110.4	1110.0	1125.2	2615	176000	7.3	418790	419150	0.5
12570	1111.2	1111.8	1111.7	1125.7	2943	176000	7.7	563920	564380	0.5
12990	1112.7	1112.5	1112.5	1126.3	3267	176000	7.7	494610	495460	26.5
13640	1117.7	1115.4	1115.5	1130.1	3045	176000	16.4	433460	434370	28.4
14440	1117.8	1117.5	1117.6	1133.8	3201	176000	8.1	423170	424490	15.2
15500	1118.5	1124.7	1123.9	1135.2	6536	176000	7.0	418800	419060	0.4
16620	1121.3	1120.7	1120.8	1136.4	3927	176000	11.5	536850	537800	12.0
17880	1126.3	1125.5	1125.7	1139.8	4006	176000	11.5	581870	582850	13.6
19520	1131.3	1131.0	1131.2	1144.2	5252	176000	8.8	559590	560500	7.9
20820	1129.7	1130.8	1130.6	1145.7	4238	176000	6.8	593390	593660	0.4
21820	1131.2	1131.0	1131.1	1146.4	3960	176000	10.7	688820	689570	9.0
22920	1129.0	1129.2	1129.2	1147.6	2553	176000	14.7	713310	713840	4.7

X =RIVER DISTANCE
Y0=INITIAL THALWEG EL (T=0 HR)
YF=FINAL THALWEG EL (T=239 HRS)
Y =THALWEG EL AT PEAK FLOW
H =W.S. EL AT PEAK FLOW
W =TOP WIDTH AT PEAK FLOW
Q =WATER DISCHARGE AT PEAK FLOW
V =MEAN VELOCITY AT PEAK FLOW
QB =BED-LOAD DISCHARGE AT PEAK FLOW (=QT-QS)
QS =SUS-LOAD DISCHARGE AT PEAK FLOW
QT =TOTAL-LOAD DISCHARGE AT PEAK FLOW
D50=MEDIAN DIAMETER OF BED MATERIAL AT PEAK FLOW

Table 24 Principal results computed by HEC-6 for the Salt River

SALT RIVER: FLUVIAL-11

X	Y0	YF	Y	H	H1	W	Q	V	QT	D50
FT	FT	FT	FT	FT	FT	FT	CFS	FPS	T/D	MM
0	1079.2	1079.2	1079.2	1089.7	1089.7	962	176000	18.0	1539110	99.2
150	1079.3	1080.0	1080.0	1091.7	1091.8	958	176000	17.0	1539110	130.0
450	1079.6	1084.5	1081.8	1092.5	1092.5	892	176000	17.4	1556330	129.8
800	1080.0	1086.8	1082.8	1095.9	1093.1	1324	176000	14.5	1482100	121.8
910	1080.0	1086.9	1078.7	1097.4	1094.8	811	176000	12.1	1374360	93.6
1520	1080.7	1086.0	1081.5	1098.2	1097.8	868	176000	12.9	1348880	81.8
1920	1081.1	1087.5	1085.0	1100.2	1100.3	1253	176000	9.9	1311730	8.5
2520	1081.7	1087.8	1086.4	1100.8	1100.6	1307	176000	10.5	1333010	21.9
3120	1084.5	1087.7	1088.0	1101.7	1101.2	1368	176000	10.8	1372080	30.7
3520	1085.5	1088.3	1086.1	1102.1	1101.4	1163	176000	11.9	1391940	48.4
4240	1087.3	1087.8	1089.3	1103.5	1102.8	1264	176000	12.0	1404320	59.0
4840	1088.8	1089.2	1093.1	1104.8	1104.5	1288	176000	12.2	1408020	70.6
5440	1090.4	1089.8	1091.3	1106.1	1105.6	1153	176000	13.2	1414570	85.8
6040	1092.0	1091.2	1091.7	1107.3	1106.8	998	176000	14.3	1427380	96.9
6910	1094.2	1092.6	1092.9	1109.9	1110.4	991	176000	14.3	1415060	102.1
7310	1095.3	1094.3	1092.6	1110.9	1111.3	947	176000	14.5	1413850	101.2
7510	1095.8	1094.7	1096.9	1111.4	1110.5	857	176000	14.7	1415560	98.3
7660	1096.2	1095.6	1095.8	1111.9	1112.9	866	176000	14.5	1395000	96.2
7860	1096.7	1096.5	1098.5	1112.8	1114.7	979	176000	13.8	1387240	93.0
8260	1097.7	1097.0	1100.7	1114.0	1115.6	1046	176000	13.4	1376920	89.8
8920	1099.4	1098.7	1102.9	1115.7	1116.6	1047	176000	13.4	1370510	91.2
9520	1101.0	1100.7	1100.8	1117.1	1117.7	1012	176000	13.7	1361690	96.6
10120	1102.6	1102.4	1105.6	1118.9	1119.0	1044	176000	13.1	1331020	97.3
10320	1103.1	1103.3	1101.8	1119.2	1119.5	1005	176000	13.4	1335000	103.1
10720	1104.6	1105.4	1104.5	1120.9	1120.8	1179	176000	11.6	1303830	88.1
11120	1106.0	1107.7	1109.0	1122.2	1122.4	1532	176000	10.3	1311230	75.6
11320	1106.8	1108.5	1106.2	1122.6	1122.7	1584	176000	10.3	1320480	79.4
11520	1107.5	1108.9	1110.6	1123.2	1122.8	1647	176000	9.7	1292520	65.0
11730	1108.3	1110.3	1112.5	1123.9	1124.1	2202	176000	8.4	1297780	22.7
12150	1109.7	1111.6	1116.6	1124.6	1124.7	2617	176000	8.5	1342760	38.8
12570	1111.2	1113.8	1118.6	1125.4	1125.1	2951	176000	8.8	1348450	76.2
12990	1112.7	1115.8	1114.5	1126.5	1125.6	3256	176000	8.8	1345750	96.2
13640	1117.7	1118.9	1114.2	1128.4	1130.4	2921	176000	10.4	1432220	116.2
14440	1117.8	1123.3	1124.2	1131.6	1133.4	2931	176000	9.2	1357850	88.2
15500	1118.5	1129.1	1129.0	1134.7	1134.7	5919	176000	5.6	1275150	2.2
16620	1121.3	1130.0	1126.2	1136.3	1135.5	3663	176000	7.8	1439330	73.8
17880	1126.3	1130.0	1126.0	1139.4	1139.4	3208	176000	9.1	1478690	100.0
19520	1131.3	1135.2	1135.7	1144.0	1143.3	5468	176000	6.2	1446450	5.9
20820	1129.7	1139.1	1138.5	1146.0	1144.8	4443	176000	6.1	1448730	1.5
21820	1131.2	1135.0	1134.3	1147.3	1145.5	4044	176000	7.0	1578960	6.4
22920	1129.0	1129.0	1129.0	1149.3	1146.6	2881	176000	9.1	1689340	60.9

X =RIVER DISTANCE
Y0=INITIAL THALWEG EL
YF=FINAL THALWEG EL
Y =THALWEG EL AT PEAK FLOW
H =W.S. EL AT PEAK FLOW
H1=W.S. EL AT PEAK FLOW (HEC-2)
NOTE: QB & QS WERE NOT COMPUTED WITH FLUVIAL-11

W = TOP WIDTH AT PEAK FLOW
Q = WATER DISCHARGE AT PEAK FLOW
V = MEAN VELOCITY AT PEAK FLOW
QT = TOTAL-LOAD DISCHARGE AT PEAK FLOW
D50= MEDIAN DIAMETER OF BED MATERIAL AT PEAK FLOW

Table 25 Principal results computed by FLUVIAL-11 for the Salt River

SALT RIVER: SEDIMENT-4H

ID	X	Y0	YF	Y	H	H1	W	Q	V	QT	D50
	FT	FT	FT	FT	FT	FT	FT	CFS	FPS	T/D	MM
5	1300	1080.5	1079.4	1079.9	1099.7	1099.8	807	172124	11.3	818000	10.0
6	1950	1082.4	1083.6	1083.1	1100.9	1101.0	1958	172122	8.3	1004000	10.0
7	2500	1083.5	1084.5	1084.2	1101.4	1101.5	1632	172118	8.7	929000	10.0
8	3050	1084.6	1084.8	1084.8	1102.0	1102.0	1459	172114	9.2	963000	10.0
9	3600	1087.0	1086.4	1086.7	1102.7	1102.7	1263	172112	10.2	1005000	10.0
10	4200	1090.2	1089.4	1089.7	1103.7	1103.8	1388	172106	10.4	1018000	10.0
11	4850	1091.8	1091.0	1091.4	1104.8	1104.9	1325	172100	10.4	997000	10.0
12	5450	1093.2	1091.9	1092.5	1105.9	1106.2	1219	172094	11.3	949000	10.0
13	6200	1095.2	1093.3	1094.1	1107.9	1108.6	1066	172088	12.5	881000	10.0
14	6900	1097.5	1095.5	1096.4	1110.3	1111.3	1043	172081	12.6	826000	10.0
15	7500	1099.0	1096.4	1097.5	1112.1	1113.3	897	172077	13.2	796000	10.0
16	7850	1099.7	1097.8	1098.7	1113.2	1114.4	1009	172075	12.3	757000	10.0
17	8300	1100.8	1099.2	1100.0	1114.4	1115.5	1072	172071	11.8	697000	10.0
18	8900	1102.3	1100.6	1101.4	1115.8	1116.9	1069	172065	11.9	637000	10.0
19	9500	1104.1	1102.2	1103.1	1117.4	1118.4	1060	172060	11.9	579000	10.0
20	10150	1106.0	1104.2	1105.0	1119.0	1120.0	1088	172054	11.6	534000	10.0
21	10700	1107.8	1106.1	1106.9	1120.3	1121.3	1213	172051	11.3	497000	10.0
22	11050	1109.3	1107.9	1108.6	1121.2	1122.1	1533	172047	10.6	468000	10.0
23	11400	1110.6	1109.1	1109.8	1122.0	1122.8	1635	172043	10.6	450000	10.0
24	11750	1111.9	1110.9	1111.4	1122.7	1123.5	2201	172039	9.8	425000	10.0
25	12100	1113.3	1112.5	1113.0	1123.6	1124.2	2635	172034	9.3	403000	10.0
26	12550	1114.9	1114.0	1114.5	1124.5	1124.9	2963	172028	9.4	393000	10.0
27	13000	1116.5	1115.4	1116.0	1125.7	1125.9	3268	172022	9.6	386000	10.0
28	13450	1118.7	1116.8	1117.7	1127.1	1127.5	3264	172018	10.3	377000	10.0
29	14050	1120.3	1118.0	1119.0	1130.2	1131.3	2818	172016	11.3	339000	10.0
30	14600	1121.2	1120.3	1120.8	1133.1	1134.5	3081	172011	8.5	259000	10.0
31	15500	1123.1	1122.6	1122.9	1134.5	1135.4	5991	172002	7.0	199500	10.0
32	16600	1126.2	1125.9	1126.0	1136.6	1137.0	3988	171996	7.4	175900	10.0
33	17800	1130.3	1129.4	1129.8	1139.9	1140.3	3081	171996	8.2	129300	10.0
34	19100	1133.9	1134.0	1134.0	1142.3	1142.9	4438	171997	5.4	58230	10.0
35	19800	1135.5	1135.6	1135.5	1143.2	1143.6	4276	171997	5.3	36000	10.0
36	20800	1131.8	1132.0	1131.9	1144.7	1144.9	4302	171997	5.9	41800	10.0
37	21800	1131.3	1131.3	1131.3	1146.8	1146.9	3717	171999	7.5	46800	10.0
38	22900	1130.7	1129.9	1130.3	1149.8	1150.1	1404	172000	11.5	62700	10.0

ID = SECTION ID
X = RIVER DISTANCE
Y0 = INITIAL THALWEG EL
YF = FINAL THALWEG EL
Y = THALWEG EL AT PEAK FLOW
H = W.S. EL AT PEAK FLOW
H1 = W.S. EL AT PEAK FLOW COMPUTED USING FIXED-BED MODEL
W = TOP WIDTH AT PEAK FLOW
Q = WATER DISCHARGE AT PEAK FLOW (MAIN AND OVERBANK AREAS)
V = MEAN VELOCITY AT PEAK FLOW
QT = TOTAL-LOAD DIS. AT PEAK FLOW
D50= MEDIAN SIZE OF BED MATERIAL AT PEAK FLOW

NOTE: RESULTS SHOWN ARE FOR ENTIRE SECTION OF MAIN AND OVERBANK AREAS

Table 26 Principal results computed by SEDIMENT-4H for the Salt River

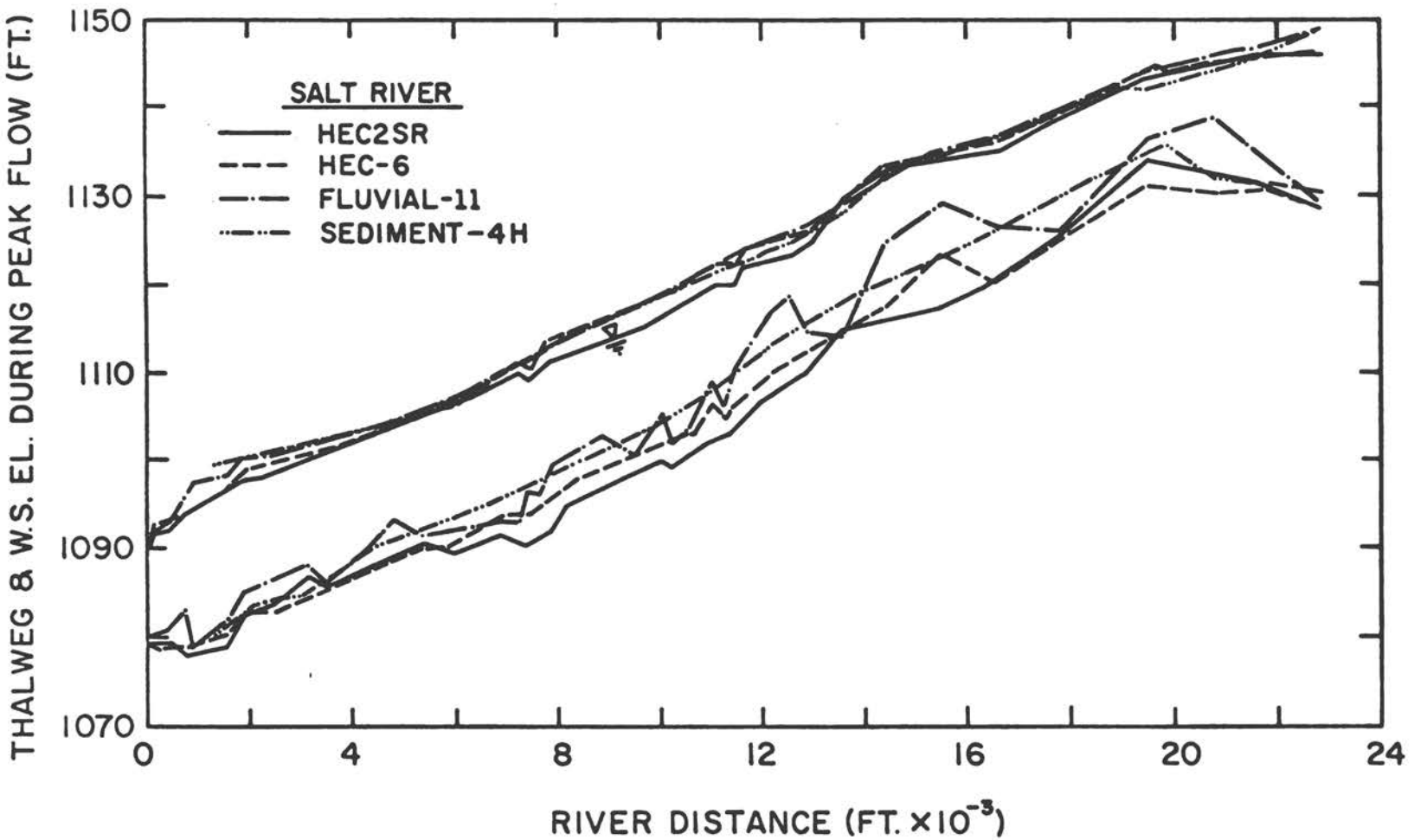

Figure 32 Comparison of thalweg and water-surface profiles at peak flow computed using the HEC2SR, HEC-6, FLUVIAL-11, and SEDIMENT-4H movable-bed models for the Salt River

Table 27 lists water-surface elevations at peak flow predicted by HEC using the HEC-6 movable-bed model, and the HEC-6 and HEC-2 fixed-bed models. The differences among these predictions of the three models are seen to be minute. It is of interest that in spite of cumulative bed deposition of 5.4 ft at a river distance of 15,500 ft, the water-surface elevation predicted by the HEC-6 movable-bed model was only 0.5 ft higher than that predicted by HEC-2, as seen in tables 24 and 27. Figure 33 shows two water-surface profiles at peak flow predicted by SDSU using HEC-2 and FLUVIAL-11; no significant differences are seen between them, although major thalweg degradation was predicted by FLUVIAL-11, as seen in table 25 (compare YO with Y).

Longitudinal distributions of mean flow velocities computed by the HEC-6, FLUVIAL-11, and SEDIMENT-4H movable-bed models are shown in figure 34. Since mean velocities of HEC2SR were very nearly equal to those of HEC-6, they are not plotted in the figure in order to simplify the graphic presentation. HEC-6 is seen to predict very high mean velocities in comparison with the other two models. The predicted total-load discharges at peak flow are compared in figure 35 (see table 28 also). Substantial differences among the predictions are seen. HEC-6 did not include transport of cobbles (sizes larger than 64 mm) or fines (finer than 0.125 mm) because of a program limitation for the former and a lack of measured data for the latter. Note that RMA tested two movable-bed cases for constant median bed-material diameters of 10 mm and 60 mm. Total-load discharges given in table 28 correspond to a median size of 60 mm according to their raw computer output, although in table 28 the median diameter is listed as 10 mm, the value reported by RMA. Post-flood median sizes predicted by HEC2SR, HEC-6, and FLUVIAL-11 are presented in table 28. Median sizes at peak flow predicted by these three models are shown in figure 36. HEC2SR and FLUVIAL-11 predicted armoring effects; however, finer sizes were predicted by HEC-6 because HEC-6 did not consider cobbles.

Finally, thalweg and water-surface elevations for rising and falling stages computed by HEC2SR, HEC-6, FLUVIAL-11 and SEDIMENT-4H are presented in tables 29, 30, 31, and 32, respectively. As can be seen in tables 29 and 30, water-surface elevations predicted by HEC2SR and HEC-6 for rising and falling stages at discharges of 95,040 cfs and 102,080 cfs, respectively, agree fairly well.

The computer model and computation time reported by each modeler are summarized in table 33.

SALT RIVER: HEC-6

X	H1	H2	H3	Q
FT	FT	FT	FT	CFS
0	1089.8	1089.7	1089.7	176000
150	1092.8	1092.0	1091.8	176000
450	1093.2	1092.7	1092.5	176000
800	1093.8	1093.7	1093.1	176000
910	1094.2	1095.0	1094.8	176000
1520	1096.4	1097.3	1097.8	176000
1920	1099.0	1099.9	1100.3	176000
2520	1099.7	1100.2	1100.6	176000
3120	1101.0	1101.0	1101.2	176000
3520	1101.4	1101.4	1101.4	176000
4240	1102.8	1102.8	1102.8	176000
4840	1104.5	1104.7	1104.5	176000
5440	1105.7	1105.8	1105.6	176000
6040	1106.2	1106.5	1106.8	176000
6910	1110.2	1111.0	1110.4	176000
7310	1111.5	1111.9	1111.3	176000
7510	1110.9	1111.1	1110.5	176000
7660	1111.9	1112.9	1112.9	176000
7860	1114.1	1115.0	1114.7	176000
8260	1115.1	1116.0	1115.6	176000
8920	1116.4	1117.0	1116.6	176000
9520	1117.7	1118.1	1117.7	176000
10120	1119.1	1119.5	1119.0	176000
10320	1119.6	1119.9	1119.5	176000
10720	1121.2	1121.3	1120.8	176000
11120	1122.7	1123.2	1122.4	176000
11320	1122.9	1123.2	1122.6	176000
11520	1123.0	1123.3	1122.8	176000
11730	1124.4	1124.7	1124.1	176000
12150	1125.2	1125.4	1124.7	176000
12570	1125.6	1125.8	1125.1	176000
12990	1126.3	1126.4	1125.6	176000
13640	1130.1	1130.2	1130.4	176000
14440	1133.8	1134.0	1133.4	176000
15500	1135.2	1135.1	1134.7	176000
16620	1136.4	1136.0	1135.5	176000
17080	1139.8	1140.1	1139.4	176000
19520	1144.2	1144.2	1143.3	176000
20820	1145.7	1145.7	1144.8	176000
21820	1146.4	1146.3	1145.4	176000
22920	1147.6	1147.6	1146.6	176000

X =RIVER DISTANCE
H1=W.S. EL. BY HEC-6 (MOVABLE BED)
H2=W.S. EL. BY HEC-6 (FIXED BED)
H3=W.S. EL. BY HEC-2 (FIXED BED)
Q =PEAK FLOW WATER DISCHARGE

Table 27 Water-surface elevations computed by the HEC-6 movable-bed and fixed-bed models and HEC-2 for the Salt River

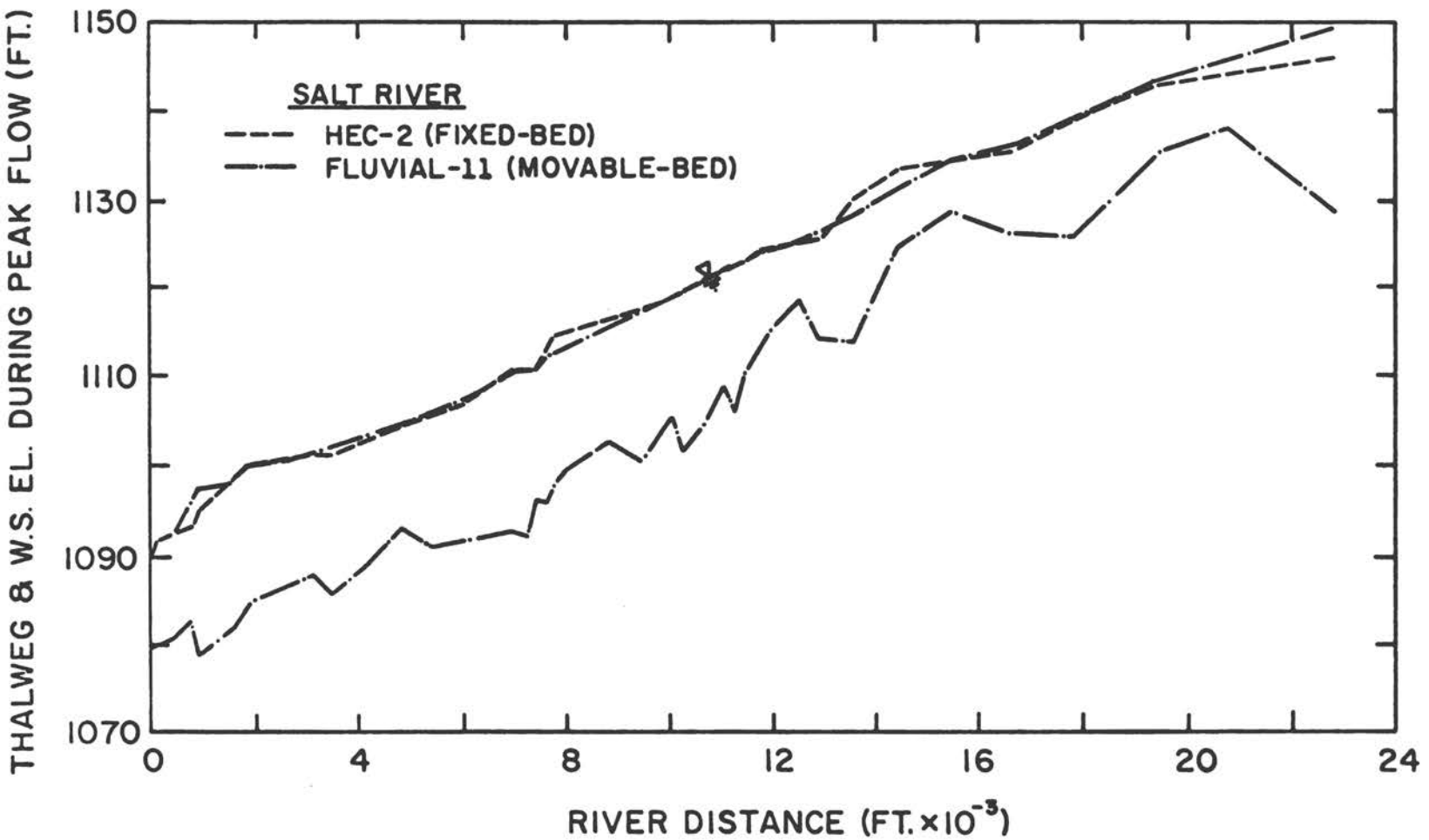

Figure 33 Comparison of water-surface profiles at peak flow computed by SDSU using HEC-2 and FLUVIAL-11

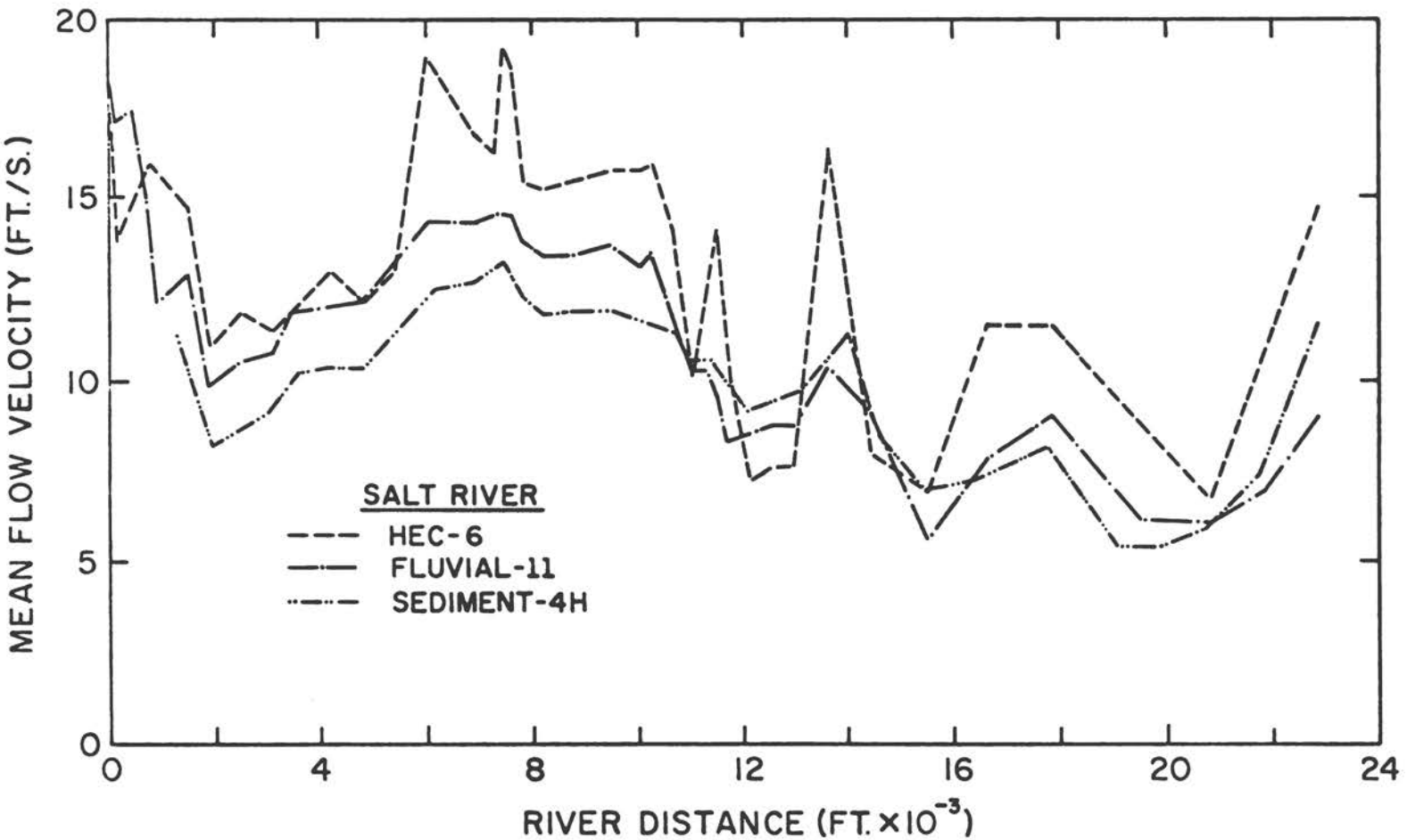

Figure 34 Longitudinal distributions of mean flow velocity at peak flow computed using the HEC-6, FLUVIAL-11, and SEDIMENT-4H movable-bed models for the Salt River

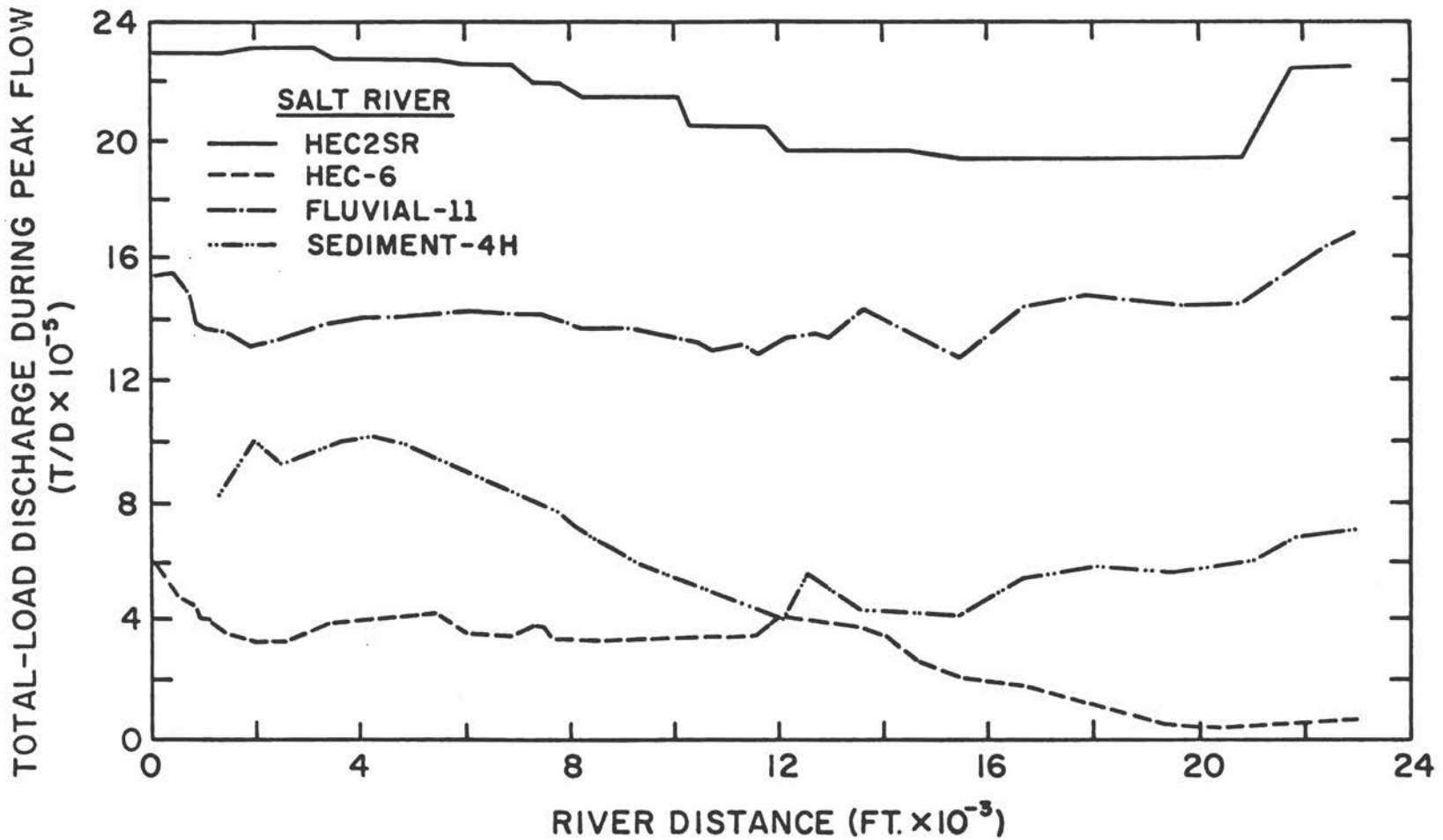

Figure 35 Total-load discharges at peak flow predicted by HEC2SR, HEC-6, FLUVIAL-11, and SEDIMENT-4H for the Salt River

SALT RIVER		(HEC-6)		(FLUVIAL-11)		(HEC2SR)		(SEDIMENT-4H)		
X	D50I	QT	D50F	QT	D50F	QT	D50F	X	QT	D50F
FT	MM	T/D	MM	T/D	MM	T/D	MM	FT	T/D	MM
0	64.0	581320	35.48	1539110	144.89	2306010	49	1300	818000	10.0
150	64.0	575880	31.59	1539110	163.14	2306010	49	1950	1004000	10.0
450	64.0	487680	15.59	1556330	163.43	2306010	49	2500	929000	10.0
800	64.0	454710	19.89	1482100	161.38	2306010	47	3050	963000	10.0
910	64.0	420080	1.45	1374360	159.55	2306010	47	3600	1005000	10.0
1520	64.0	348690	14.32	1348880	2.17	2306010	47	4200	1018000	10.0
1920	64.0	323210	21.61	1311730	2.59	2321440	87	4850	997000	10.0
2520	64.0	326930	2.29	1333010	4.48	2321440	87	5450	949000	10.0
3120	64.0	372330	7.25	1372080	13.18	2321440	87	6200	881000	10.0
3520	64.0	385960	11.61	1391940	19.04	2284790	20	6900	826000	10.0
4240	64.0	396040	16.25	1404320	26.68	2284790	20	7500	796000	10.0
4840	64.0	413210	19.86	1408020	45.02	2284790	20	7850	757000	10.0
5440	64.0	427590	19.78	1414570	48.09	2284790	20	8300	697000	10.0
6040	64.0	351480	22.01	1427380	73.88	2264580	94	8900	637000	10.0
6910	64.0	345010	25.84	1415060	95.85	2264580	94	9500	579000	10.0
7310	64.0	375020	18.59	1413850	92.44	2202860	84	10150	534000	10.0
7510	64.0	380180	3.77	1415560	107.22	2202860	84	10700	497000	10.0
7660	64.0	333550	17.85	1395000	101.46	2202860	84	11050	468000	10.0
7860	64.0	329860	24.47	1387240	100.00	2202860	84	11400	450000	10.0
8260	64.0	322850	26.37	1376920	69.84	2151420	54	11750	425000	10.0
8920	64.0	327330	26.19	1370510	77.11	2151420	54	12100	403000	10.0
9520	64.0	331200	26.69	1361690	82.74	2151420	54	12550	393000	10.0
10120	64.0	335420	28.91	1331020	104.41	2151420	54	13000	386000	10.0
10320	64.0	335051	31.47	1335000	103.92	2050060	26	13450	377000	10.0
10720	64.0	336380	35.37	1303830	94.37	2050060	26	14050	339000	10.0
11120	64.0	334550	27.71	1311230	90.92	2050060	26	14600	259000	10.0
11320	64.0	337640	24.77	1320480	94.71	2050060	26	15500	199500	10.0
11520	64.0	344260	1.22	1292520	105.41	2050060	26	16600	175900	10.0
11730	64.0	370610	3.33	1297780	98.72	2050060	26	17800	129300	10.0
12150	64.0	419150	8.63	1342760	116.40	1963050	46	19100	58230	10.0
12570	64.0	564380	24.23	1348450	105.89	1963050	46	19800	36000	10.0
12990	64.0	495460	27.61	1345750	118.31	1963050	46	20800	41800	10.0
13640	64.0	434370	30.08	1432220	103.63	1963050	46	21800	46800	10.0
14440	64.0	424490	29.47	1357850	107.23	1963050	46	22900	62700	10.0
15500	64.0	419060	9.11	1275150	112.37	1940900	17	-	-	-
16620	64.0	537800	25.96	1439330	70.51	1940900	17	-	-	-
17880	64.0	582850	24.05	1478690	88.45	1940900	17	-	-	-
19520	64.0	560500	27.46	1446450	144.83	1940190	33	-	-	-
20820	64.0	593660	2.76	1448730	16.81	1940190	33	-	-	-
21820	64.0	689570	25.93	1578960	31.87	2271650	49	-	-	-
22920	64.0	713840	24.72	1689340	60.89	2271650	49	-	-	-

ID = SECTION I.D.
X = RIVER DISTANCE
D50I = INITIAL MEDIAN SIZE OF BED MATERIAL (PRE-FLOOD)
D50F = FINAL MEDIAN SIZE OF BED MATERIAL (POST-FLOOD)
QT = TOTAL-LOAD DISCHARGE AT PEAK-FLOW DISCHARGE OF 176,000 CFS

Table 28 Total-load discharges at peak flow and final median bed-material sizes computed by HEC2SR, HEC-6, FLUVIAL-11, and SEDIMENT-4H for the Salt River

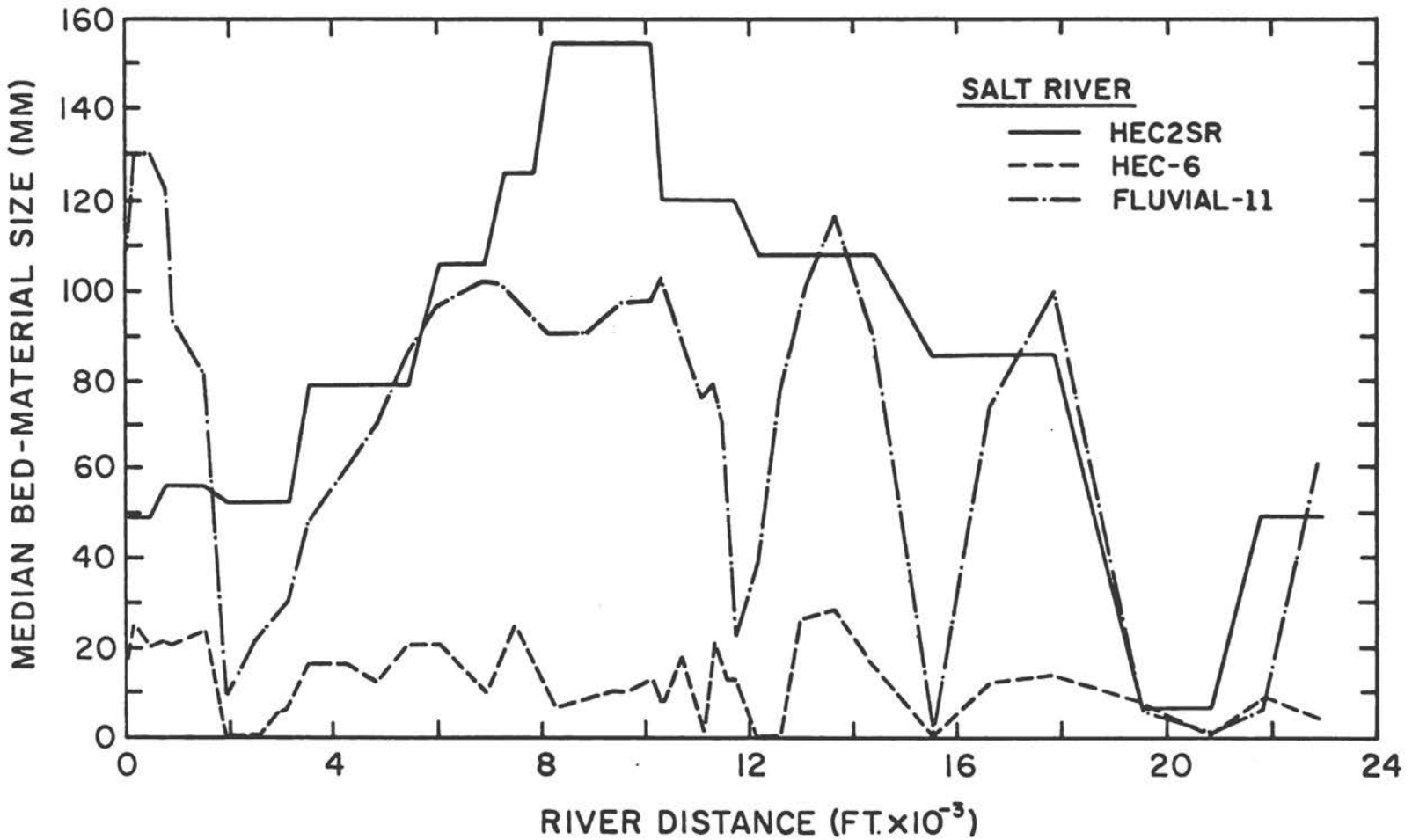

Figure 36 Longitudinal distributions of median bed-material size at peak flow computed using HEC2SR, HEC-6, and FLUVIAL-11 for the Salt River

SALT RIVER: HEC2SR

X	YR	HR	YFA	HFA
FT	FT	FT	FT	FT
0	1079.2	1086.2	1079.2	1086.5
150	1079.3	1088.2	1079.3	1088.5
450	1079.6	1089.0	1079.6	1089.4
800	1079.1	1090.2	1078.4	1090.8
910	1079.1	1090.6	1078.4	1091.2
1520	1079.8	1092.2	1079.1	1092.4
1920	1081.7	1093.5	1081.8	1093.4
2520	1082.8	1094.1	1082.8	1094.3
3120	1085.5	1095.5	1085.6	1096.2
3520	1085.3	1096.5	1084.9	1097.4
4240	1087.1	1098.5	1086.8	1098.9
4840	1088.6	1100.6	1088.2	1100.9
5440	1090.2	1101.8	1089.9	1102.1
6040	1090.8	1103.2	1088.9	1103.7
6910	1093.0	1105.8	1091.1	1105.2
7310	1093.1	1106.9	1090.3	1106.3
7510	1093.4	1106.8	1090.4	1106.3
7660	1093.9	1107.5	1090.8	1106.5
7860	1094.5	1108.7	1091.7	1107.2
8260	1096.8	1109.4	1094.5	1107.7
8920	1098.5	1111.1	1096.2	1109.8
9520	1100.1	1112.7	1097.8	1111.3
10120	1101.7	1114.3	1099.5	1113.0
10320	1100.6	1115.3	1098.3	1113.9
10720	1102.2	1115.8	1099.8	1114.4
11120	1103.4	1116.5	1101.2	1115.1
11320	1104.1	1116.7	1101.9	1115.7
11520	1104.8	1117.2	1102.5	1116.6
11730	1105.7	1119.2	1103.8	1118.3
12150	1107.7	1119.6	1106.9	1119.7
12570	1109.2	1121.2	1108.4	1121.2
12990	1110.7	1122.9	1109.9	1123.0
13640	1115.6	1128.1	1114.9	1128.2
14440	1116.3	1130.8	1115.8	1130.9
15500	1118.0	1131.8	1117.9	1131.9
16620	1120.8	1133.3	1120.7	1133.5
17880	1125.7	1136.7	1125.6	1136.9
19520	1132.3	1140.9	1134.1	1142.1
20820	1130.7	1142.5	1132.6	1144.3
21820	1131.2	1143.2	1131.2	1145.0
22920	1129.0	1144.4	1129.0	1145.4

X =RIVER DISTANCE
YR =THALWEG EL AT Q=95,040 CFS (RISING STAGE)
HR =W.S. EL AT Q=95,040 CFS (RISING STAGE)
YFA=THALWEG EL AT Q=102,080 CFS (FALLING STAGE)
HFA=W.S. EL AT Q=102,080 CFS (FALLING STAGE)

Table 29 Thalweg and water-surface elevations during rising and falling stages computed by HEC2SR for the Salt River

SALT RIVER: HEC-6

X	YR	HR	YFA	HFA
FT	FT	FT	FT	FT
0	1079.3	1086.3	1079.3	1086.6
150	1079.1	1088.5	1078.6	1089.2
450	1079.4	1089.2	1078.7	1089.7
800	1079.8	1090.1	1078.7	1090.4
910	1079.8	1090.7	1079.0	1090.6
1520	1080.6	1092.5	1080.3	1092.1
1920	1082.9	1093.9	1083.0	1093.8
2520	1082.3	1095.0	1083.8	1095.0
3120	1084.4	1095.9	1084.7	1097.0
3520	1085.4	1096.8	1085.4	1097.7
4240	1087.1	1098.8	1086.9	1099.3
4840	1088.8	1100.9	1088.7	1101.1
5440	1090.3	1102.2	1090.0	1102.5
6040	1091.0	1103.1	1090.4	1103.2
6910	1093.9	1106.3	1094.0	1106.3
7310	1094.5	1107.4	1094.1	1107.8
7510	1094.6	1107.4	1093.8	1107.9
7660	1095.3	1107.9	1094.5	1108.2
7860	1096.3	1109.3	1095.5	1109.4
8260	1097.9	1110.4	1097.7	1110.3
8920	1099.3	1112.0	1099.1	1112.2
9520	1100.7	1113.4	1100.7	1113.6
10120	1102.2	1114.9	1101.9	1115.2
10320	1103.2	1115.4	1103.1	1115.6
10720	1104.1	1116.7	1103.1	1117.0
11120	1106.2	1118.4	1107.5	1118.0
11320	1105.5	1118.4	1105.3	1118.9
11520	1106.5	1118.4	1106.6	1118.9
11730	1107.6	1119.9	1106.9	1120.3
12150	1109.7	1121.2	1110.3	1121.4
12570	1111.2	1122.1	1112.0	1122.5
12990	1112.6	1123.4	1112.5	1123.9
13640	1116.0	1128.5	1115.4	1128.6
14440	1117.7	1131.2	1117.5	1131.4
15500	1120.3	1132.2	1127.1	1132.8
16620	1120.7	1133.7	1120.8	1134.8
17880	1125.9	1137.2	1125.6	1137.3
19520	1131.1	1141.4	1131.1	1141.7
20820	1129.7	1142.9	1130.9	1143.3
21820	1131.1	1143.1	1131.0	1143.7
22920	1129.0	1145.3	1129.2	1145.6

X =RIVER DISTANCE
YR =THALWEG EL AT Q=95,040 CFS (RISING STAGE)
HR =W.S. EL AT Q=95,040 CFS (RISING STAGE)
YFA=THALWEG EL AT Q=102,080 CFS (FALLING STAGE)
HFA=W.S. EL AT Q=102,080 CFS (FALLING STAGE)

Table 30 Thalweg and water-surface elevations during rising and falling stages computed by HEC-6 for the Salt River

SALT RIVER: FLUVIAL-11

X	YR	HR	YFA	HFA
FT	FT	FT	FT	FT
0	1079.2	1086.2	1079.2	1086.7
150	1079.6	1088.4	1080.2	1088.2
450	1080.7	1089.0	1081.2	1089.6
800	1082.4	1090.3	1083.1	1092.3
910	1079.3	1093.5	1082.3	1093.7
1520	1080.3	1094.2	1083.8	1095.6
1920	1083.9	1095.2	1086.3	1097.2
2520	1085.1	1095.6	1086.9	1097.8
3120	1085.0	1096.6	1087.7	1098.6
3520	1086.8	1097.3	1086.1	1099.0
4240	1090.0	1099.1	1087.4	1100.4
4840	1092.9	1100.7	1088.4	1101.6
5440	1091.3	1102.1	1089.3	1102.8
6040	1092.1	1103.6	1091.2	1104.1
6910	1096.8	1106.3	1092.3	1106.2
7310	1096.3	1107.4	1093.0	1107.3
7510	1094.8	1107.7	1097.1	1108.3
7660	1096.4	1108.4	1096.4	1108.6
7860	1096.8	1109.3	1096.2	1109.1
8260	1100.3	1110.4	1096.6	1110.2
8920	1100.8	1111.9	1098.3	1111.9
9520	1100.8	1113.3	1101.1	1113.4
10120	1102.2	1114.8	1104.9	1115.0
10320	1102.8	1115.3	1102.6	1115.4
10720	1104.3	1116.5	1104.3	1116.8
11120	1107.9	1117.8	1107.1	1117.9
11320	1106.2	1118.3	1107.8	1118.4
11520	1106.5	1118.8	1110.9	1119.0
11730	1110.4	1119.7	1111.4	1119.8
12150	1115.5	1120.8	1112.7	1121.3
12570	1117.6	1122.0	1114.1	1122.8
12990	1114.2	1123.5	1116.4	1124.5
13640	1114.2	1127.0	1114.2	1126.8
14440	1120.2	1130.7	1124.0	1129.5
15500	1122.0	1132.3	1129.2	1132.8
16620	1125.9	1134.0	1129.2	1135.1
17880	1126.0	1137.2	1126.6	1137.5
19520	1132.9	1141.5	1135.8	1141.6
20820	1134.7	1143.1	1139.2	1144.2
21820	1132.1	1144.1	1134.8	1145.6
22920	1129.0	1145.8	1129.0	1147.4

X =RIVER DISTANCE
YR =THALWEG EL AT Q=94,400 CFS (RISING STAGE)
HR =W.S. EL AT Q=94,400 CFS (RISING STAGE)
YFA=THALWEG EL AT Q=106,400 CFS (FALLING STAGE)
HFA=W.S. EL AT Q=106,400 CFS (FALLING STAGE)

Table 31 Thalweg and water-surface elevations during rising and falling stages computed by FLUVIAL-11 for the Salt River

SALT RIVER: SEDIMENT-4H

ID	X	YR	HR	YFA	HFA
	FT	FT	FT	FT	FT
5	1300	1080.5	1095.3	1079.3	1095.8
6	1950	1081.0	1095.9	1080.0	1096.4
7	2500	1082.2	1096.5	1081.4	1097.2
8	3050	1084.0	1097.1	1083.1	1097.9
9	3600	1085.4	1097.9	1084.1	1098.7
10	4200	1087.1	1099.2	1085.4	1099.7
11	4850	1088.7	1100.5	1087.1	1100.8
12	5450	1090.0	1101.9	1087.9	1102.0
13	6200	1092.0	1104.2	1089.1	1103.7
14	6900	1094.3	1106.9	1091.2	1105.8
15	7500	1095.8	1108.7	1092.5	1107.3
16	7850	1096.5	1109.7	1093.8	1108.3
17	8300	1097.7	1110.8	1095.2	1109.5
18	8900	1099.1	1112.1	1096.5	1111.0
19	9500	1100.9	1113.7	1098.1	1112.7
20	10150	1102.7	1115.3	1100.3	1114.2
21	10700	1104.4	1116.6	1102.3	1115.5
22	11050	1105.8	1117.7	1103.7	1116.7
23	11400	1107.1	1118.6	1104.9	1117.8
24	11750	1108.2	1119.5	1106.3	1118.9
25	12100	1109.6	1120.6	1107.7	1120.4
26	12550	1111.0	1121.8	1109.0	1122.1
27	13000	1112.6	1123.2	1110.1	1123.8
28	13450	1115.4	1125.1	1111.8	1125.6
29	14050	1117.5	1128.4	1114.3	1128.6
30	14600	1118.0	1131.0	1116.1	1131.2
31	15500	1119.6	1132.2	1118.4	1132.5
32	16600	1122.8	1134.2	1122.0	1134.5
33	17800	1126.9	1137.7	1125.3	1137.4
34	19100	1130.6	1140.2	1130.5	1139.7
35	19800	1132.0	1140.9	1132.1	1140.8
36	20800	1131.8	1142.0	1132.0	1142.3
37	21800	1131.3	1143.7	1131.3	1144.3
38	22900	1130.6	1146.0	1129.6	1146.3

ID = SECTION ID
X = RIVER DISTANCE
YR = THALWEG EL AT Q=92,110 CFS (RISING STAGE)
HR = W.S. EL AT Q=92,110 CFS (RISING STAGE)
YFA= THALWEG EL AT Q=104,530 CFS (FALLING STAGE)
HFA= W.S. EL AT Q=104,530 CFS (FALLING STAGE)

Table 32 Thalweg and water-surface elevations during rising and falling stages computed by SEDIMENT-4H for the Salt River

MODEL	MODE	COMPUTER MODEL	CPU TIME (SEC)
(SAN LORENZO RIVER)			
HEC2SR	MOVABLE-BED	CDC CYBER 172	800.0
KUWASER	MOVABLE-BED	CDC CYBER 172	117.1
UUWSR	MOVABLE-BED	CDC CYBER 172	210.0
HEC-6	MOVABLE-BED	CDC 7600	13.5
HEC-6	MOVABLE-BED	HARRIS 500	199.1
HEC-6	FIXED-BED*	CDC 7600	0.3
HEC-6	FIXED-BED*	HARRIS 500	9.7
HEC-2	FIXED-BED*	CDC 7600	0.5
HEC-2	FIXED-BED*	HARRIS 500	14.3
FLUVIAL-11	MOVABLE-BED	VAX 11/780	606.0
SEDIMENT-4H	MOVABLE-BED	PRIME 550	7,200.0
(SAN DIEGUITO RIVER)			
HEC2SR	MOVABLE-BED	CDC CYBER 172	526.5
UUWSR	MOVABLE-BED	CDC CYBER 172	209.1
FLUVIAL-11	MOVABLE-BED	VAX 11/780	1,291.0
SEDIMENT-4H	MOVABLE-BED	PRIME 550	7,200.0
(SALT RIVER)			
HEC2SR	MOVABLE-BED	CDC CYBER 172	530.0
HEC-6	MOVABLE-BED	CDC 7600	17.6
HEC-6	FIXED-BED*	CDC 7600	0.4
HEC-2	FIXED-BED*	CDC 7600	0.6
FLUVIAL-11	MOVABLE-BED	VAX 11/780	831.0
SEDIMENT-4H	MOVABLE-BED	PRIME 550	7,200.0

*: FOR A PEAK DISCHARGE ONLY

Table 33 List of computer models used in the present study and their computing times

V. LIMITATIONS OF ALLUVIAL-RIVER-FLOW MODELS

The computer-based alluvial-river flow models utilized in this study account for the effects of changes in river-bed elevation on flood stages. Degradation or aggradation occurs in a subreach when the sediment-transport capacity of the flow at the upstream boundary of a reach differs from that at the downstream boundary. Degradation results when the sediment output across the downstream boundary of the reach exceeds the sediment input into the upstream end of the reach, while aggradation occurs when the sediment input exceeds the output. These sediment-transport imbalances occur along the river reach when there is a change in flow characteristics or the sediment input to the reach is changed without accompanying changes in the sediment-transport capacity. Alluvial-river-flow models compute changes in river-bed elevation (degradation or aggradation) by means of the sediment-continuity equation, and determine the new flow field on the basis of the altered bed elevation and slope using the flow-continuity and the flow-momentum or flow-energy equations. Interaction or feedback between changing river bed and flow characteristics is handled by the numerical schemes described in Chapter II. Common to all alluvial-river-flow models are requirements for input data on channel geometry, sediment, and hydrologic characteristics. The input-data requirements for the individual models tested in the present study are summarized in Chapter II. Even if adequate data are provided for a study river, there still remains a need to calibrate and verify the model by means of field data. In most natural rivers, only extremely limited geometric, sediment, and hydrologic field data are available for high flood stages, and, consequently, adequate calibration or verification of the models usually cannot be obtained.

The limitations of the individual models tested are described in Chapter II, and attention here will be focused on several important considerations that may explain some of the discrepancies among the computed results presented in Chapter IV. First, it should be pointed out that the initial channel-geometry condition is in general not completely known. Strictly speaking, the initial condition must be specified at the time a 100-year-flood simulation is initiated. In most practical cases, rather old river cross-

section profiles are provided as input data; however, the river geometry may in reality be undergoing changes in a somewhat random manner as a consequence of floods during the period between the time of cross-section surveys and the 100-year flood. This means that a movable-bed model should have the capability of predicting the random initial condition by statistical means using flood-frequency records. Randomness of the initial conditions has not been incorporated into any of the available models.

Second, the bed-armoring process during channel degradation is not well understood, and has not been adequately formulated. Armoring and the result coarsening of the bed-material size have a direct effect on the sediment-discharge capacity and the channel roughness or bed friction factor, and, thereby, impact on the velocity, depth, and energy slope of the flow. Moreover, bed armoring greatly impedes degradation. Finally, the field data available on the horizontal and vertical distributions of bed-material size generally are inadequate to make use of even the imperfect armoring formulations available. Many of the seeming anomalies and discrepancies in the results computed by the various models presented in Chapter IV may have resulted from the differences among the armoring and bed-material sorting formulations utilized. In order to stress this point, the median-bed sizes predicted by different models at narrow and wide cross sections during peak flow are summarized in table 34 for SDR and SR. At narrow, constricted cross sections, channel degradation and attendant armoring (or coarsening of the bed-material size) are generally expected during peak flow. However, as seen in table 34, only HEC2SR predicted the coarsening at the narrower sections for both SDR and SR. However, the final SDR post-flood median bed-material size predicted by HEC2SR at a river distance of 3,600 ft is coarser than that computed during peak flow. FLUVIAL-11 predicted the coarser post-flood bed-material sizes at the narrower sections for both SDR and SR. Because each sediment-transport function has its own independent variables, the characteristics of the sediment-transport formula in an alluvial-river-flow model have a strong effect on the flow characteristics and the sediment-discharge prediction. As has been pointed out in Chapter IV, greatly different sediment discharges were predicted by the models tested in this study.

MODEL	X FT	W FT	V FT/S	D50 MM	D50F MM
SAN DIEGUITO RIVER					
HEC2SR	3,600	170	11.6	0.86	0.92
	4,350	1,143	1.2	0.38	0.30
FLUVIAL-11	3,600	266	6.9	0.27	0.28
	4,350	829	5.1	0.28	0.30
SEDIMENT-4H*	4,200	237	9.0	0.46	0.46
	4,950	944	1.8	0.46	0.46
SALT RIVER					
HEC2SR	7,510	645	15.6	126.0	84.0
	13,640	1,513	12.3	108.0	46.0
HEC-6**	7,510	850	19.3	24.8	3.8
	13,640	3,045	16.4	28.4	30.1
FLUVIAL-11	7,510	857	14.7	98.3	107.2
	13,640	2,921	10.4	116.2	103.6
SEDIMENT-4H*	7,500	897	13.2	10.0	10.0
	13,450	3,264	10.3	10.0	10.0

X = RIVER DISTANCE
W = COMPUTED TOP WIDTH AT PEAK FLOW
D50 = COMPUTED MEDIAN DIAMETER OF BED MATERIAL AT PEAK FLOW
D50F = COMPUTED POST-FLOOD MEDIAN DIAMETER OF BED MATERIAL
* = SEDIMENT-4H DOES NOT CONSIDER SEDIMENT SORTING
** = HEC-6 DID NOT CONSIDER TRANSPORT OF COBBLES (COARSER THAN 64 MM) OR WASH LOAD (FINER THAN 0.125 MM) FOR SR

Table 34 Typical median bed-material sizes computed during peak flow and post-flood bed-material sizes for the San Dieguito and Salt Rivers

Third, it should be pointed out that the boundary conditions applied to alluvial-river-flow models play important roles in their simulations. For example, if the upstream sediment input is a boundary condition and is greater than the computed sediment-transport capacity of the flow at the first cross section, the first subreach will aggrade until the bed slope increases until the imposed sediment discharge is transported by the resulting increased flow velocity. The local aggradation propagates downstream until the entire reach is sufficiently steep to produce a velocity that is competent to pass the imposed sediment discharge through the system. The boundary condition used to account for erodible banks is also extremely important in cases where banks are susceptible to erosion during floods. Unless some computational means are employed to account for changing movable-bed width, predicted flood levels in rivers with very erodible banks become less reliable. FLUVIAL-11 is the only model among the models tested in this study that incorporates width variations.

Finally, the effects of uncertainty surrounding variations in the channel roughness or friction factor on flooded stages are not well understood. Because of the strong dependence of the friction factor on the sediment discharges, the effects of suspended- and bed-load sediment on the friction factor should be accounted for.

VI. SUMMARY, CONCLUSIONS, AND RECOMMENDATIONS

The report summaries that were prepared and submitted in letter form to the Committee by the individual modelers are first quoted, in order to present their views regarding their modeling experience in the present study.

1. SLA. "In general, the conventional rigid-boundary flood analysis based on HEC-2 is adequate for a river system experiencing adequate armoring control, equilibrium or near equilibrium conditions. However, this method of analysis underestimates or overestimates the flood level in a reach that has experienced significant aggradation or degradation before the flood peak. The results of application of HEC2SR, KUWASER, and UUWSR to the study reaches are very similar. Minor differences are a product of the various assumptions associated with the individual models. While each model is especially applicable to specific situations, we recommend adoption of HEC2SR. The primary advantage of this model is its compatibility with HEC-2. This feature would expedite application of HEC2SR to flood insurance studies."

2. HEC. "With regard to the subject of the study, it should be noted that, as the hydraulic computations in both HEC-2 and HEC-6 are steady state, neither one can be accurately termed a "flood routing model". In general, the computed water surface profiles for the peak flood discharges differed little between the fixed-bed and movable-bed simulations. This may be due to certain peculiarities of the data sets. The Salt River data set, as provided, included no information on inflowing sediment load, an essential ingredient of movable bed river modeling. The inflowing load had to be assumed to be in equilibrium with the bed material throughout the range of discharges on the flood hydrograph. Therefore, little scour or deposition would be expected, as is seen in the simulation results. The San Lorenzo River flood event was of very short duration. It appears that this factor, plus local hydraulic control at the tidal downstream boundary condition, minimizes any overall bed elevation changes. Furthermore, we have not previously applied HEC-6 to short-term, single flood event simulations. We certainly would not conclude that fixed and movable boundary simulations will always produce similar water surface profiles as these results indicate. Because no data were provided for model calibration, these results should not be considered to be an engineering analysis of water surface profiles. Use of these results should be limited to intermodel comparisons".

3. SDSU. "If a river channel is in the state of approximate equilibrium, river-channel changes during floods are usually not sufficiently significant to result in major differences in the flood level. Such are the cases for the San Lorenzo River and the Salt River. However, if the natural equilibrium of a river is significantly distorted, river-channel changes during floods are such that major differences in the flood level can be expected. Such is the case for the San Dieguito River, for which

the water-surface profile as well as special variations in velocity obtained using the fixed-bed model are shown to be unrealistic; the computed flood level is not substantiated by measured data. On the other hand, the FLUVIAL-11 results are supported by measured data. Since a small difference in flood level may involve a large difference in the inundated area, the accuracy of flood-level prediction is of major importance in flood-plain management. River-channel changes may include channel-bed aggradation and degradaton, width variation, and lateral migration in channel bends. These changes are interrelated as they may occur concurrently. Changes in channel-bed elevation are inseparable from changes in channel width because a channel tends to become narrower during degradation while it tends to widen during aggradation. Therefore, a hydrodynamic model for erodible channels must include these variables."

4. RMA. "The accuracy of model simulations depend on the accuracy with which initial conditions, sediment properties, etc., are specified. In all of the cases we modeled, the data available were sparse and certainly insufficient for using model results for design. We have been able to demonstrate here, however, the significance of accounting for bottom changes in flood routing."

The principal conclusions and recommendations arrived at by the Committee in this study may be summarized as follows:

1. None of the movable-bed models evaluated was found to yield wholly satisfactory results. However, all of the models seem to make reasonably accurate predictions of flood water-surface profiles provided appropriate friction factors are utilized in the computations. This conclusion is attested to by the fact that the HEC2SR, HEC-6, FLUVIAL-11, and SEDIMENT-4H movable-bed models all predicted closely the water-surface profiles for the lower reach of SLR (X = 0 - 10,150 ft), for which Manning's n values obtained from the February 1980 flood records were provided in the input. At over one-half of the stations in this reach, the difference between the highest and lowest stages predicted by the four models were not more than two feet. However, water-surface profiles predicted by the same models for the upper reach of this study section deviated widely, apparently because the available field data were inadequate to determine n values. It is concluded, therefore, that a major deficiency of all movable-bed models is their inability to accurately predict channel roughness or friction factor from the input variables provided. Because the friction factor has a major effect on river stages, this deficiency is a major one.

2. The effects of uncertainty surrounding variations in the channel roughness on flood stages are far greater than the effects of bed erodibility and the attendant degradation/aggradation. Accordingly, until models are developed which include better friction-factor or channel-roughness predictors, and then except in situations in which extensive input and calibration data on channel geometry, bed-material composition, water and sediment hydrographs, etc. are available, the added cost of utilizing movable-bed rather than fixed-bed models is not justified in most cases.

3. An exception to the recommendation set forth in item 2, above, arises in the case of severely disturbed rivers (e.g., by channel straightening or aggregate mining), or channels in very unstable conditions. If adequate input and calibration data are available, erodible-bed models should be utilized in these cases, because the large-scale geometry changes occurring during a flood can have significant flood-stage effects. It is repeated, for emphasis, that localized channel-bed degradation/aggradation has such minor effects on flood-stage elevations that this feature of channel change is masked by uncertainties about the channel roughness and friction factor, initial conditions, and sediment input to the study reach.

4. In order to instill more confidence in fixed-bed models, and to provide guidance concerning the extent and accuracy of the input data required to achieve a specified level of precision, there is a need to undertake a detailed sensitivity analysis of the results to such input variables as channel roughness, channel slope, cross-section geometry, and input hydrograph characteristics (including unsteadiness). In the HEC study of Line Creek, Mississippi (HEC, 1970), HEC-2 was found to be very sensitive to these variables. In particular, the findings of this study showed that the increases in water-surface levels attendant to larger values of Manning's n tend to increase as channel slope decreases; the influence of inaccuracies in channel cross-section geometry tends to increase as channel slope increases; and the influence of discharge errors decreases with increasing channel slope.

5. Because degradation and aggradation are the result of streamwise gradients in the sediment-transport capacity of streams, a very reliable sediment-transport relation is a prerequisite to reliable estimates of channel-geometry changes. It is in the calculation of sediment-discharge

capacities that the various models examined differed most widely. The SLA approach of expressing sediment-transport capacity as a power-law function of local mean velocity and flow depth seems to be reasonable, provided that adequate data are available for the stream being modeled to evaluate the coefficient and exponents appearing in the transport relation. As presently utilized, however, this approach does not make an adequate accounting of the critically important effects of bed armoring.

6. A conspicuous stumbling block in making predictions of channel degradation is the poor understanding and formulation of the bed-armoring process, and the effect of armoring on channel roughness and the sediment-discharge capacity of the flow. Until the formulation of these phenomena are improved, all movable-bed models are likely to be somewhat unreliable in predicting thalweg-elevation changes. Improved formulation of these phenomena must, in turn, await further research.

7. Future alluvial-channel modeling efforts should be directed toward improved incorporation of channel-width changes and channel-pattern migration. There is also a need to improve the formulation of large-scale, abrupt, tributary-sediment inputs to rivers. The approach utilized by SDSU in incorporating these features appears to be in the right direction.

8. It is unlikely that a movable-bed model will be forthcoming that is applicable to all types of rivers. Instead, each model will be more dependable for rivers of the type for which it was developed. Accordingly, there is a need to undertake an effort to classify natural rivers in terms of their hydraulic and geomorphological characteristics to provide for selection and application of appropriate models that use appropriate, constituent formulations for sediment discharge, channel roughness, bank erodibility, etc.

APPENDIX: BIOGRAPHICAL SKETCHES OF COMMITTEE MEMBERS AND CONSULTANT

JOHN F. KENNEDY is Director of the Iowa Institute of Hydraulic Research and Carver Distinguished Professor in the Energy Engineering Division of The University of Iowa. He studied Civil Engineering at Notre Dame University where he received the BSCE in 1955. He entered graduate school at California Institute of Technology, where he received his M.S. in 1956 and, after a period of service as a Second Lieutenant in the U.S. Army Corps of Engineers, his Ph.D. in 1960, both in Civil Engineering. He was a Research Fellow at Caltech from 1960 to 1961, when he became Assistant Professor at Massachusetts Institute of Technology, where he was promoted to the rank of Associate Professor in 1964. In 1966 he accepted the position of Director of the Iowa Institute of Hydraulic Research and Professor of Fluid Mechanics at The University of Iowa. From 1974 to 1976 he also served as Chairman of UI's Division of Energy Engineering, and in July 1981 was named Carver Distinguished Professor. He has received many awards; among these was his election to membership in the National Academy of Engineering in 1973; receipt of ASCE's Stevens (in 1961), Huber (in 1964), and Hilgard (in 1974 and 1978) prizes; selection as ASCE's Hunter Rouse Lecturer in 1981; and his election to the Presidency of the International Association for Hydraulic Research in 1980. He was re-elected to that office in 1982 and currently is serving his second two-year term. His principal technical interests include river hydraulics, ice engineering, cooling-tower technology, and density-stratified flows.

DAVID R. DAWDY is a hydrologic consultant in San Francisco, California. He received his B.A. in History in 1948 from Trinity University in San Antonio, Texas, and his M.S. in Statistics in 1962 from Stanford University. He served 25 years in the United States Geological Survey, where he did research in statistical flood frequency analysis, stochastic simulation of streamflows, rainfall-runoff modeling, and resistance to flow and sediment transport in alluvial streams. For the last 6 years he has been in private consulting, involved with the National Flood Insurance Program, design storm analysis for major dams in South America,

and scour at river crossings. He is Chairman, U.S. National Committee for International Association of Hydrological Sciences; member, U.S. National Committee for International Union of Geodesy and Geophysics; and Adjunct Professor of Civil Engineering, University of Mississippi.

CARL F. NORDIN is a research hydrologist with the U.S. Geological Survey in Denver, Colorado. He received his B.S. and M.S. in Civil Engineering from the University of New Mexico and his Ph.D. from Colorado State University. He is a specialist on sediment transport in rivers, and on stochastic processes in hydraulics and hydrology. He has served on committees of the American Society of Civil Engineers, American Geophysical Union, International Association for Hydraulic Research, and the National Research Council.

JOHN C. SCHAAKE, Jr., is presently responsible for the river and flood forecast operations of the National Weather Service. His position is Chief, Hydrologic Services Division and he also serves as NWS Deputy Associate Director for Hydrology. He first joined the NWS in 1974 as Deputy Director, Hydrologic Research Laboratory. From 1968 to 1974, he was a member of the MIT Civil Engineering Faculty. Prior to that he held joint appointments at the University of Florida in Environmental Engineering and in Industrial and System Engineering. He received B.E.S. and Ph.D. degrees from the John Hopkins University, and held a Post-Doctoral Fellowship at Harvard University. Throughout his career, he has been involved in areas of consulting engineering practice associated with his research in urban hydrology, water resources planning and in both stochastic and determining modeling of hydrologic systems.

STANLEY A. SCHUMM is Professor of Geology at Colorado State University, Fort Collins, Colorado. He received his B.A. in Geology from Upsala College in 1950 and Ph.D. in Geomorphology from Columbia University in 1955. He served 12 years as a geologist for the U.S. Geological Survey. He was a Visiting Lecturer at the University of California, Berkeley from 1959 to 1960; and a Visiting Fellow at the University of Sydney, Australia, from 1964 to 1965. In 1967, he accepted his present position with Colorado

State University and during 1972-1973 was Acting Associate Dean for Research. He received the Horton Award in 1957 from the American Geophysical Union, and in 1970 he received "Honorable Mention" for his paper "Geomorphic Approach to Erosion Control in Semiarid Regions" from the American Society of Agricultural Engineers. In 1979, he received the Kirk Bryan Award of the Geological Society of America for his book "The Alluvial System." In 1980, he received the Distinguished Alumni Award for scientific contributions from Upsala College and the L.W. Durrell Award for research and creativity from Colorado State University. He is presently a member of the NAS-NRC Committee on Disposal of Excess Spoil. He also has served on other technical and advisory Committees of the National Research Council, Geological Society of America, American Geophysical Union, International Geographical Union, American Society of Civil Engineers, U.S. Forest Service and National Park Service.

VITO A. VANONI is Professor of Hydraulics Emeritus, California Institute of Technology (Caltech), Pasadena, California. Since retiring in 1974, he has been active in consulting on sedimentation problems. All of his academic training was at Caltech where he received B.S., M.S., and Ph.D. degrees in Civil Engineering in 1926, 1932, and 1940, respectively. He started his research in sedimentation with the U.S. Soil Conservation Service in 1935 and continued it without interruption while on the Caltech faculty, which he joined in 1947. His research has been experimental in nature and has dealt mostly with the mechanics of sediment suspension, flow resistance, temperature effects, and alluvial bed forms. He has been active for many years consulting on river problems. Among his clients have been the U.S. Army Corps of Engineers, the California Division of Water Resources, and the Bechtel Corporation. He has lectured on sedimentation and consulted on river problems in several countries in Latin America. He was awarded the ASCE Hilgard prizes in 1949 and 1976 for his ASCE paper on suspended-sediment transport mechanics and for his editing of the ASCE monograph "Sedimentation Engineering", respectively. He was elected to the National Academy of Engineering in 1977.

TATSUAKI NAKATO is a Research Scientist at the Iowa Institute of Hydraulic Research of The University of Iowa. He received his B.S. and M.S. degrees in Civil Engineering at Nagoya University, Nagoya, Japan in 1966 and 1968; and his Ph.D. degree in Mechanics and Hydraulics at The University of Iowa in 1974. Since 1975, he has conducted research in sediment-transport processes and been engaged in numerous hydraulic-model investigations at the Iowa Institute of Hydraulic Research.

LIST OF REFERENCES

Amein, M., and Chu, H.L., "Implilcit numerical modeling for unsteady flows," Journal of the Hydraulics Division, ASCE, Vol. 101, No. HY6, June 1975.

Anderson-Nichols/West, "Design review of the Salt River channelization project," prepared by Roberts, B.R., et al., for Corps of Engineers, Sacramento, Californnia, November 1980.

Ariathurai, R., "Erosion and sedimentation downstream from Harry S. Truman Dam as a result of hydropower operations," prepared for Corps of Engineers, Kansas City, Missouri, May 1980.

Brown, C.B., "Sediment transportation," Engineering Hydraulics, H. Rouse ed., John Wiley and Sons, Inc., New York, N.Y., 1950.

Chang, H.H., and Hill, J.C., "Computer modeling of erodible flood channels and deltas," Journal of the Hydraulics Division, ASCE, Vol. 102, No. HY10, October 1976.

Chang, H.H., and Hill, J.C., "Minimum stream power for rivers and deltas," Journal of the Hydrauulic division, ASCE, Vol. 103, No. hY12, December 1977.

Chang, H.H., "Mathematical model for erodible channels," Journal of the Hydraulics Division, ASCE, Vol. 108, No. HY5, May 1982.

Colby, B.R., "Relationship of unmeasured sediment discharge to mean velocity," Transactions, American Geophysical Union, Vol. 38, No. 5, October 1957.

Engelund, F. and Hansen, E., "A monograph on sediment transport in alluvial streams," Teknisk Vorlag, Copenhagen, Denmark, 1967.

Gessler, J., "Beginning and ceasing of sediment motion," River Mechanics, Vol. 1, Colorado State University, Fort Collins, Colorado, 1971.

Graf, W.H., "Hydraulics of sediment transport," McGraw-Hill Book Co., Inc., New York, N.Y. 1971.

Hydrologic Engineering Center, "National Academy of Sciences study of computer based flood and sediment routing models, San Lorenzo River, California and Salt River, Arizona," prepared by MacArthur, R.C., and Gee, M.D., Corps of Engineers, Davis, California, January 1982.

Hydrologic Engineering Center, "Sensitivity analysis of factors that influence water surface profiles: HEC-2," Corps of Engineers, Davis, California, October 1970.

Hydrologic Engineering Center, "Scour and deposition in rivers and reservoirs," Computer Program HEC-6, Corps of Engineers, Davis, California, March 1977.

Jennings, M.E., and Land, L.F., "Simulation studies of flow and sediment transport using a mathematical model, Atchafalaya River basin, Louisiana," U.S.G.S. Water-Resources Investigation 77-14, May 1977.

Jones-Tillson & Associates, et al., "San Lorenzo River study, stage II, field and simulation studies," prepared for Corps of Engineers, San Francisco, California, September 1980.

Laursen, E.M., "The total sediment load of streams," Journal of the Hydraulics Division, ASCE, Vol. 54, February 1958.

Nakato, T., and Vadnal, J.L., "Field study and tests of several one-dimensional sediment-transport computer models for Pool 20, Mississippi River," IIHR Report No. 237, Iowa Institute of Hydraulic Research, The University of Iowa, July 1981.

Prasuhn, A.L., and Sing, E.F., "Modeling of sediment transport in Cottonwood Creek," Proceedings of the Specialty Conference on Computer and Physical Modeling in Hydraulic Engineering, ASCE, Chicago, Illinois, August 1980.

Resource Management Associates, "Flood routing with movable bed," prepared by Ariathurai R., and Smith, D.J., March 1982.

Rouse, H., "Modern conception of the mechanics of fluid turbulence," Transactions, ASCE, Vol. 102, Paper No. 1965, 1937.

San Diego State University, "Computer-based flood and sediment routing model: case studies of San Dieguito River, California; San Lorenzo River, California; and Salt River, Arizona," prepared by Chang, H.H., and Hill, J.C. for National Research Council, January 1982.

Simons, Li & Associates, Inc., "Erosion, sedimentation, and debris analysis of Boulder Creek (24th Street Bridge to 30th Street Bridge), Boulder, Colorado," prepared for URS Company, Denver, Colorado, 1980.

Simons, Li & Associates, Inc., "Scour and sedimentation analysis of the proposed channelization of the Salt River for protecting the Sky Harbor International Airport in Phoenix, Arizona," prepared for HNTB, Kansas City, Missouri, December 1980.

Simons, Li & Associates, Inc., "River response analysis associated with Rio Nuevo-Santa Cruz River flood control and channelization project, Tucson, Arizona," prepared for Cella Barr Associates, 1981.

Simons, Li & Associates, Inc., "Cañada del Oro Wash flood control project - Oro Valley, Pima County, Arizona," prepared for Department of Water Resources, Phoenix, Arizona, 1981.

Simons, Li & Associates, Inc., "Sediment transport analysis of Rillito River and tributaries for regional flood control element of the Tucson urban study," 1981.

Simons, Li & Associates, Inc., "Application of hydrodynamic computer models to flood analysis," prepared for National Research Council, February 1982.

Simons, D.B., Li, R.M., and Brown, G.O., "Sedimentation study of the Yazoo River basin-user manual for Program KUWASER", Report No. CER79-80DBS-R, Colorado State University, August 1979.

Simons, D.B., et al., "A geomorphic study of Pools 24, 25, and 26 in the Upper Mississippi and Lower Illinois Rivers," Report No. CER74-75DBS-SAS-MAS-YHC-PFL8, Colorado State University, March 1975.

Simons, D.B., and Chen, Y.H., "A mathematical model study of Pool 4 in the Upper Mississippi and Lower Chippewa Rivers," Report No. CER76-77DBS-YHC-8, Colorado State University, October 1976.

Simons, D.B., and Chen, Y.H., "Investigation of the effects of Chippewa River erosion and silt reduction measures," Report No. CER76-DBS-YHC-54, Colorado State Univesity, 1977.

Simons, D.B., Chen, Y.H., and Saez-Benito, J.M., "A mathematical model of Pools 5 through 8 in the Upper Mississippi River system," Report no. CER79-80DBS-YHC-JMS21, Colorado State University, December 1979.

Simons, D.B., and Chen, Y.H., "A mathematical model of the Lower Chippewa River network system," Report No. CER78-79-DBS-YHC58, Colorado State University, June 1979.

Simons, D.B., and Chen, Y.H., "Assessment of hydraulic impacts of the Atchafalaya River flood control program on the Lower Mississippi River," Report No. CER77-78DBS-YHC38, Colorado State University, August 1978.

Thomas, W.A., and Prasuhn, A.L., "Mathematical modeling of scour and deposition," Journal of the Hydraulics Division, ASCE, Vol. 103, No. HY8, August 1977.

Toffaleti, F.B., "A procedure for computation of the total river sand discharge and detailed distribution, bed to surface," Technical Report No. 5, Committee on Channel Stabilization, Corps of Engineers, Vicksburg, Mississippi, November 1968.

Williams, D.T., "Effects of dam removal: an approach to sedimentation," Technical Paper No. 50, Hydrologic Engineering Center, Corps of Engineers, Davis, California, October 1977.

Yang, C.T., "Incipient motion and sediment transport," Journal of the Hydraulics Division, ASCE, Vol. 99, No. HY10, October 1973.